SYNTHESIS AND COORDINATION CHEMISTRY OF AZULENE- AND FERROCENE-BASED ISOCYANIDE LIGANDS

By

Copyright 2011

David Michael McGinnis

Submitted to the graduate degree program in the Department of Chemistry and the Graduate Faculty of the University of Kansas in partial fulfillment of the requirements for the degree of Doctor of Philosophy.

_____

Chairperson, Dr. Mikhail V. Barybin

_____

Dr. David R. Benson

_____

Dr. Cindy L. Berrie

_____

Dr. Kyle V. Camarda

_____

Dr. Timothy A. Jackson

Date Defended: June 29, 2011

The Dissertation Committee for David Michael McGinnis

certifies that this is the approved version of the following dissertation:

SYNTHESIS AND COORDINATION CHEMISTRY OF AZULENE- AND FERROCENE-BASED ISOCYANIDE LIGANDS

_____

Chairperson, Dr. Mikhail V. Barybin

Date approved: July 7, 2011

Abstract

Nonbenzenoid aromatic isocyanides feature attractive structural and electronic properties for the potential design of optoelectronic devices. Prior to the work of Barybin and coworkers, examples of nonbenzenoid isocyanides were limited to isocyanoferrocene and 1,1'-diisocyanoferrocene. This thesis describes the design of nonbenzenoid isocyanides featuring ferrocene and/or azulene moieties.

The first nonbenzenoid aromatic isocyanide featuring both azulene and ferrocene in one molecule is described. Electrochemical results indicate stable redox activity leading to the potential use in the design of redox-addressable materials. A new bis-iridium complex of 1,1'-diisocyanoferrocene was synthesized and showed the possible existence of two isomeric forms when in solution. Redox properties indicate reversibility which is likely iron-based. Preliminary crystallographic data for this complex features a symmetrical structure with C-N-C angles of approximately 176°.

A synthetic pathway for the formation of 2,2'-diisocyano-6,6'-biazulenylacetylene π-linker is documented. This diisocyanide exhibits a relatively stable stepwise two-electron reduction process on the electrochemical time scale indicating the likelihood of a closed shell dianion. Coordination chemistry of the mono and dinuclear tungsten diisocyanide complexes illustrates evidence for a metal-to-bridge charge-transfer. A self assembled monolayer of the ligand coordinated to Au(111) indicates an upright orientation when on the surface. Synthesis of a tetranuclear(I) gold rectangle featuring the 2,2'-diisocyano-6,6'-biazulenyl linker is presented and its interesting luminescent properties will be compared to relevant complexes. A crystallographically defined half gold ring featuring the 2-isocyanoazulenyl moiety exhibits an aurophilic interaction between two Au(I) centers.

An optimized regioselective amination of 2,2'-biazuene is presented in good yield. This ligand undergoes a stepwise, reversible two-electron reduction according to an electrochemical study . This ligand acts as a precursor to the targeted 6-isocyano-2,2'-biazulene. The formation of a self assembled monolayer featuring 6-isocyano-2,2'-biazulene coordinated in an upright fashion on a Au(111) surface is mentioned.

The first accessible planar-chiral isocyanide ligand is presented in high enantiomerically purity. This ligand exhibits robust redox activity upon coordination on the electrochemical time scale. Results from the electrochemical studies in addition to the other spectroscopic evidence will be presented.

Acknowledgements

First of all, I express many thanks to my research mentor, Dr. Mikhail Barybin. Misha has an unbelievable mentoring ability that all of his graduate students witness first hand. His incredible scientific intellect and passion for the field is impressive. It has been an honor to work with someone of his caliber during my graduate career. I am indebted to him for allowing me to work in his lab and I look forward to maintaining our friendship in the future.

I must thank the faculty of the Chemistry Department at the University of Kansas. I appreciate all of their efforts in my graduate student training and for those that have been regular participants for the inorganic colloquium series. I especially would like to thank Dr. David Benson, Dr. Cindy Berrie, Dr. Kyle Camarda, and Dr. Timothy Jackson for agreeing to serve as members of my committee. I greatly appreciate your support.

I am thankful for the people I have worked with during my studies at the University of Kansas. I must start off by thanking Dr. Tom Holovics, Dr. Stephan Deplazes, and Dr. Tiffany Maher for their assistance in getting me up to speed with research. Tiffany is a good friend and I appreciated all of her constructive criticism when she was a member of the Barybin group. I am grateful to have worked alongside some outstanding individuals. John Meyers and Brad Neal were very helpful in providing fruitful feedback during the writing process. We've had our fair share of good times resulting in laughter and making for a fun lab environment. I look forward to maintaining our friendships in the future. In addition to John and Brad, I must also thank Kolbe Scheetz, Andrew Spaeth, and Chris Palmer for helping make the Barybin group what it is today. I'd like to think that our research group is a tight knit core of guys that are like brothers. I am a better person after working with them and am looking forward to hearing about their progress into the future. I've had the opportunity to work with a few exceptional undergraduates

during the REU summer research program at KU. Special thanks goes out to Chris Smith, Nils Wittenbrink, and Sergio Perez-Conessa for choosing to work in the Barybin group and giving me the opportunity to learn how to supervise them.

I would also like to thank Dr. Victor Day for his expertise pertaining to X-ray crystallography. Thanks Dr. Richard Givens for allowing me to use the Cary 100 and the Eclipse fluorimeter in your lab. Also, I would like to thank Dr. Justin Douglas and Sarah Neuenswander for their assistance over the years in the NMR laboratories. Thanks to my close friends Dr. Chris Thomas and Dr. John Hershberger for their conversations and friendships during their time at KU. I would like to thank the folks in the stockroom, the main office, and to anyone else at KU that helped during my graduate career.

I thank Dr. Roy Williams and Dr. Mark Elliott from my days at Old Dominion University. These professors were the ones that inspired me to swing for the fences and attempt to pursue graduate school at the University of Kansas. I am forever indebted to them both and am grateful that they saw potential in me. I fondly remember eating lunch at the O'Sullivans Wharf and Pizza Inn between classes sharing in discussion of science. Thanks for allowing me to be in your company and for inspiring me to obtain my goal.

Finally, I would like to acknowledge my family beginning with my wife, Carrie, whom has been my biggest fan. She has sacrificed, worked hard, and supported me in every step of the way during my endeavors. Without her, I would not be where I am today. I love her very much and look forward to starting the next phase of our lives together. My parents, Mike and Rita, were instrumental in teaching me the value of hard work from an early age. They allowed for me to decide my own path and never dissuaded me in any way. To my second mom and dad, Bob and Darlene, I greatly appreciate them for making me feel like their son and not just a

typical son-in-law. I am indebted to Bob for his wisdom as I pursued my degree. I thank both sets of parents for their tremendous support; I love you guys. And last but not least, I thank my siblings, Michelle and Jay, and the rest of my extended family for their continuous support.

TABLE OF CONTENTS

Abstract iii

Acknowledgments v

LIST OF TABLES xii

LIST OF FIGURES xiii

LIST OF SCHEMES xvi

CHAPTER I 1

I. Redox-active Organic Isocyanides Featuring Azulenyl and Ferrocenyl Moieties in One Molecule 1

I.1 Introduction 2

I.2 Work Described in Chapter I 8

I.3 Experimental Section 9

I.3.1 General Procedures 9

I.3.2 Synthesis of Acetylferrocene 11

I.3.3 Synthesis of 1-chlorovinylformylferrocene 11

I.3.4 Synthesis of ethynylferrocene 12

I.3.5 Synthesis of 2-amino-1,3-diethoxycarbonyl-6-azulenylethynylferrocene 13

I.3.6 Synthesis of 2-formamido-1,3-diethoxycarbonyl-6-azuleneferrocenyl acetylene 13

I.3.7 Synthesis of 2-isocyano-1,3-diethoxycarbonyl-6-azuleneferrocenyl acetylene 14

I.3.8 Synthesis of bis(2-isocyano-1,3-diethoxycarbonyl-6-azuleneferrocenyl acetylene)Palladium(II)iodide 15

I.3.9 Preliminary small scale synthesis of hexakis(2-isocyano-1,3-diethoxycarbonyl-6-azuleneferrocenyl acetylene)chromium (0 and I) 15

I.3.10 Synthesis of 1,1'-diisocyanoferrocenebis (pentamethylcyclopentadienyl-dichloroiridium(III)) 16

I.4 Results and Discussion 17

I.5 Conclusions and Outlook 30

I.6 References 32

CHAPTER II 35

II. Chemistry of a Linear Symmetric π-Linker Featuring Isocyanide Termini and Two Azulenic Moieties Separated by an Acetylene Spacer 35

II.1 Introduction 36

II.2 Work Described in Chapter II 41

II.3 Experimental Section 42

II.3.1 General Procedures 42

II.3.2 Synthesis of 2-amino-6-trimethylsiylylacetylene-1,3-diethoxycarbonylazulene 44

II.3.3 Synthesis of 2-amino-6-ethynyl-1,3-diethoxycarbonylazulene 44

II.3.4 Synthesis of 2,2'-diamino-1,1',3,3'-tetraethoxycarbonyl-6,6'-biazulenylacetylene 45

II.3.5 Synthesis of 2,2'-bisformamido-1,1',3,3'-tetraethoxycarbonyl-6,6'-biazulenylacetylene 45

II.3.6 Synthesis of 2,2'-diisocyano-1,1',3,3'-tetraethoxycarbonyl-6,6'-biazulenylacetylene 46

II.3.7 Synthesis of a dinuclear tungsten pentacarbonyl complex featuring 2,2'- diisocyano-1,1',3,3'-tetraethoxycarbonyl-6,6'-biazulenylacetylene 47

II.3.8 Synthesis of a mononuclear tungsten pentacarbonyl complex featuring 2,2'-diisocyano-1,1',3,3'-tetraethoxycarbonyl-6,6'-biazulenylacetylene 48

II.3.9 Synthesis of [dcpm(Au)$^{1}_{2}$bis(1,3-diethoxycarbonyl-2-isocyanoazulene]$^{2+}$([OTF]$^{-}$)$_2$ 48

II.3.10 Synthesis of bis[dcpm(Au)$^{1}_{2}$(2,2'-diisocyano-1,1',3,3'- tetraethoxycarbonyl -6,6'-biazulenylacetylene]$^{4+}$([OTF]$^{-}$)$_4$ 49

II.4 Results and Discussion 50

II.5 Conclusions and Outlook 73

II.6 References 75

CHAPTER III 78

III. Regioselective Monofunctionalization of the 2,2'-Biazulenyl Scaffold: Chemistry of the 6-Isocyano-2,2'-biazulenyl Ligand 78

III.1 Introduction 79

III.2 Work Described in Chapter III 84

III.3 Experimental Section 85

III.3.1 General Procedures 85

III.3.2 Synthesis of 6-amino-2,2'-biazulene 87

III.3.3 Synthesis of 6-formamido-2,2'-biazulene 87

III.3.4 Synthesis of 6-isocyano-2,2'-biazulene 88

III.4 Results and Discussion 89

III.5 Conclusions and Outlook 98

III.6 References 99

CHAPTER IV 101

IV. Synthesis, Properties and Complexation of ($_p$*S*)-1-Isocyano-2-methylferrocene, the First Planar-chiral Isocyanide Ligand 101

IV.1 Introduction....102
IV.2 Work Described in Chapter IV....103
IV.3 Experimental Section....104
IV.3.1 General Procedures....104
IV.3.2 Synthesis of ($_p$S)-1-amino-2-methylferrocene....106
IV.3.3 Synthesis of ($_p$S)-1-formamido-2-methylferrocene....106
IV.3.4 Synthesis of ($_p$S)-1-isocyano-2-methylferrocene....107
IV.3.5 Synthesis of trans-[PdI_2{($_p$S)-1-isocyano-2-methylferrocene}$_2$]....108
IV.4 Results and Discussion....109
IV.5 Conclusions and Outlook....118
IV.6 References....119
Appendix 1. Crystallographic Data for Compound 2.8....122
Appendix 2. Preliminary Crystallographic Data for Compound 3.1....154
Appendix 3. NMR Spectra of Selected Compounds from Chapter I....165
Appendix 4. NMR Spectra of Selected Compounds from Chapter II....171
Appendix 5. NMR Spectra of Selected Compounds from Chapter III....182

LIST OF TABLES

Table I.1. C-N-C bond angles in bimetallic complexes of 1,1'-diisocyanoferrocene 29

Table II.1. ^{1}H NMR data in ppm of selected azulenic based compounds in $CDCl_3$ and/or CD_2Cl_2 at 25°C 53

Table II.2. Reduction and oxidation potentials of 1.3, 1.6, and selected compounds from the literature in CH_2Cl_2 versus FcH/FcH^+ in volts 56

Table II.3. Electronic transitions for azulenic compounds in CH_2Cl_2 and pentane 58

Table II.4. MBCT and binucleation energies for selected compounds conducted in CH_2Cl_2 62

Table II.5. Selected bond distances and/or angles from X-ray diffraction 68

Table II.6. Emission data of selected gold-gold based compounds in CH_2Cl_2 at 24°C.....70

Table III.1. Isocyanide stretching frequencies for selected isocyanoazulene derivatives.....92

Table III.2. Half-wave redox potentials for 3.1, 3.3, and several other azulenic derivatives in CH_2Cl_2 versus FcH/FcH^+.....94

Table IV.1. Selected bond distances for **4.4** 114

Table IV.2. Cyclic voltammetry data for FcNC, **4.2**, **4.3**, and **4.4** 117

LIST OF FIGURES

Figure I.1. Resonance structures of isocyanide and carbonyl ligands 2

Figure I.2. Synergistic metal-ligand interactions allow an isocyanide to act as a σ-donor and π-acceptor 3

Figure I.3. Examples of 1,1'-diisocyanoferrocene coordination chemistry 6

Figure I.4. Ferrocene azulenylium and guaiazulenylium carbocations 7

Figure I.5. Cyclic voltammogram of 1.6 in CH_2Cl_2 referenced to the FcH/FcH^+ couple. Scan rate = 100 mV/sec 18

Figure I.6. Cyclic voltammogram of 1.3 in CH_2Cl_2 referenced to the FcH/FcH^+ couple. Scan rate = 100 mV/sec 19

Figure I.7. Cyclic voltammogram of 2-isocyano-1,3'-diethoxycarbonylazulene in CH_2Cl_2 referenced to the FcH/FcH^+ couple. Scan rate = 100 mV/sec 20

Figure I.8. A zwitterionic resonance form of compound 1.6 21

Figure I.9. FTIR spectrum of compound 1.6 in CH_2Cl_2 at 25°C 23

Figure I.10. FTIR spectrum of compound 1.8a in CH_2Cl_2 at 25°C 23

Figure I.11. FTIR spectrum of compound 1.8b in CH_2Cl_2 at 25°C 24

Figure I.12. FTIR spectrum of compound 1.9 in CH_2Cl_2 at 25°C 26

Figure I.13. FTIR spectrum of compound 1.9 in Nujol at 25°C 26

Figure I.14. ^1H NMR spectrum of compound 1.9 in $CDCl_3$ at 25°C 27

Figure I.15. Possible isomeric structures of 1.9 in solution 27

Figure I.16. Cyclic voltammogram of 1.9 in CH_2Cl_2 referenced to the FcH/FcH^+ couple. Scan rate = 100mV/sec 28

Figure I.17. Preliminary X-ray structure of compound 1.9 29

Figure I.18. Proposed redox active complex featuring two isocyanoazulenic motifs 31

Figure II.1. A homologous series of linear diisocyanoarene linkers based on the nonbenzenoid 2,6-azulenic framework 36

Figure II.2. Cyclic Voltammogram of 2,2'diisocyano 6,6'-biazulene....39

Figure II.3. Cyclic voltammogram of 2.5 in CH_2Cl_2 with an internal FcH/FcH^+ ref. at a scan rate of 50mV/sec....54

Figure II.4. Differential pulse voltammogram of 2.5 in CH_2Cl_2 with an internal FcH/FcH^+ ref....54

Figure II.5. Cyclic voltammogram of 2.3 in CH_2Cl_2 with an internal FcH/FcH^+ ref. at a scan rate of 500mV/sec....55

Figure II.6. Cyclic voltammogram of 2.4 in CH_2Cl_2 with an internal FcH/FcH^+ ref. at a scan rate of 500mV/sec....55

Figure II.7. LUMO of 2.5 using a simple Hückel calculation....57

Figure II.8. Potential representation of the closed shell dianion for 2.5....57

Figure II.9. Coordination of 2.5 with tungsten pentacarbonyl....60

Figure II.10. FTIR of compound 2.6 in CH_2Cl_2 at 25°C....61

Figure II.11. FTIR of compound 2.7 in CH_2Cl_2 at 25°C....61

Figure II.12. Cyclic voltammogram of 2.6 in CH_2Cl_2 with an internal FcH/FcH^+ ref. at a scan rate of 100mV/sec....63

Figure II.13. X-ray structure of compound 2.8....66

Figure II.14. X-ray structure of the1,1' diisocyanoferrocenyl gold rectangle and 2.8....67

Figure II.15. X-ray structure of Puddephatt's tetragold(I) rectangle....67

Figure II.16. SAM of 6,6'-biazulenyl ligands on Au(111). Left: SAM of compound 2.5. Right: SAM of 2,2'-diisocyano-6,6'-biazulenyl....71

Figure III.1. Azulene: atom numbering scheme and the resonance form emphasizing its polar nature....79

Figure III.2. Aromatic delocalization energies for select aromatics in kcal/mol....79

Figure III.3. The hypothetical 2,6-azulenic linker....80

Figure III.4. Three possible linear diisocyanobiazulene frameworks....81

Figure III.5. Neutral and zwitterionic resonance forms of compound 3.1 91

Figure III.6 Neutral and zwitterionic resonance forms of compound 3.3 92

Figure III.7. Cyclic voltammogram of compound 3.1 in CH_2Cl_2 versus FcH/FcH^+. Scan rate = 100mV/sec 93

Figure III.8. Differential pulse voltammogram of compound 3.1 in CH_2Cl_2 with an internal FcH/FcH^+ reference 93

Figure III.9. Top: FTIR spectrum of 3.3 in CH_2Cl_2. Bottom: FTIR spectrum of 3.3 absorbed on Au(111) 95

Figure III.10. Preliminary X-ray crystal structure of the compound 3.1 97

Figure IV.1 Chiral HPLC traces (identical conditions) for *rac*-1-amino-2-methylferrocene (A), *($_p$S)*- 1-amino-2-methylferrocene (B), and *($_p$R)*- 1-amino-2-methylferrocene (C). Adapted from S. F. Deplazes, Ph.D. Thesis, The University of Kansas, 2007 111

Figure IV.2 ORTEP diagrams of two independent molecules A (top) and B (bottom) in the asymmetric unit of **4.4**. Thermal ellipsoids are drawn at the 50% probability level 113

Figure IV.3 Cyclic voltammogram of **4.2** in 0.1 M $[^nBu_4N][PF_6]/CH_2Cl_2$ vs. Cp_2Fe^+/Cp_2Fe. Scan rate = 100 mV/s. Internal Cp_2Co^+/Cp_2Co reference 115

Figure IV.4 Cyclic voltammogram of **4.3** in 0.1 M $[^nBu_4N][PF_6]/CH_2Cl_2$ vs. Cp_2Fe^+/Cp_2Fe. Scan rate = 100 mV/s. Internal Cp_2Co^+/Cp_2Co reference 115

Figure IV.5. Cyclic voltammogram of **4.4** in 0.1 M $[^nBu_4N][PF_6]/CH_2Cl_2$ at positive potentials vs. Cp_2Fe^+/Cp_2Fe. Scan rate = 100 mV/s. External Cp_2Fe^+/Cp_2Fe reference. Adapted from S. F. Deplazes, Ph.D. Thesis, The University of Kansas, 2007 116

LIST OF SCHEMES

Scheme I.1. Synthetic route for 1,1'-diisocyanoferrocene 5

Scheme I.2. Synthesis of ethynylferrocene adopted from Polin and co-workers 17

Scheme I.3. Synthesis of the isocyanide ligand featuring ferrocenyl and azulenyl moieties 17

Scheme I.4. Preliminary syntheses of neutral and cationic homoleptic complexes of compound 1.6.....22

Scheme I.5. Synthesis of a bis(iridium(III)) complex of 1,1'-diisocyanoferrocene 24

Scheme II.1. First reported 6,6'-biazulene synthesis.....37

Scheme II.2. Synthesis of 2,2'-diisocyano 6,6'-biazulene.....38

Scheme II.3. Synthesis of precursors for the 6,6'-biazulenylacetylene chemistry 50

Scheme II.4. Synthesis of the 2,2'-diamino-6,6'-biazulenylaceylene scaffold 51

Scheme II.5. Synthesis of the 2,2'-diisocyano-6,6'-biazulenylacetylene linker.....52

Scheme II.6. Synthesis of the 1,4-diisocyanodurene tetragold(I) rectangle 64

Scheme II.7. Synthesis of the 1,1'-diisocyanoferrocene digold(I) rectangle.....65

Scheme II.8. Synthesis of compound 2.8.....66

Scheme II.9. Synthesis of compound 2.9.....69

Scheme III.1. Synthesis of 2,2'-biazulene 89

Scheme III.2. Synthesis of the 6-isocyano-2,2'-biazulene 90

Scheme IV.1. Synthesis of compounds **4.1** – **4.4** from *($_p$S)*-1-bromo-2-methylferrocene.....110

CHAPTER I

I. Redox-active Organic Isocyanides Featuring Azulenyl and Ferrocenyl Moieties in One Molecule

I.1. Introduction

Organic isocyanides are isolable molecules that feature a lone pair of electrons on a terminal carbon atom of the functional group. Isocyanides are isoelectronic with the carbonyl ligand (Figure I.1), which also has a lone pair of electrons on its carbon atom. Isocyanide complexes of transition metals play an important role in organic and organometallic synthesis, catalysis, and radiological medicine.[1-7]

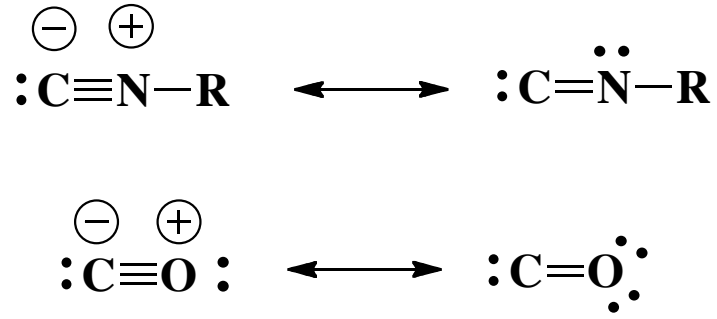

Figure I.1. Resonance structures of isocyanide (top) and carbonyl (bottom) ligands.

Isocyanides as ligands exhibit several noteworthy structural characteristics. The most obvious is associated with the possibility of tuning the nature of the substituent "R". In addition, the cylindrical symmetry of π-electron density of the isocyano group is well suited for supporting metal-to-ligand electron delocalization. The metal-isocyanide bonding in transition metal complexes can be considered in terms of two synergic interactions: σ-donation of the carbon atom's lone pair to vacant metal-based orbitals and transfer of electron density from the filled metal d-orbitals of π-symmetry into the isocyanide π*-antibonding orbitals. The latter interaction is known as π back-bonding (Figure I.2), which in the case of aryl isocyanide ligands can delocalize metal electron density into the π*-system of the aryl fragment. The vast majority of aryl isocyanides known by the turn of the last century contain benzenoid aromatic

substituents. Such ligands are commonly quite air and thermally sensitive under ambient conditions, more so compared to their alkyl congeners.[8] A fundamental advantage of the aryl isocyanides over their alkyl counterparts is the electronic coupling between the π-systems of the isocyanide group and the organic fragment in the former.[3-5, 9-15] Thus, there has been an interest in designing stable isocyanide complexes that would feature electron delocalization mediated by the isocyano junction(s).

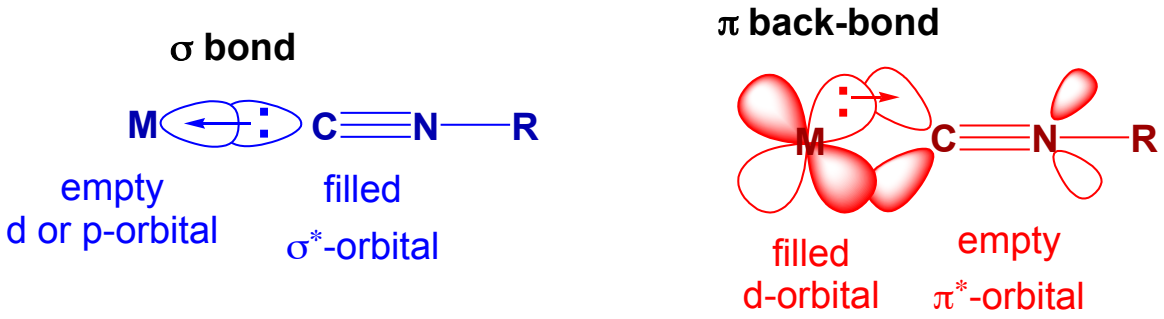

Figure I.2. Synergistic metal-ligand interactions allow an isocyanide to act as a σ-donor and a π-acceptor.

Recently, a new class of aryl isocyanide molecules, which incorporate nonbenzenoid aromatic substituents, has been popularized by Barybin *et al*.[16] The first two examples of nonbenzenoid isocyanides were isocyanoferrocene and 1,1'-diisocyanoferrocene. Until a few years ago, the chemistry of isocyanoferrocene had remained scarcely developed since the discovery of the compound in the late 1980s.[1, 17-19] This is most likely due to the tedious and low-yielding synthesis of aminoferrocene available at the time as well as a somewhat unreliable conversion of its amino group to the isocyano substituent originally reported in the 1980s. Recently, significantly more efficient synthetic routes to aminoferrocene have emerged.[20] Heinze and coworkers were able to obtain nearly quantitative yields for the formation of aminoferrocene

on the gram scale.[20] However, formylation of aminoferrocene followed by dehydration of the resulting formamidoferrocene remained problematic. In 1990, Knox *et al.* described the synthesis of isocyanoferrocene from aminoferrocene in poorly reproducible yields of 25-90%.[15]

In 2002, Barybin and coworkers published an substantially improved and highly reliable synthesis of isocyanoferrocene.[1] Based on the similar values of the Hammett constants for the methyl and ferrocenyl substituents, it was thought for a long time that isocyanoferrocene would behave akin to methyl isocyanide as a ligand.[17-18] Thus, despite many parallels in the chemistries of ferrocene and arenes, consideration of ferrocenyl's π-system as a potential electron acceptor has not been addressed experimentally prior to the work done by Barybin and coworkers.[21] In their work, the studied homoleptic complexes of isocyanoferrocene and low-valent chromium exhibited properties which made the ferrocenyl substituent comparable to an aryl moiety.[21]

In 2001, Hessen and coworkers published the synthesis of 1,1'-diisocyanoferrocene that avoids the use of unstable 1,1'-diaminoferrocene as a precursor.[19] The route is reproducible and yields 50% of 1,1'-diisocyanoferrocene at the conclusion of the synthesis. (Scheme I.1). This ligand should be an attractive redox-active linker for multi-metallic ensembles and coordination polymers.[19]

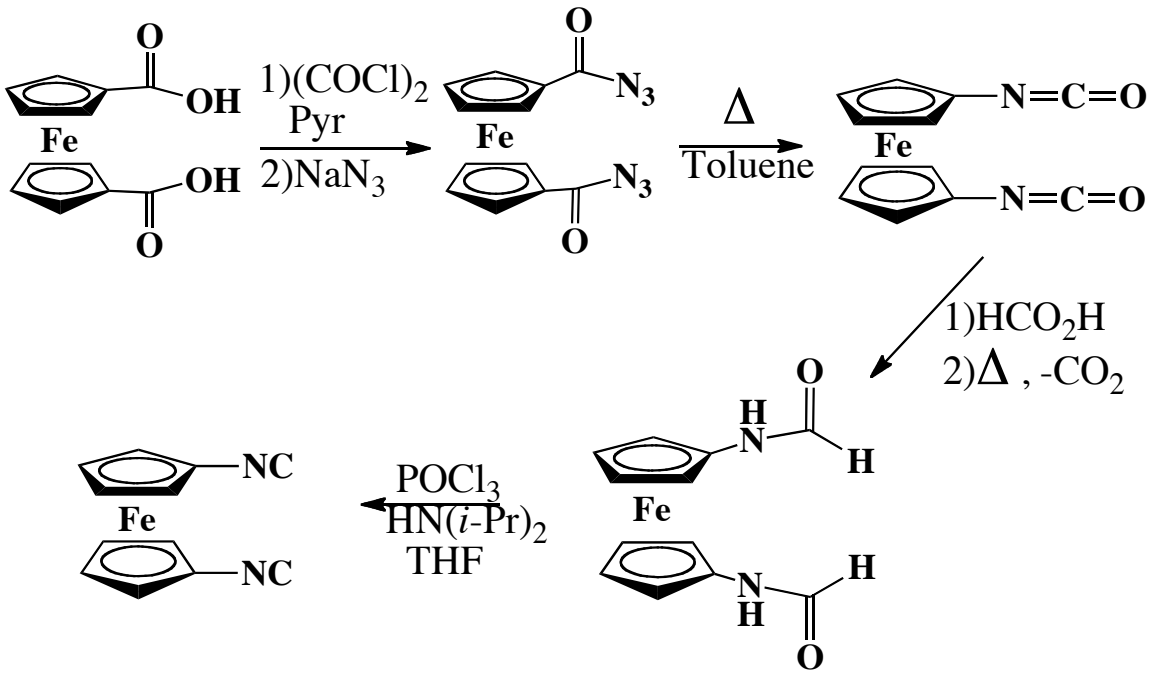

Scheme I.1. Synthetic route to 1,1'-diisocyanoferrocene.[19]

Siemeling and coworkers have pioneered the efforts towards the construction of organometallic systems where the 1,1'-diisocyanoferrocene linker was involved in coordination to gold(I) and copper(I) metal centers (Figure I.3).[22-25] The 1D organometallic polymer formed by the interaction of diisocyanoferrocene with gold(I) chloride (Figure I.3, right) is particularly interesting as it may serve as a model for understanding the interaction of diisocyanoferrocene with the gold(111) surface.[22] In addition, the interplanar distance between the cyclopentadienyl rings in the ferrocene moiety is about 3.3 Å, which is quite similar to many M-M single bond lengths, including the Au-Au interaction. This suggests that 1,1-diisocyanoferrocene should indeed be a useful building block for constructing organometallic molecular rectangles that incorporate the ferrocene motif.

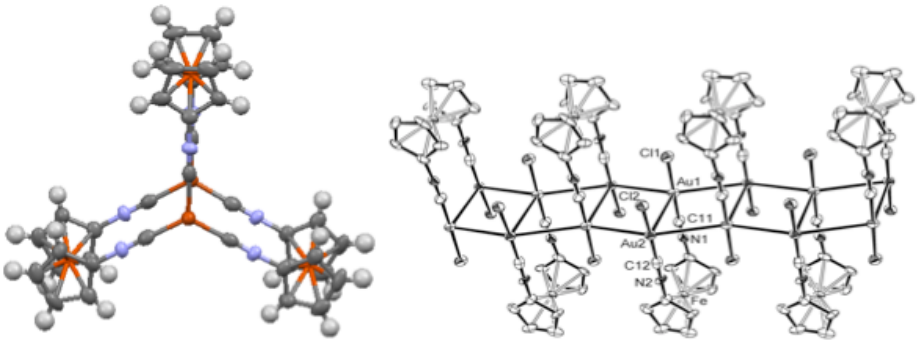

Figure I.3. Examples of 1,1'-diisocyanoferrocene coordination chemistry. [16, 22-25]

Nonlinear optics (NLO) is a field that has become increasingly important during the electronic age as technology uses the movement of electrons to acquire, store, and process information.[26] When light from the near-infrared to the blue end of the visible range impinges on the NLO material, electrons will oscillate in response to an optical field.[26] Light intensity can play a factor. For instance, a high light intensity will lead to the oscillation of the electrons to be antiharmonic in turn leading to potential emission at frequencies different than that of the incident light. A considerable amount of research related to the design of nonlinear optical materials and devices has been done in the past twenty years.[27-30] A well-established strategy to obtain materials with high values of hyperpolarizability is to connect a donor fragment and an acceptor moiety with a conjugated bridge.[31] Hermann reasoned that the combination of an organometallic fragment with well-known donor properties such as ferrocene with an aromatic compound exhibiting unusual electron distribution, e.g., azulene, might lead to molecular systems with unique properties and potentially enhanced NLO coefficients.[31] Another intriguing property of such materials would be their redox activity. Ferrocene is well known for its stability and robust redox behavior. Thus, the electronically coupled ferrocene/azulene combination could very well lead to interesting results.

Farrell and coworkers studied azulenylium and guaiazulenylium cations (Figure I.4) to develop understanding of mutual donor-acceptor electronic influence using cyclic voltammetry.[32]

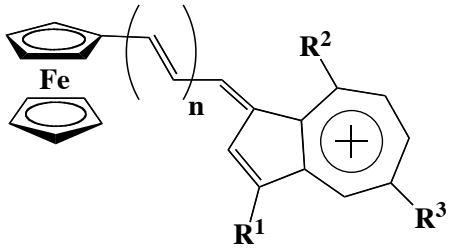

$R^1 = R^2 = R^3 = H$; n = 0-2; azulenylium cations
$R^1 = R^2 =$ Me, $R^3 =$ *i*-Pr; n = 0-2; guaiazulenylium carbocations

Figure I.4. Ferrocene azulenylium and guaiazulenylium carbocations.[32]

Cyclic voltammetry helped uncover a greater extent of ground state electronic communication between the azulenylium based acceptors and the ferrocenyl termini compared to the system containing the electronically and structurally related tropylium and ferrocenyl units.[32] The experiment also indicated that the HOMO of these molecules is primarily ferrocene-based whereas the LUMO is azulenylium-based and there is an increased negative shift of the reduction potential upon decreased donor-acceptor separation.[32]

I.2. Work Described in Chapter I

In this Chapter, the synthesis and properties of the isocyanide ligand featuring both azulenyl and ferrocenyl moieties is presented. Preliminary results pertaining to the coordination chemistry of this novel ligand are discussed as well. In addition, new aspects of the coordination chemistry involving 1,1'-diisocyanoferrocene are described. Future directions based on the research reported herein are outlined at the conclusion of the Chapter.

I.3. Experimental Section

I.3.1 General Procedures and Starting Materials

Unless specified otherwise, all operations were performed under an atmosphere of 99.5% argon further purified by passage through columns of activated BASF catalyst and molecular sieves. All connections involving the gas purification systems were made of glass, metal, or other materials impermeable to air. Solutions were transferred via stainless steel cannulas whenever possible. Standard Schlenk techniques were employed with a double manifold vacuum line. CH_2Cl_2 and Et_3N were distilled over CaH_2. THF and toluene were distilled over Na/benzophenone. Following purification, all distilled solvents were stored under argon.

Solution infrared spectra were recorded on a PerkinElmer Spectrum 100 FTIR spectrometer with samples sealed in 0.1mm gas tight NaCl cells. NMR samples were analyzed using Bruker DRX-400 and Bruker Avance 500 spectrometers. ^{1}H and ^{13}C chemical shifts are given with reference to residual ^{1}H and ^{13}C solvent resonances relative to Me_4Si. UV-vis spectra were recorded in CH_2Cl_2 at 24°C using a CARY 100 spectrophotometer.

Cyclic voltammetric (CV) and differential pulse voltammetric (DPV) experiments on 2×10^{-3} M solutions of selected compounds in CH_2Cl_2 were conducted at room temperature using an EPSILON (Bioanalytical Systems, INC., West Lafayette, IN) electrochemical workstation. The electrochemical cell was placed in an argon-filled Vacuum Atmospheres dry-box. Tetrabutylammonium hexafluorophosphate (0.1 M solution in CH_2Cl_2) was used as the supporting electrolyte. CV data were obtained using a three component system consisting of a platinum working electrode, platinum wire auxillary electrode, and a glass encased non-aqueous silver/silver chloride reference electrode. The reference Ag/Ag^{+} electrode was monitored with the ferrocenium/ferrocene couple. IR compensation was achieved prior to each CV scan by

measuring the uncompensated solution resistance followed by incremental compensation and circuit stability testing. Background CV scans of the electrolyte solution were recorded before adding the analytes. The half-wave potentials ($E_{1/2}$) were determined as averages of the cathodic and anodic peak potentials of reversible couples and are referenced to the external FcH^+/FcH couple.[33]

2-Amino-6-bromo-1,3-diethoxycarbonylazulene, acetic-formic anhydride and 1,1'-diisocyanoferrocene were prepared according to literature procedures.[19, 34-35] The synthetic procedures leading up to ethynylferrocene constitute modified versions of the published syntheses involved in the preparation of this compound.[36] Other reagents were obtained from commercial sources and used as received.

I.3.2 Synthesis of Acetylferrocene (1.1)

Acetyl chloride (0.942 g, 12.0 mmol) was added to a solution of ferrocene (2.046 g, 11.00 mmol) in 10 mL dichloromethane and the resulting mixture was immediately cooled to 0°C. Aluminum(III) chloride (1.467 g, 11.00 mmol) was added in small increments over a 20 minute period. The reaction was allowed to stir for 2 hr while warming to room temperature. The reaction was quenched by slowly adding 4×0.5 mL portions of cold deionized water. An additional 3 mL of cold water was added and the contents were transferred into a separatory funnel. The organic layer was collected and the aqueous layer was extracted with 50 mL dichloromethane. The combined organic fractions were washed with 50 mL brine and dried over anhydrous Na_2SO_4. The drying agent was filtered off and the filtrate was concentrated via rotatory evaporation under vacuum. The residue was subjected to column chromatography on silica using 9:1 hexanes/ethyl acetate as eluent. An orange band was collected. The product was dried at 10^{-2} Torr to afford an 89% yield of **1.1** (2.23 g, 9.78 mmol) as a red-orange powder. ^{1}H NMR (400MHz, $CDCl_3$, 25°C): δ 2.40 (s, 3H, CH_3), 4.22 (s, 5H, C_5H_5), 4.51 (s, 2H, C_5H_4), 4.78 (s, 2H, C_5H_4) ppm.

I.3.3 Synthesis of 1-chlorovinylformylferrocene (1.2)

Phosphorous(V) oxychloride (3.92 g, 25.6 mmol) was added to a flask containing 2.34 mL of cold (0 °C) DMF and the resulting solution was stirred for 30 minutes at 0 °C while acquiring a red color.. The resulting red mixture was transerred to a flask containing a suspension of acetylferrocene (2.16 g, 9.47 mmol) in 2.34 mL of DMF at 0 °C over a 30-minute period. The reaction mixture stirred for 2 hrs at 0 °C. Then, 7.5 mL of diethyl ether was added and the mixture was stirred for an additional 20 minutes. Sodium acetate trihydrate (10.95 g, 80.49 mmol) was added to this cold mixture and it was vigorously stirred for 1 hr while warming

up to room temperature. The color of the reaction mixture turned from blue to purple to wine-red during this period.. After stirring for 3 additional hours, the deep red mixture was transferred into a separatory funnel. Deionized water (50 mL) was added and the mixture was extracted with diethyl ether until the organic extracts were colorless. The combined organic extracts were washed with 50 mL of saturated aqueous sodium bicarbonate and dried over anhydrous Na_2SO_4. The drying agent was filtered off and all solvent was removed from the filtrate under vacuum to afford an 81% yield of **1.2** (2.11 g, 7.68 mmol) as purple needles. ^{1}H NMR (400MHz, $CDCl_3$, 25°C): δ 4.26 (s, 5H, C_5H_5), 4.58 (s, 2H, C_5H_4), 4.77 (s, 2H, C_5H_4), 6.41 (s, 1H, C*H*), 10.3 (s, br, 1H, C*H*O) ppm.

I.3.4 Synthesis of ethynylferrocene (1.3)

1-Chlorovinylformylferrocene (1.00 g, 3.64 mmol) dissolved in 15 mL of dioxane was was heated to reflux in a side-armed round-bottom flask equipped with a reflux condencer. Then, 15 mL of boiling 1 N aqueous NaOH was added to the flask and refluxing was continued for 25 additional minutes. The mixture was then allowed to cool to room temperature, poured intoice,and neutralized to pH of 7 using 1 N aqueous HCl. After extraction with 100 mL of hexanes, the organic extract was separated, washed with 5 mL of saturated aqueous sodium bicarbonate, and dried over anhydrous Na_2SO_4 The drying agent was filtered off and the filtrate was concentrated on a rotary evaporator. The resulting residue was chromatographed on silica gel using 100% hexanes to collect an orange band. Solvent removal and drying of the product at 10^{-2} Torr afforded an 86% yield of **1.3** (0.655 g, 3.12 mmol) as orange microcrystals. ^{1}H NMR (400MHz, $CDCl_3$, 25°C): δ 2.71 (s, 1H, C*H*), 4.27 (s, 7H, C_5H_4 ,C_5H_5), 4.51 (s, 2H, C_5H_4) ppm.

I.3.5 Synthesis of 2-amino-1,3-diethoxycarbonyl-6-azulenylethynylferrocene (1.4)

An orange mixture of tetrakis(triphenylphosphine)palladium(0) (0.157 g, 0.136 mmol), copper(I) iodide (0.052 g, 0.273 mmol), triphenylphosphine (0.065 g, 0.246 mmol), 2-amino-6-bromo-1,3-diethoxycarbonylazulene (0.500 g, 1.36 mmol), and ethynylferrocene (0.301 g, 1.43 mmol) in 150 mL of toluene was treated with 6 mL of freshly distilled triethylamine via syringe. The resulting mixture was allowed to stir for 21 hrs. The red reaction mixture was poured into 150 mL of 10% aqueous NH_4Cl and the organic layer was separated. The aqueous layer was extracted with dichloromethane (2×75 mL). The combined organic fractions were washed with 150 mL of deionized H_2O, dried over anhydrous $MgSO_4$, and filtered through a short bed of Celite. The resulting solution was concentrated on a rotary evaporator to give a residue that was subjected to column chromatography on silica gel (10:1 hexanes/ethyl acetate). A red band was collected. All solvent was removed *in vacuo* to afford a 97% yield of **1.4** (0.660 g, 1.33 mmol) as a red powder. MP: 178-182°C. ^{1}H NMR (400MHz, $CDCl_3$, 25°C): δ 1.49 (t, 6H, CH_3, $^3J_{HH}$ = 8 Hz), 4.28 (s, 5H, C_5H_5), 4.32 (t, 2H, C_5H_4, 2 Hz), 4.48 (q, 4H, CH_2, 8 Hz), 4.56 (t, 2H, C_5H_4, 2 Hz), 7.72 (d, 2H, $H^{5,7}$, 12 Hz), 7.84 (s, 2H, NH_2), 9.02 (d, 2H, $H^{4,8}$, 12 Hz) ppm. $^{13}C\{^1H\}$ NMR (100.6MHz, $CDCl_3$, 25°C): δ 14.87 (CH_3), 60.14 (CH_2), 64.76, 69.58, 70.31, 71.88 (*cyclopentadienyl C atoms*), 89.83, 92.27 (*alkyne C atoms*), 100.68, 129.09, 130.15, 135.34, 145.45, 162.50 (aromatic C), 166.66 (CO_2R) ppm. UV-Vis (CH_2Cl_2): λ_{max}(log ε) 499 nm (3.34), 437 nm (3.67), 344 nm (3.98), 249 nm (3.87).

I.3.6 Synthesis of 2-formamido-1,3-diethoxycarbonyl-6-azuleneferrocenyl acetylene (1.5)

A red solution of 2-amino-1,3,-diethoxycarbonyl-6-azuleneferrocenylacetylene (0.660 g, 1.33 mmol) in 100 mL of dichloromethane was treated with formic acid (25 mL) and acetic-formic anhydride (8.5 mL) while being vigorously stirred.. The resulting dark purple reaction

mixture was stirred for 2 hrs and then quenched with 10% aqueous Na_2CO_3. The organic layer was separated and the light purple aqueous layer was extracted with dichloromethane (2×75 mL). The organic fractions were combined, washed with 150 mL of deionized H_2O, and dried over anhydrous Na_2SO_4. The drying agent was filtered off and the filtrate was concentrated via rotary evaporation. The product was recrystallized from dichloromethane/pentane to afford a 98% yield of **1.5 (**0.684 g, 1.31 mmol) as a purple powder. ^{1}H NMR (400MHz, $CDCl_3$, 25°C): δ 1.47 (t, 6H, CH_3, $^3J_{HH}$ = 7 Hz), 4.30 (s, 5H, C_5H_5), 4.39 (s, 2H, C_5H_4), 4.48 (q, 4H, CH_2, 7 Hz), 4.61 (s, 2H, C_5H_4), 7.84 (d, 2H, $H^{5,7}$, 12 Hz), 8.66 (s, br, 1H, N*H*), 9.25 (d, 2H, $H^{4,8}$, 12 Hz), 10.26 (s, br, 1H, CH*O*) ppm. UV-Vis (CH_2Cl_2): λ_{max}(log e) 537 nm (3.82), 419 nm (4.34), 351 nm (4.55), 348 nm (4.55), 250 nm (4.33), 228 nm (4.34).

I.3.7 Synthesis of 2-isocyano-1,3-diethoxycarbonyl-6-azuleneferrocenyl acetylene (1.6)

A cold (0° C) purple solution of 2-formamido-1,3,-diethoxycarbonyl-6-azuleneferrocenylacetylene (0.265 g, 0.506 mmol) and 1 mL of triethylamine in 30 mL of dichloromethane was treated via cannula with a cold (0 °C) solution of triphosgene (0.165 g, 0.556 mmol) in 25 mL of dichloromethane . Gas evolution was observed as the reaction mixture changed from purple to blue-green over the course of a minute. After 15 minutes of stirring, the reaction mixture was quenched with 25 mL 10% aqueous Na_2CO_3. The organic layer was separated and the aqueous layer was extracted with dichloromethane (2×50 mL). The combined organic fractions were washed with 50 mL of deionized H_2O and dried over anhydrous Na_2SO_4. The drying agent was filtered off and the filtrate was concentrated via rotary evaporation. The residue was passed through a plug of neutral alumina using neat dichloromethane. Recrystallization from dichloromethane/pentane afforded a 71% yield of **1.6** (0.181 g, 0.358 mmol) as a green powder. MP: decomposes at 150 °C. FTIR (CH_2Cl_2): ν_{CN}

2125 cm^{-1}. ^1H NMR (400MHz, $CDCl_3$, 25°C): δ 1.52 (t, 6H, CH_3, $^3J_{HH}$ = 8 Hz), 4.31 (s, 5H, C_5H_5), 4.45 (t, 2H, C_5H_4, 2 Hz), 4.52 (q, 4H, CH_2, 8 Hz), 4.65 (t, 2H, C_5H_4, 2 Hz), 7.90 (d, 2H, $H^{5,7}$, 11 Hz), 9.64 (d, 2H, $H^{4,8}$, 11 Hz) ppm. UV-Vis (CH_2Cl_2): λ_{max}(log ε) 577 nm (3.90), 411 nm (4.42), 348 nm (4.44), 289 nm (4.22), 237 nm (4.44). MS (ESI+): 506.1 $[M-H]^+$.

I.3.8 Synthesis of bis(2-isocyano-1,3-diethoxycarbonyl-6-azuleneferrocenyl acetylene)Palladium(II) iodide (1.7)

A mixture containing 2-isocyano-1,3-diethoxycarbonyl-6-azuleneferrocenylacetlylene (0.120 g, 0.237 mmol) and palladium(II) iodide (0.043 g, 0.119 mmol) in 30 mL of dichloromethane was stired for 105 minutes at room temperature. The resulting forest green mixture was then filtered through a plug of Celite. The filtrate was concentrated via rotary evaporation and the residue was recrystallized from dichloromethane/pentane to afford a 42% yield of **1.7** (0.069 g, 0.050 mmol) as purple microcrystals. FTIR (CH_2Cl_2): ν_{CN} 2198 cm^{-1}. ^1H NMR (400MHz, $CDCl_3$, 25°C): δ 1.61 (t, 6H, CH_3, $^3J_{HH}$ = 8 Hz), 4.33 (s, 5H, C_5H_5), 4.48 (t, 2H, C_5H_4, 2 Hz), 4.59 (q, 4H, CH_2, 8 Hz), 4.68 (t, 2H, C_5H_4, 2 Hz), 7.96 (d, 2H, $H^{5,7}$, 12 Hz), 9.78 (d, 2H, $H^{4,8}$, 12 Hz) ppm.

I.3.9 Preliminary small scale synthesis of hexakis(2-isocyano-1,3-diethoxycarbonyl-6-azuleneferrocenyl acetylene)chromium(0 and I) (1.8a and 1.8b)

A solution of bis(naphthalene)chromium(0) (0.018 g, 0.058 mmol) in 3 mL of THF was added dropwise to a solution of 2-isocyano-1,3,-diethoxycarbonyl-6-azuleneferrocenylacetylene (0.175 g, 0.346 mmol) in 10 mL of THF at room temperature. After stirring for *ca.* 15 hrs, 40 mL of heptane was added to the reaction mixture to crashed out the product, which was filtered off, washed with heptane, and dried at 10^{-2} Torr to afford a 78% yield of **1.8a** (0.139 g, 0.045 mmol) as a dark green-brown powder. FTIR (CH_2Cl_2): ν_{CN} 1967 cm^{-1}.

The above dark green-brown solid was dissolved in 50 mL of dichloromethane. A solution of silver hexafluoroantimonate (0.012 g, 0.036 mmol) in 20 mL of dichloromethane was added to this solution via cannula at room temperature. The reaction mixture was stirred for 1hr while acquiring a light green color. The mixture was then passed through a short plug of Celite. The Celite was washed with dichloromethane until the washings were colorless. The filtrate was concentrated under vacuum and layered with pentane for recrystallization to afford a 62% yield of **1.8b** (0.066 g, 0.020 mmol) as a dark green microcrystalline powder. FTIR (CH_2Cl_2): ν_{CN} 2058 cm^{-1}.

I.3.10 Synthesis of 1,1'-diisocyanoferrocenebis(pentamethylcyclopentadienyl-dichloroiridium(III)) (1.9)

A solution of 1,1'-diisocyanoferrocene (0.045 g, 0.193 mmol) and bis(pentamethylcyclopentadienyldichloroiridium(III)) (0.154 g, 0.193 mmol) in 50 mL of dichloromethane was stirred for 2 hrs at room temperature. About 25 mL of the solvent was removed under vacuum and the product was then crashed out with about 50 mL of pentane. The resulting yellow-orange solid was dried and recrystallized from dichloromethane/heptane to afford a 76% yield of **1.9** (0.100 g, 0.097 mmol) as golden microcrystals. FTIR (CH_2Cl_2): ν_{CN} 2159 (s), 2181 cm^{-1}(s). FTIR (nujol): ν_{CN} 2147 (s), 2176 (w) cm^{-1}. ^1H NMR (400 MHz, $CDCl_3$, 25 °C): δ 1.86 (s, 15H, $C_5(CH_3)_5$), 4.45 (t, 2H, C_5H_4, 4 Hz), 4.76 (t, 2H, C_5H_4, 4 Hz) ppm. MS (ESI+): 997.1 $[M\text{-}Cl]^+$.

I.4. Results and Discussion

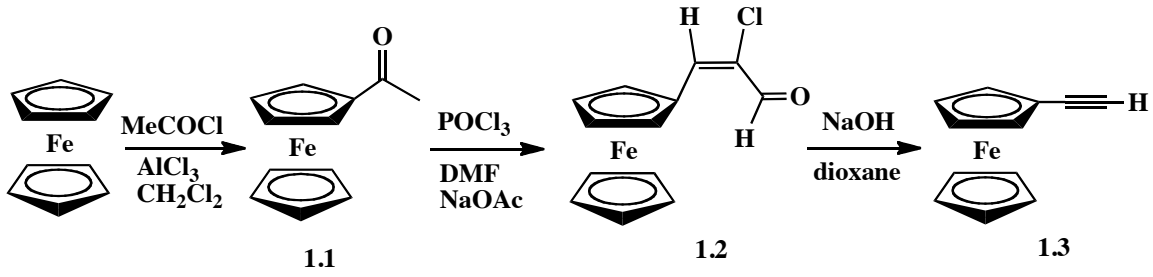

Scheme I.2. Synthesis of ethynylferrocene adopted from Polin and co-workers.[36]

The synthesis of the novel isocyanide ligand **1.6** from ferrocene begins with the preparation of ethynylferrocene **1.3** via the modified procedures of Polin and co-workers (Scheme I.2).[36] It should be noted that the modifications of the procedures for the reaction steps summarized in Scheme I.2 provide somewhat higher yields of the products compared to the corresponding original syntheses.[36]

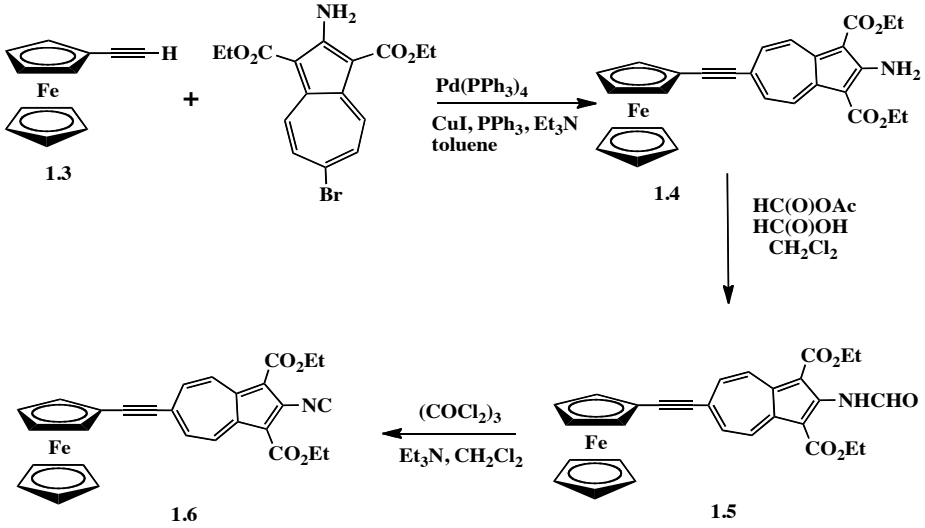

Scheme I.3. Synthesis of the isocyanide ligand featuring ferrocenyl and azulenyl moieties.

Scheme I.3 illustrates the synthetic pathway for the preparation of the 2-isocyanoazulene derivative **1.6** that involves Sonogashira coupling of ethynylferrocene to the azulenic moiety as the critical step. This Sonogashira cross-coupling affords the ferrocenyl/azulenyl-substituted acetylene **1.4** in a nearly quantitative yield. The brick-red compound **1.4** contains a primary amine functionality that undergoes facile formylation with excess acetic-formic anhydride and formic acid to provide the corresponding formamide in a yield of 97%. Following recrystallization, the formamide is subjected to dehydration with triphosgene and triethylamine to give the isocyanide ligand **1.6** in a 71% yield. The dehydration process is accompanied by an obvious color change and can be conveniently monitored by TLC and IR spectroscopy. Unlike its formamide precursor, the isocyanide **1.6** can be purified by column chromatography on neutral alumina. The presence of the isocyanide group in **1.6** is unambiguously indicated by the characteristic ν_{CN} band at 2125 cm^{-1} observed in the FTIR spectrum of this compound.

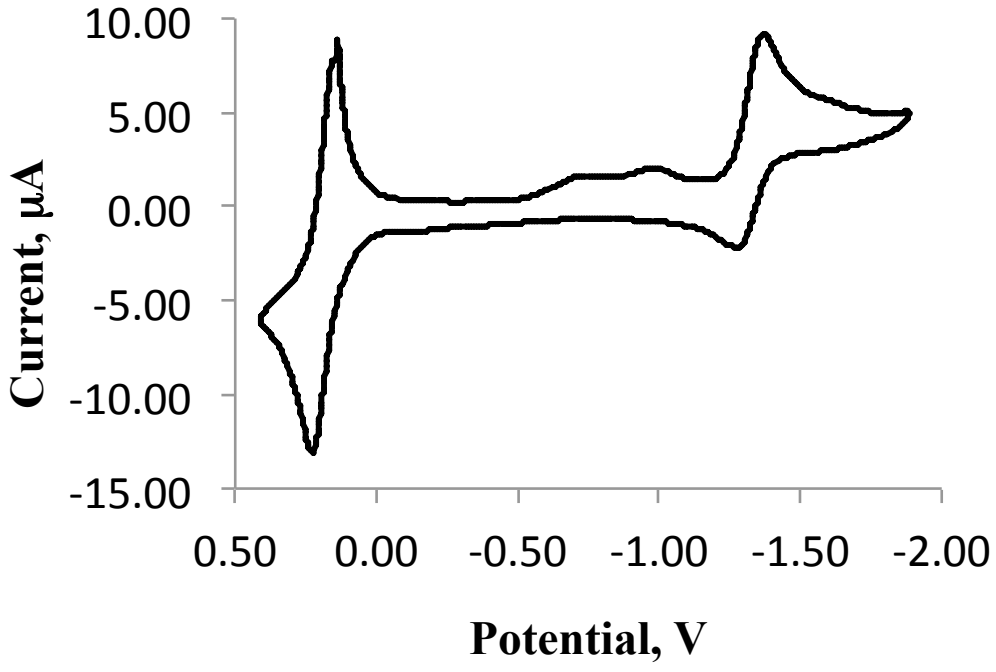

Figure I.5. Cyclic voltammogram of 1.6 in CH_2Cl_2 referenced to the FcH/FcH^+ couple. Scan rate = 100 mV/sec.

The cyclic voltammogram (CV) of a solution of **1.6** is shown in Figure I.5. This CV profile exhibits two main features. the wave at $E_{1/2}$ = + 0.183 V corresponds to the fully reversible oxidation of the iron center of the ferrocenyl moiety. The positive $E_{1/2}$ value for this process indicates that the substituted ethynyl moiety in **1.6** has a slightly electron-withdrawing effect with respect to the ferrocenyl fragment. The feature with $E_{1/2}$ = -1.32 V reflects the largely reversible one-electron reduction of the azulenic portion of the compound. Thus, the scaffold of **1.6** can be oxidized and reduced without compromising its structural integrity, at least on the electrochemical time scale. It is interesting to compare the redox behavior of **1.6** with those of ethynylferrocene **1.3** and 2-isocyano-1,3-diethoxycarbonylazulene, which are the building blocks used to assemble **1.6**.

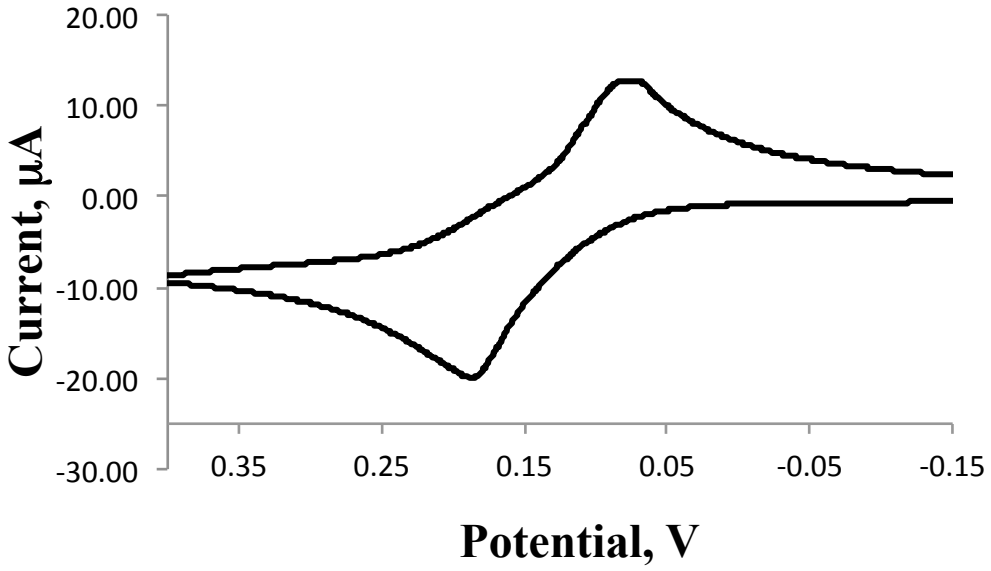

Figure I.6. Cyclic voltammogram of 1.3 in CH_2Cl_2 referenced to the FcH/FcH^+ couple. Scan rate = 100 mV/sec.

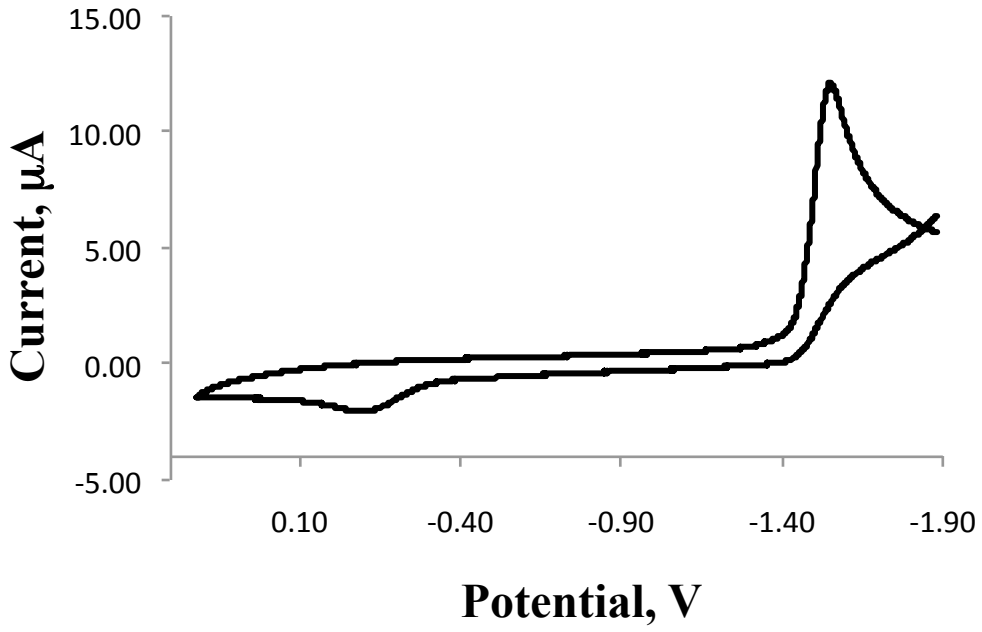

Figure I.7. Cyclic voltammogram of 2-isocyano-1,3-diethoxycarbonylazulene in CH_2Cl_2 referenced to the FcH/FcH^+ couple. Scan rate = 100 mV/sec.

Figure I.6 illustrates the cyclic voltammogram for **1.3** recorded under the conditions identical to those used to obtain the CV for **1.6**. The $E_{1/2}$ for the oxidation of **1.3** is +0.136 V. This value is 45 mV less positive than the corresponding half-wave potential observed for the oxidation of **1.6**. This indicates that (a) the ferrocenyl and azulenyl π-systems in **1.6**, separated by the –C≡C– linker, are mutually electronically coupled and (b) the 6-azulenyl moiety in **1.6** is somewhat electron-withdrawing with respect to the ferrocenylethynyl fragment. Figure I.7 displays the cyclic voltammogram for 2-isocyano-1,3-diethoxycarbonylazulene. Unlike **1.6**, this compound undergoes an irreversible one-electron reduction at $E_{p,c}$ = -1.55 V vs. FcH/FcH^+ in CH_2Cl_2. The marked difference in the reduction reversibility between **1.6** and 2-isocyano-1,3-diethoxycarbonylazulene clearly indicates that the π-system of the ferrocenylethynyl moiety in **1.6** stabilizes the azulene-based radical anion forming upon the reduction of **1.6**. Thus, compound **1.6** incorporates both donor (ferrocenyl) and acceptor (azulenyl) functionalities. An

internal charge transfer involving these functional groups may be represented by the zwitterionic resonance structure shown in Figure I.8.

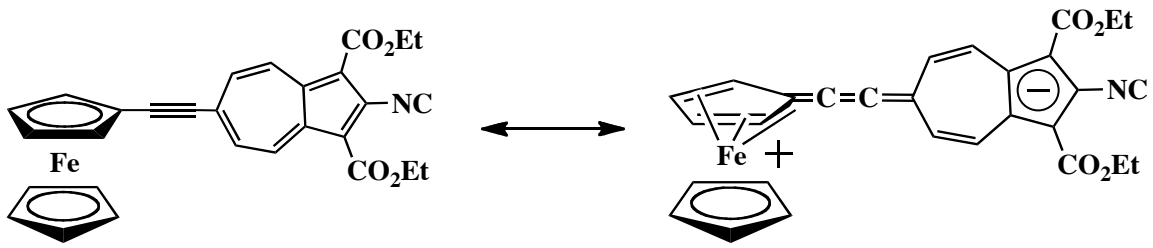

Figure I.8. A zwitterionic resonance form of compound 1.6.

Similar to other aryl isocyanides, compound **1.6** reacts with palladium(II) iodide in a 2:1 molar ratio to yield the corresponding complex *trans*-PdI_2(**1.6**)$_2$ (compound **1.7**). Upon complexation of **1.6** to Pd(II), the ν_{CN} band shifts to 2198 cm^{-1}, an increase of 75 cm^{-1} compared to the free isocyanide **1.6.** The rather high isocyanide stretching frequency observed for **1.7** suggests that the ligand **1.6** behaves primarily as a σ-donor in the complex.

Preliminary small-scale experiments indicate that treatment of bis(naphthalene)chromium(0), a storable source of atomic Cr,[37] with 6 equivalents of **1.6** under O_2- and H_2O-free conditions afforded the green-brown, zero-valent homoleptic complex **1.8a** (Scheme I.4). This species can be oxidized with one equivalent of $Ag^+[SbF_6]^-$ to give light green, low-spin d^5 complex **1.8b** (Scheme I.4). The transformations **1.6 → 1.8a → 1.8b** can be conveniently followed by FTIR spectroscopy in the ν_{CN} stretching region (Figures I.9, I.10, and I.11). Indeed, upon coordination of **1.6** to the Cr(0) center to form **1.8a**, the ν_{CN} value decreases from 2125 to 1967 cm^{-1} due to the substantial extent of back-bonding interaction within the electron-rich complex **1.8a**. On the other hand, oxidation of **1.8a** is accompanied by a decrease

in the extent of backbonding, which is reflected by the 91 cm^{-1} shift of ν_{CN} to higher energy upon proceeding from **1.8a** to **1.8b**.

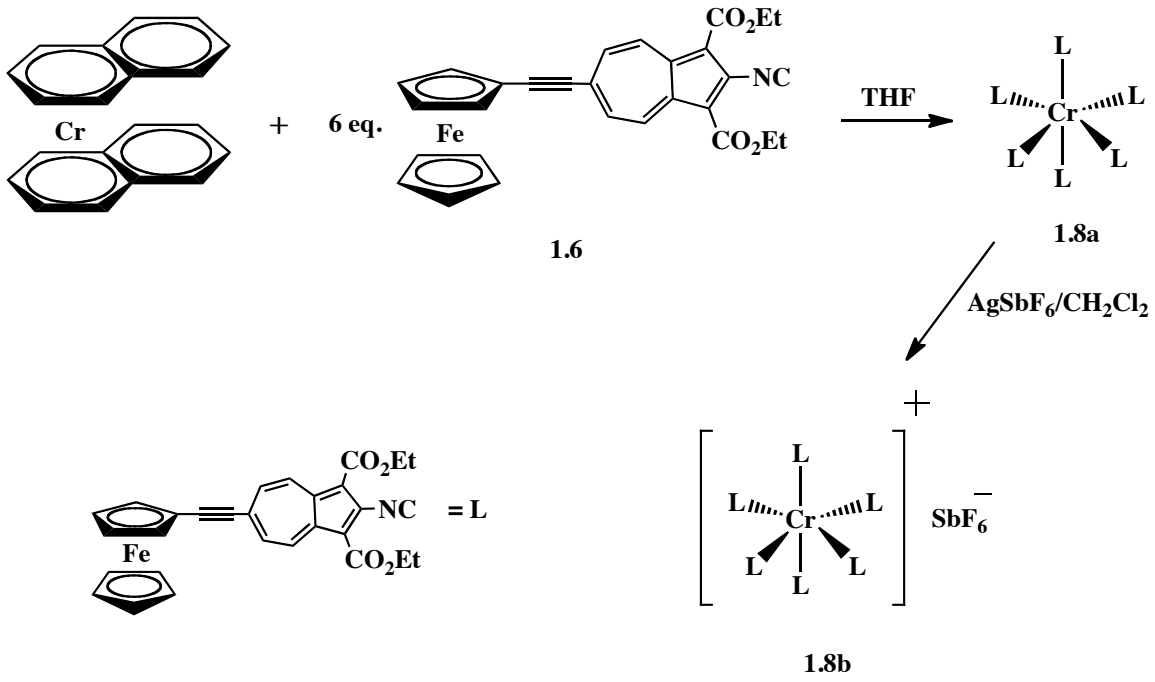

Scheme I.4. Preliminary syntheses of neutral and cationic homoleptic complexes of compound 1.6.

The above FTIR observations correlate well with several other studies of homoleptic isocyanide complexes of chromium published by the Barybin group.[1,16,21,38] Once greater quantities of the pure paramagnetic, low-spin d^5 complex **1.8b** are available, this species will be subject to detailed ^1H, ^{13}C, and ^{14}N NMR studies to gain insight into the mechanism and extent of the unpaired electron spin delocalization from the Cr(I) center into the entire π-system of the ligand **1.6**.[21,34]

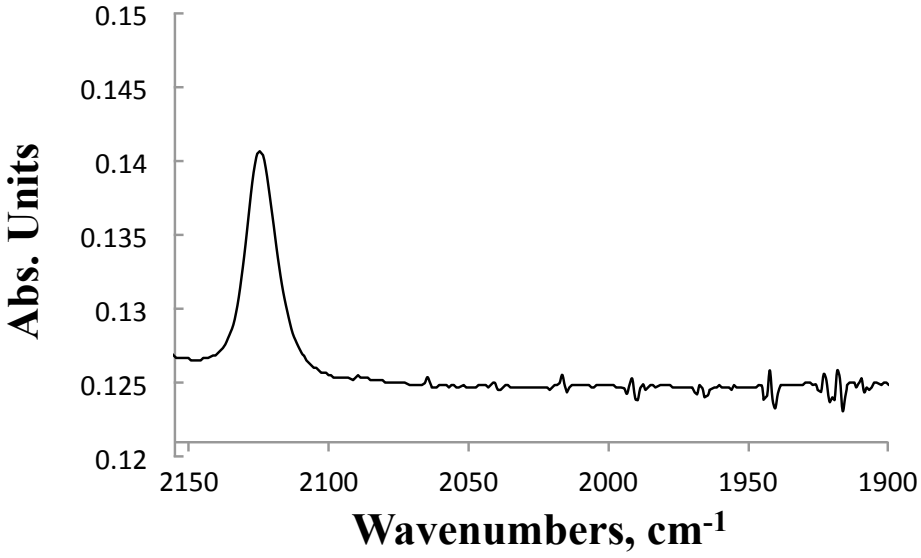

Figure I.9. FTIR spectrum of compound 1.6 in CH_2Cl_2 at 25 °C.

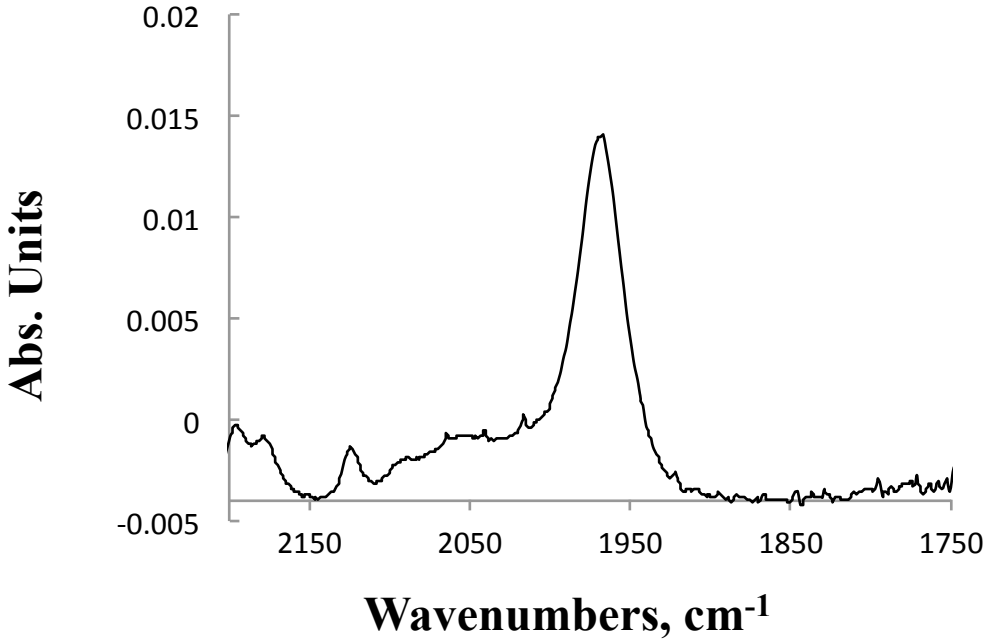

Figure I.10. FTIR spectrum of compound 1.8a in CH_2Cl_2 at 25 °C.

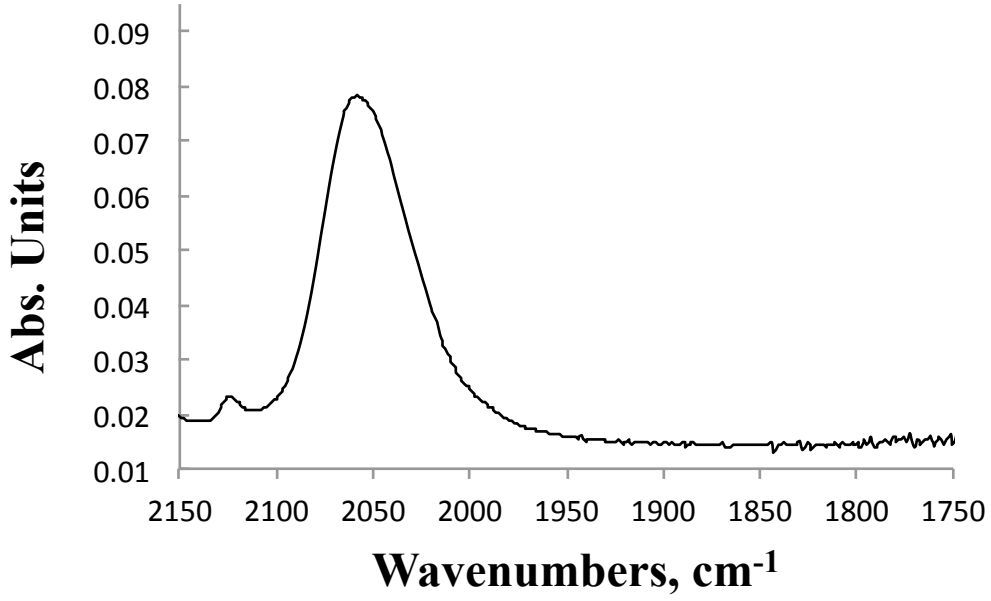

Figure I.11. FTIR spectrum of compound 1.8b in CH_2Cl_2 at 25 °C.

The remainder of this Chapter is dedicated to the discussion of new coordination chemistry of 1,1'-diisocyanoferrocene, a ditopic redox-active building block that has been drawing increasing interest in the past few years .[22-25]

Scheme I.5 illustrates the complexation of 1,1'-diisocyanoferrocene with pentamethylcyclopentadienyliridium(III) dichloride dimer ($[Cp^*IrCl_2]_2$). One equivalent of 1,1'-diisocyanoferrocene was mixed with one equivalent of $[Cp^*IrCl_2]_2$ over the span of two hours in dichloromethane. The yellow-orange product, compound **1.9**, was precipitated with pentane and purified by recrystallization to provide a 76% yield.

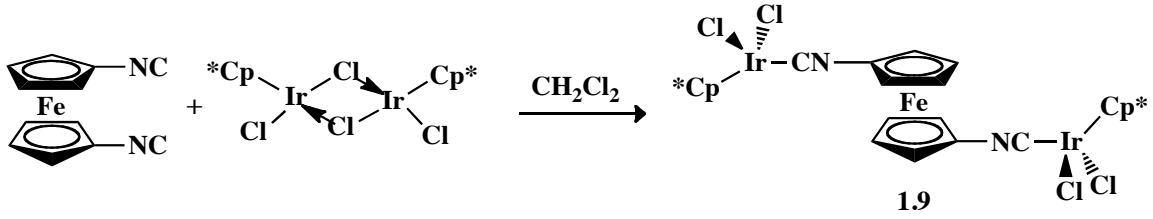

Scheme I.5. Synthesis of a bis(iridium(III)) complex of 1,1'-diisocyanoferrocene.

Interestingly, the FTIR spectrum of compound **1.9** in dichloromethane solution features two bands in the ν_{CN} stretching region (Figure I.12). This observation is certainly not consistent with the structure of **1.9** drawn in Scheme I.5 as only one isocyanide C-N stretching band would be expected. While the energy of the band at 2159 cm^{-1} is in the typical range for complexes of the type $Cp^*IrCl_2(CNR)$,[39] the second band occurring at 2181 cm^{-1} suggests isocyanide coordination to a less electron-rich Ir center. Repeated attempts to obtain solution IR spectra of **1.9** that included thorough protection of the samples from air and moisture invariably yielded the same results. The IR spectrum of **1.9** in the solid state (as a Nujol mull) is shown in Figure I.13. This spectrum features a very strong ν_{CN} band at 2147 cm^{-1} and a significantly weaker peak at 2176 cm^{-1}. Remarkably, the ^1H NMR spectrum of **1.9** in $CDCl_3$ at room temperature exhibits only one Cp* and one C_5H_4NC environments (Figure I.14). Thus, this compound probably exists in solution as a mixture of two isomers that interconvert rapidly on the NMR time scale but this interconversion is slow on the IR time scale. A reasonable pair of such interconverting isomers is shown in Figure I.15. One of these corresponds to the expected neutral structure of **1.9**, while the other constitutes an ionic substance with a chloride-bridged "Ir_2" cation and a Cl^- anion. The higher energy ν_{CN} band in the IR spectra of **1.9** would be consistent with such a cation. Interestingly, the ESI mass spectrum of **1.9** in the positive regime features a strong peak with m/z = 997.1. This peak has the largest m/z value and formally corresponds to the molecular ion of **1.9** that lost one Cl (i.e., the cationic portion of the ionic form of **1.9** in Figure I.15).

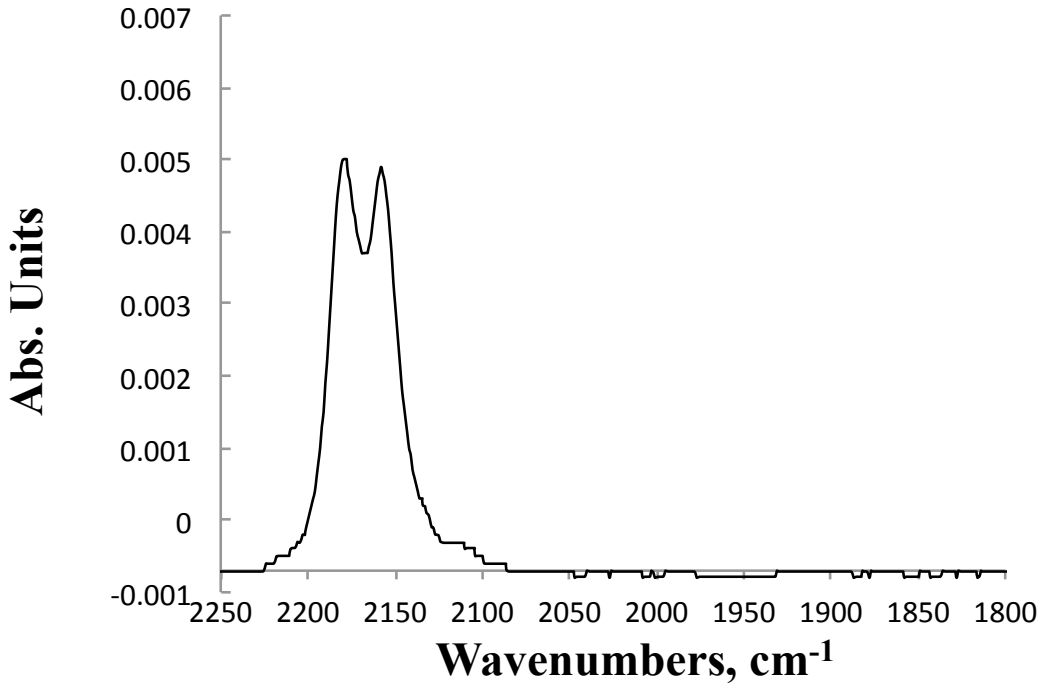

Figure I.12. FTIR spectrum of compound 1.9 in CH_2Cl_2 at 25 °C.

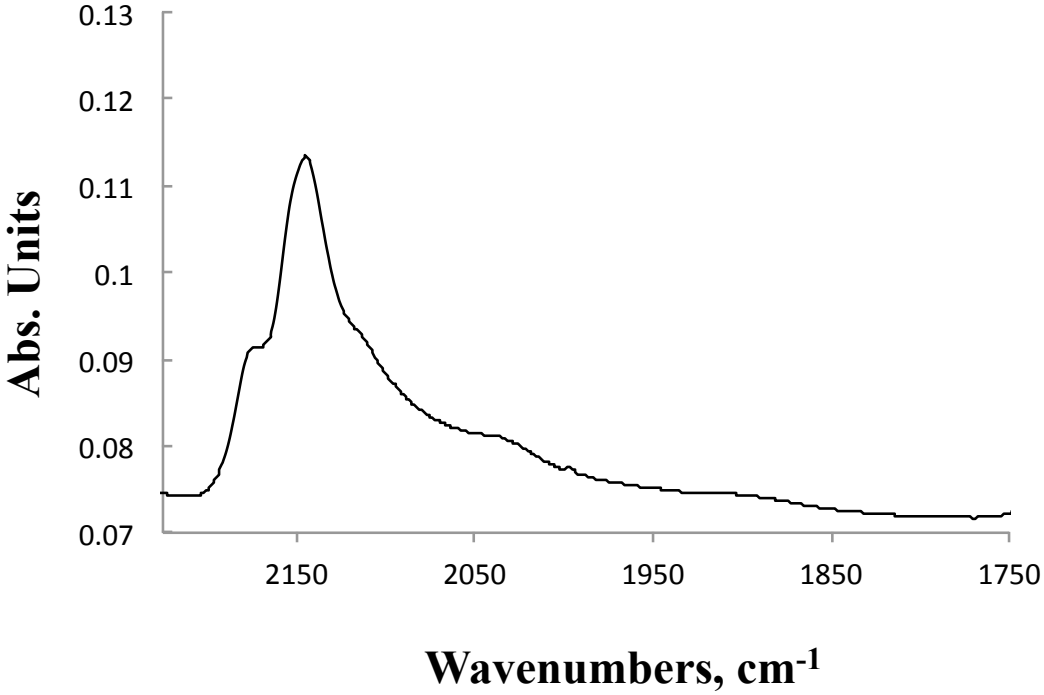

Figure I.13. FTIR spectrum of compound 1.9 in Nujol at 25 °C.

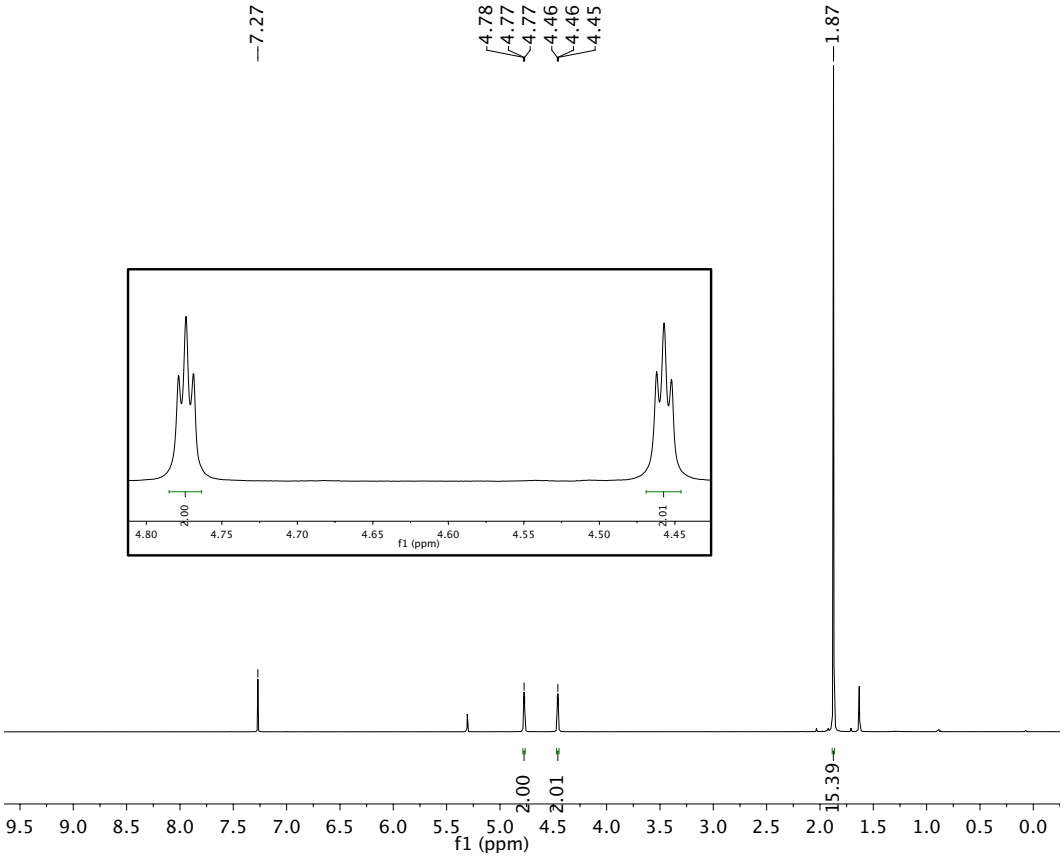

Figure I.14. ^{1}H NMR spectrum of compound 1.9 in $CDCl_3$ at 25 °C.

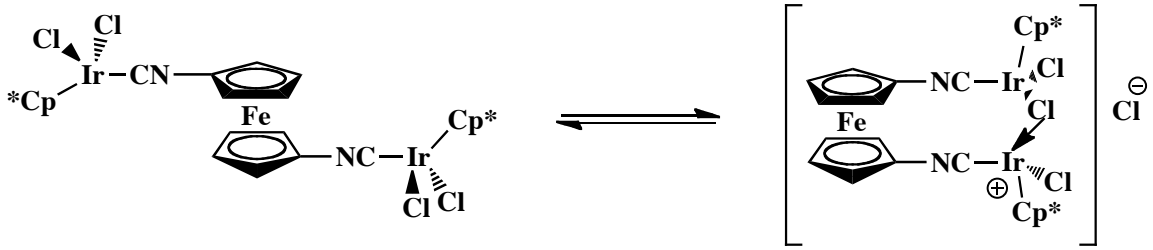

Figure I.15. Possible isomeric structures of 1.9 in solution.

A cyclic voltammogram of compound **1.9** recorded in dichloromethane is shown in Figure I.16. This CV features a reversible oxidation wave with $E_{1/2}$ = 0.543V that corresponds to the oxidation of Fe(II) to Fe(III) within the coordinated 1,1'-diisocyanoferrocene ligand. This $E_{1/2}$ potential is somewhat more positive than that observed for the oxidation of "free" 1,1-diisocyanoferrocene, which is consistent with the ν_{CN} data and also reflects the fact that the the diisocyanide ligand in **1.9** functions primarily as a σ-donor. In addition, the CV of **1.9** exhibits two irreversible oxidations at 1.019 V and 1.337 V that are likely Ir-based.

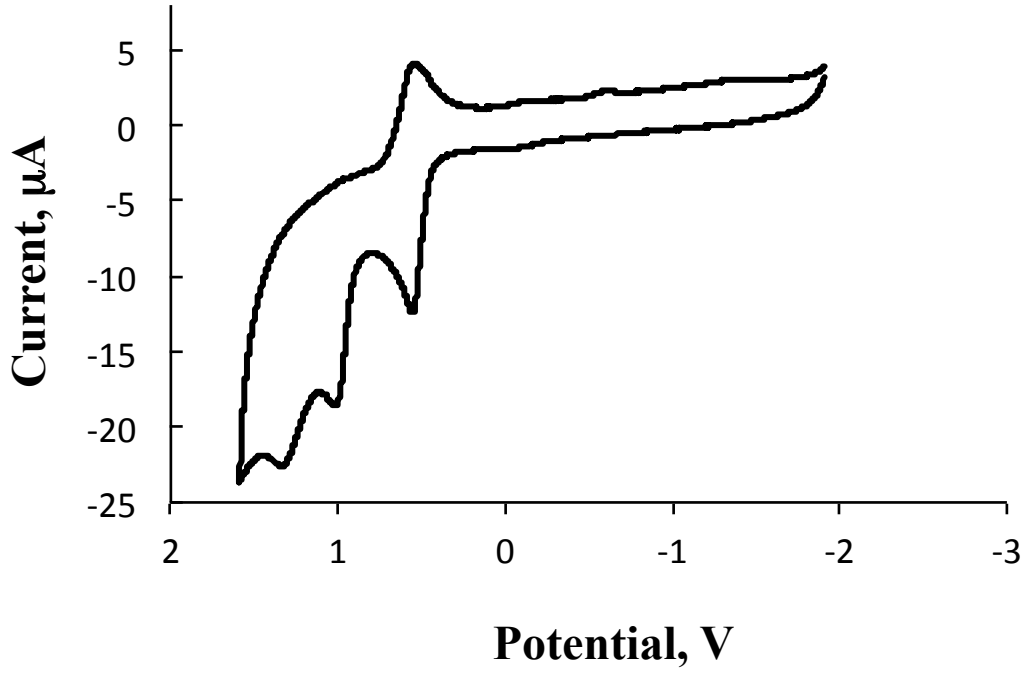

Figure I.16. Cyclic voltammogram of 1.9 in CH_2Cl_2 referenced to the FcH/FcH^+ couple. Scan rate = 100mV/sec.

Small crystals of compound **1.9** were grown by slow diffusion of pentane into its solution in dichloromethane. Repeated attempts to acquire X-ray diffraction data for these crystals indicated twinning complications. Nevertheless, a preliminary crystal structure of **1.9** was

obtained with the R-factor value around 10% (Figure I.17). While the quality of this X-ray structure is marginal at best at this point, it clearly indicates that this crystalline form of **1.9** features both isocyanide junctions in identical chemical environments and both Ir-centers carrying a pair of terminal chloride ligands. The C-N-C angles of 176° documented for **1.9** are quite similar to those observed for a few other bimetallic complexes of 1,1'-diisocyanoferrocene (Table I.1).

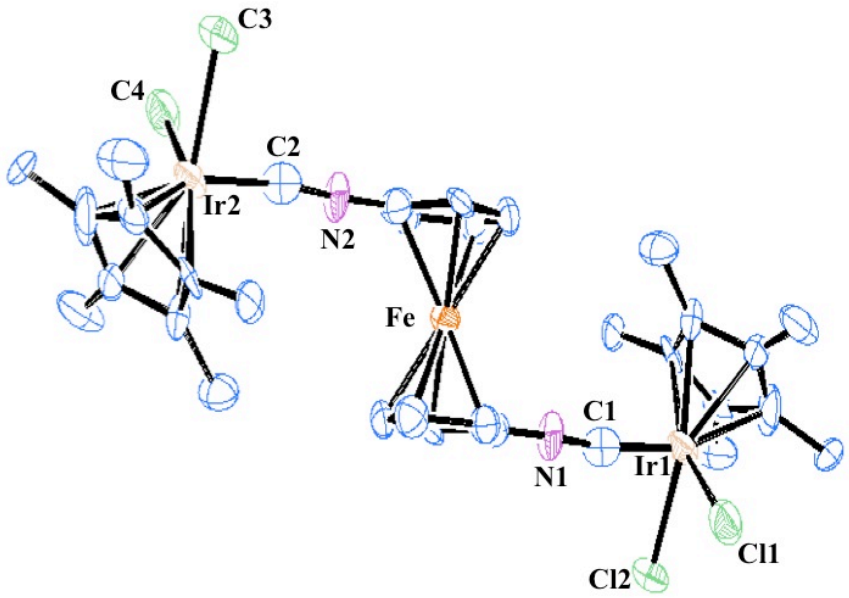

Figure I.17. Preliminary X-ray structure of compound 1.9.

Table I.1. C-N-C bond angles in bimetallic complexes of 1,1'-diisocyanoferrocene.[22-25]

Compound	C-N-C Bond Angle (°)
1.9	176.0
$[Cr(CO)_5]_2(\mu\text{-}(CNC_5H_4)_2Fe)$	170.2
$[AuCl]_2(\mu\text{-}(CNC_5H_4)_2Fe)$	178.9
$[Cu_2(\mu\text{-}(CNC_5H_4)_2Fe)_3]^{2+}$	176.9

I.5. Conclusions and Outlook

In this Chapter, the chemistry of the new nonbenzenoid aromatic isocyanide ligand **1.6** featuring both azulene (acceptor) and ferrocene (donor) moieties was introduced. This species can be reversibly oxidized and reduced, at least on the electrochemical time scale. The stable redox activity of **1.6** offers the possibility of electrochemical modification of its properties as a ligand (e.g., electron donor/acceptor characteristics). This will allow designing new redox-addressable substances and materials in the future. In particular, self-assembly of molecular films of **1.6** on various metal surfaces will be pursued and studied in the context of potential electronics and optical applications. The electron delocalization within the entire π-system of **1.6** will be studied by analyzing the ^{1}H, ^{13}C, and ^{14}N NMR spectra of its paramagnetic octahedral homoleptic complexes with Cr(I).

The new bis-iridium complex of 1,1'-diisocyanoferrocene described herein appears to exist in two interconverting isomeric forms, at least in the solution phase. Both of these forms are very attractive as building blocks for assembling either novel redox-active polymers or compact three-dimensional organometallic electron reservoirs containing the ferrocene moieties. In addition, synthesis and coordination and surface chemistry of the bis-(isocyanoazulenyl) ligand shown in Figure I.18 will be developed in the future.

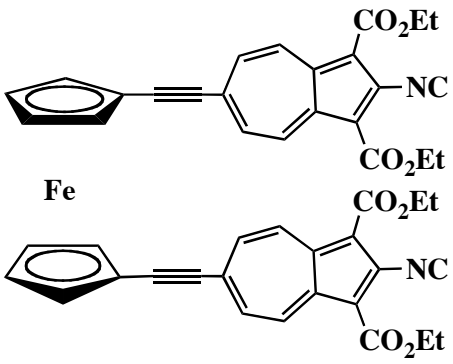

Figure I.18. Proposed redox active complex featuring two isocyanoazulenic motiffs.

I.6 References

1. Barybin, M. V.; Holovics, T. C.; Deplazes, S. F.; Lushington, G. H.; Powell, D. R.; Toryiama, M. *Journal of the American Chemical Society*. **2002**, *124*, 13668.
2. Singleton, E.; Oosthuizen, H. E. *Advances in Organometallic Chemistry*. **1983**, *22*, 209.
3. Treichel, P. M. *Advances in Organometallic Chemistry*. **1973**, *11*, 21.
4. Carnahan, E. M.; Protasiewicz, J. D.; Lippard, S. J. *Accounts of Chemical Research*. **1993**, *26*, 90.
5. Weber, L. *Angewandte Chemie, International Edition*. **1998**, *37*, 1515.
6. Sharma, V.; Piwnica-Worms, D. *Chemical Reviews*. **1999**, *99*, 2545.
7. Malatesta, L. *Progr. in Inorg. Chem. (F. Albert Cotton, editor. Interscience Publishers, Inc.)* **1959**, *1*, 283.
8. Yamamoto, Y. *Coordination Chemistry Reviews*. **1980**, *32*, 193.
9. Weber, L. *Angewandte Chemie, International Edition*. **1998**, *37*, 1515.
10. Hahn, F. E. *Angewandte Chemie*, **1993**, *105*, 681 (see also *Angewandte Chemie, International Edition*, **1993**, *32*, 650).
11. Chen, J.; Calvert, L. C.; Reed, M. A.; Carr, D. W.; Grubisha, D. S.; Bennett, D. W. *Chemical Physics Letters*, **1999**, *313*, 741.
12. Henderson, J. I.; Feng, S.; Bein, T.; Kubiak, C. P. *Langmuir*, **2000**, *16*, 6183.
13. Wagner, N. L.; Laib, F. E.; Bennett, D. W. *Inorganic Chemistry Communications*, **2000**, *3*, 87.
14. Hanack, M.; Kamenzin, S.; Kamenzin, L.; Subramanian, L. *Synthetic Metals*, **2000**, *11*, 93.

15. Knox, G. R.; Pauson, P. L.; Willison, D.; Solcaniova, E.; Toma, S. *Organometallics*, **1990**, *9*, 301.

16. Barybin, M. V. *Coordination Chemistry Reviews*, **2010**, *254*, 1240.

17. El-Shihi, T.; Sigmuller, F.; Hermann, R.; Carvalho, M. F. N. N.; Pomberio, A. J. L. *Journal of Organometallic Chemistry*, **1987**, *335*, 239.

18. El-Shihi, T.; Sigmuller, F.; Hermann, R.; Carvalho, M. F. N. N.; Pomberio, A. J. L. *Portugaliae Electrochimica Acta* , **1987**, *5*, 179.

19. van Leusen, D. V.; Hessen, B. *Organometallics*, **2001**, *20*, 224.

20. Heinze, K.; Schlenker, M. *European Journal of Inorganic Chemistry*, **2004**, 2974.

21. Holovics, T. C.; Deplazes, S. F.; Toriyama, M.; Powell, D. R.; Lushington, G. H.; Barybin, M. V. *Organometallics*, **2004**, *23*, 2927.

22. Siemeling, U.; Rother, D.; Bruhn, C.; Fink, H.; Weidner, T.; Trager, F.; Rothenberger, A.; Fenske, D.; Priebe, A.; Maurer, J.; Winter, R. *Journal of the American Chemical Society*, **2005**, *127*, 1102.

23. Siemeling, U.; Rother, D.; Bruhn, C. *Chemical Communications*, **2007**, 4227.

24. Siemeling, U.; Rother, D.; Bruhn, C. *Organometallics*, **2008**, *27*, 6419.

25. Siemeling, U.; Klapp, L. R. R.; Bruhn, C. *Zeitschrift fur Anorganische und Allgemeine Chemie*, **2010**, *636*, 539.

26. Shi, S. *Optoelectronic Properties of Inorganic Compounds* (*D. Max Roundhill and John P. Fackler, editors. Plenum Press)* **1999**.

27. Lambert, C.; Gaschler, W.; Zabel, M.; Matschiner, R.; Wortmann, R. *Journal of Organometallic Chemistry*, **1999**, *592*, 109.

28. Wolff, J. J.; Wortmann, R. *Advanced Physical Organic Chemistry*, **1999**, *32*, 121.

29. Whittall, I. R.; McDonagh, A. M.; Humphrey, M. G.; Samoc, M. *Advanced Organometallic Chemistry*, **1998**, *42*, 2911.

30. Long, N. J. *Angewandte Chemie*, **1995**, *107*, 37.

31. Hermann, R.; Pedersen, B.; Wagner, G.; Youn, J. H. *Journal of Organometallic Chemistry*, **1998**, *571*, 261.

32. Farrell, T.; Friedrichsen, T. M.; Malessa, M.; Haase, D.; Saak, W.; Asselberghs, I.; Wostyn, K.; Clays, K.; Persoons, A.; Heck, J.; Manning, A. R. *Journal of the Chemical Society, Dalton Transactions*, **2001**, 29.

33. Connelly, N. G.; Geiger, W. E. *Chemical Reviews*. **1996**, *96*, 877.

34. Holovics, T. H.; Robinson, R. E.; Weintrob, E. C.; Toriyama, M.; Lushington, G. H.; Barybin, M. V. *Journal of the American Chemical Society*, **2006**, *128*, 2300.

35. Krimen, L. I. *Organic Synthesis*. **1970**, *50*, 1.

36. Polin, J.; Schottenberger, H. *Organic Synthesis*. **1998**, *9*, 411.

37. Pomije, M. K.; Kurth, C. J.; Ellis, J. E.; Barybin, M. V. *Organometallics*. **1997**, *16*, 3582.

38. Robinson, R. E.; Holovics, T. C.; Deplazes, S. F.; Powell, D. R.; Lushington, G. H.; Thompson, W. H.; Barybin, M. V. *Organometallics*. **2005**, *24*, 2386.

39. Suzuki, H.; Tajima, N.; Tatsumi, K.; Yamamoto, Y. *Chemical Communications*. **2000**, 1801.

CHAPTER II

II. Chemistry of a Linear Symmetric π-Linker Featuring Isocyanide Termini and Two Azulenic Moieties Separated by an Acetylene Spacer

II.1. Introduction

The azulenic framework constitutes an edge sharing combination of 5-and 7-membered sp^2-carbon rings. This motif occurs naturally as a defect in carbon nanotubes and is believed to be responsible for enhancing conductivity of these nanostructures.[1] Recently, the Barybin group has become engaged in the design of linear 2,6-azulenic pi-bridges for future nanotechnological applications.[2] The general structure of the targeted systems is illustrated in Figure II.1. The π^* system of the azulenic unit(s) in this design is exceptionally well suited for supporting charge delocalization between the electron-rich termini. Depending on the nature of the metal termini, the junction groups X could be isocyanides, thiolates, or carboxylates. It is important to note that for n =2, three different combinations of the azulenic moieties can be envisioned: two symmetric with 2,2'- or 6,6'-connectivities and one asymmetric with 2,6'-connectivity of the azulenic fragments. The above three biazulenic bridges will have fundamentally very different electron delocalization and transport profiles as well as different responses to reductive doping. For example, reduction of the 6-6' biazulenic unit would force the biazulenyl moiety to adopt a more planar geometry,[3] which should have a profound effect on its absorption characteristics.

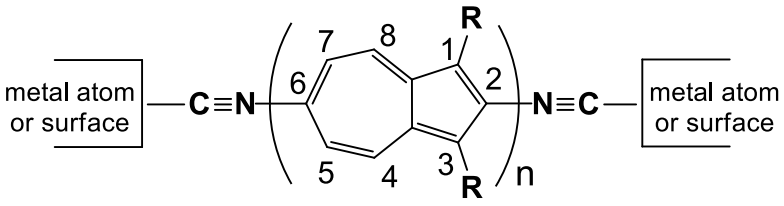

Figure II.1. A homologous series of linear diisocyanoarene linkers based on the nonbenzenoid 2,6-azulenic framework.[3]

While many reports involving 1,3-polyazulenes have been published to date,[4-5] the chemistry of biazulenic derivatives of any connectivity remains extremely scarce. Hanke and Jutz described the first synthesis of 6,6'-biazulene summarized in Scheme II.1.[6] This synthetic

protocol was inspired by Hafner's azulene synthesis,[7] affords 6,6-biazulene in a 30% yield, and does not rely on transition metal catalysis. Very limited information is available regarding functionalized 6,6'-biazulenes.Sugihara and coworkers synthesized a 2,2'-diamino-6,6'-biazulene derivative using a Miyaura borylation / Suzuki cross-coupling approach for a combined yield of 17%.[8] Last year, Barybin and coworkers published a dramatically improved, one-pot route to 2,2-diamino-1,1',3,3'-tetra(ethoxycarbonyl)-6,6'-biazulene and converted this species into the corresponding structurally characterized diisocyanide as summarized in Scheme II.2.[3]

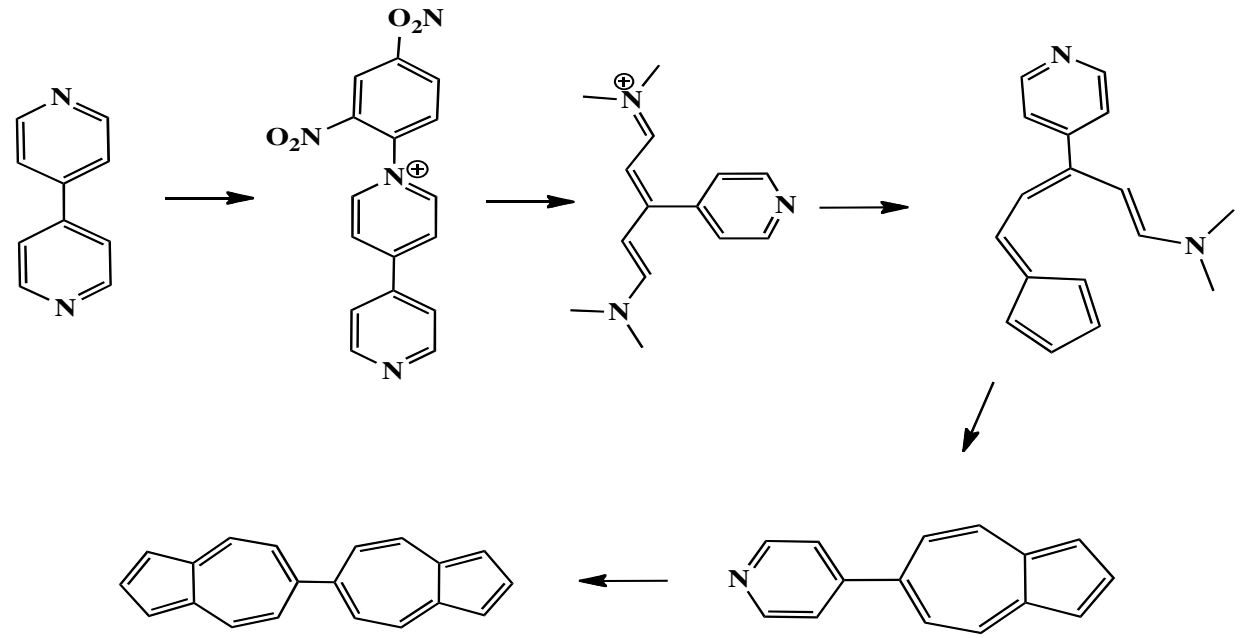

Scheme II.1. Hanke and Jutz's 6,6'-biazulene synthesis.[6]

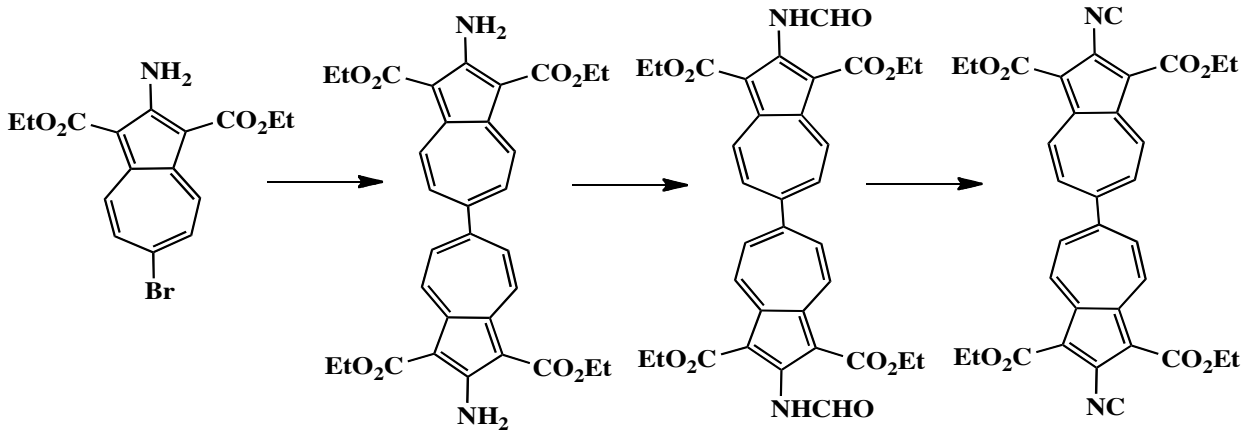

Scheme II.2. Synthesis of 2,2'-diisocyano 6,6'-biazulene.[3]

The 2,2'-diisocyano-6,6'-biazulene exhibits a reversible 2 electron reduction on the electrochemical time scale which makes it attractive for materials applications. The crystal structure of this ligand indicates an interplanar angle of approximately 67° due to crystal packing forces involving the tetraethoxycarbonyl substituents.[3] A way to make the linear 6,6'-biazulene more planar would be to introduce a spacer group between the seven membered rings.

Ito and coworkers synthesized the first 6,6'-biazulenylacetlyene ligand in a series of three steps beginning with azulene halogenated at the 6 position.[9] The coupling of 6-ethynylazulene with 6-bromoazulene was made possible with the use of Sonogashira conditions. The yields for each of the reactions were reported to be greater than 80%. Cyclic voltammetry studies by Ito showed that the 6,6'-biazulenylacetylene ligand forms a two electron closed shell dianion upon electrochemical reduction.[9] This discovery is indeed similar to the electrochemical data recently obtained in the Barybin group for the 6,6'-biazulene system and for the data supported by Hunig and Ort (Figure II.2).[3,10-11]

DFT studies of the 2,2'-6,6'-biazulene system indicated the formation of the singlet dianion upon reduction would lead to the shortening of the central C-C bond leading to double bond character with a 30 degree decrease in angle between the rings.[3]

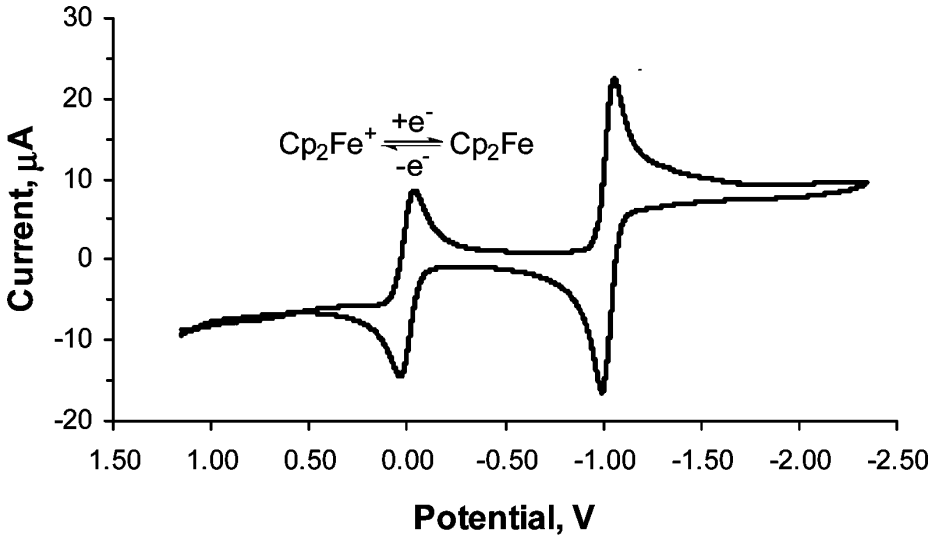

Figure II.2. Cyclic Voltammogram of 2,2'diisocyano 6,6'-biazulene.[3]

Recent efforts by the Barybin and Ito groups have opened the door for the construction of the linear 2,2'-diisocyano-6,6'-biazulenylacetylene electronic bridge.[3,9,12-14] This molecule is expected to be intriguing due to its coplanar character that should allow for better orbital overlap and enhanced conjugation. To the best of the author's knowledge, there is only one example of the non-benzenoid 6,6'-biazulene used for coordination to metals in a linear fashion.[3]

Aromatic benzenoid ligands have been used in the design of organogold complexes during the past two decades. These complexes exhibit rich luminescent properties and have the ability to form rigid polymer networks in some cases.[15-26] Luminescence of linear gold (I) complexes is thought by many to originate from aurophilic interactions. These secondary gold-gold interactions have the same bond energy as that of a hydrogen bond.[27-28] Strength of these

aurophilic interactions are enhanced by relativistic effects.[27-28] Organogold(I) complexes are considered to be emissive due to these strong aurophilic interactions. Up to this point, the only known examples of organogold(I) complexes seem to be mostly benzenoid in nature.

In this chapter, the synthetic scheme for the first 2,2'-diisocyano-6,6'-biazulenylacetylene is shown. Electrochemical studies on a series of ligands from the diisocyanide synthetic scheme will also be addressed. Synthesis of mono and bistungsten pentacarbonyl complexes using the 2,2'-diisocyano-6,6'-biazulenyl bridge will be discussed. Metal to bridge charge transfer results from the tungsten coordination studies will be compared to other known systems involving 1,4-diisocyanobenzene and 2,6-diisocyanoazulene.

The first examples of azulenic gold(I) architectures will be showcased. These Gold complexes exhibit luminescent emission due in part to aurophilic interactions. The subsequent synthesis of a large tetranuclear gold(I) rectangle of the 2,2'-diisocyano-6,6'-biazulenylacetylene linker will be addressed. The luminescent results of this complex will be compared with a few other complexes prepared in our lab.

II.2. Work Described in Chapter II

This Chapter is focused on the chemistry of a symmetric linear biazulenic pi-linker featuring two isocyanide termini and an ethynylene spacer between the azulenic moieties. Syntheses, characterization, redox behavior, complexation, and formation and properties of self-assembled monolayer films of this novel nonbenzenoid pi-bridge on metallic gold are discussed. In addition, some relevant coordination chemistry of a 2-isocyanoazulene derivative is presented as well

II.3. Experimental Section

II.3.1 General Procedures and Starting Materials

Unless specified otherwise, all operations were performed under an argon atmosphere of 99.5% argon further purified by passage through columns of activated BASF catalyst and molecular sieves. All connections involving the gas purification systems were made of glass, metal, or other materials impermeable to air. Solutions were transferred via stainless steel cannulas whenever possible. Standard Schlenk techniques were employed with a double manifold vacuum line. CH_2Cl_2 and Et_3N were distilled over CaH_2. THF and Toluene were distilled over Na/benzophenone. Following purification, all distilled solvents were stored under argon.

Solution infrared spectra were recorded on a PerkinElmer Spectrum 100 FTIR spectrometer with samples sealed in 0.1mm gas tight NaCl cells. NMR samples were analyzed using Bruker DRX-400 and Bruker Avance 500 spectrometers. ^{1}H and ^{13}C chemical shifts are given with reference to residual ^{1}H and ^{13}C solvent resonances relative to Me_4Si. UV-vis spectra were recorded in CH_2Cl_2 at 24°C using a CARY 100 spectrophotometer. Emission spectra were recorder in CH_2Cl_2 at 24°C using a CARY Eclipse fluorimeter.

Cyclic voltammetric (CV) and differential pulse voltammetric (DPV) experiments on 2 x 10^{-3}M solutions of selected compounds in CH_2Cl_2 were conducted at room temperature using an EPSILON (Bioanalytical Systems, INC., West Lafayette, IN) electrochemical workstation. The electrochemical cell was placed in an argon-filled Vacuum Atmospheres dry-box. Tetrabutylammonium hexafluorophosphate (0.1M solution in CH_2Cl_2) was used as the supporting electrolyte. CV data was recorded at room temperature using a three component system consisting of a platinum working electrode, platinum wire auxillary electrode, and a glass

encased non-aqueous silver/silver chloride reference electrode. The reference Ag/Ag^+ electrode was monitored with the ferrocenium/ferrocene couple. IR compensation was achieved prior to each CV scan by measuring the uncompensated solution resistance followed by incremental compensation and circuit stability testing. Background CV scans of the electrolyte solution were recorded before adding the analytes. The half-wave potentials ($E_{1/2}$) were determined as averages of the cathodic and anodic peak potentials of reversible couples and are referenced to the external FcH^+/FcH couple.[29]

Elemental analysis was carried out by Chemisar/Guelph Chemical Laboratories Ltd, Ontario, Canada.

Compounds 2-amino-6-bromo-1,3-diethoxycarbonylazulene[30], acetic formic anhydride[31], $[bis(dcpmAu_2$1,4'-diisocyanodurene$)]^{4+}4OTF^-$ [32], and $[dcpmAu_2$1,1'diisocyanoferrocene$)]^{2+}2OTF^-$ [33] were prepared according to literature procedures. Other reagents were obtained from commercial sources and used as received.

II.3.2 Synthesis of 2-amino-6-trimethylsiylylacetylene-1,3-diethoxycarbonylazulene (2.1)

Dichlorobis(triphenylphosphine)palladium(II) (0.143 g, 0.204 mmol), copper(I) iodide (0.052 g, 0.272 mmol), triphenylphosphine (0.071 g, 0.272 mmol), and 2-amino-6-bromo-1,3-diethoxycarbonylazulene (0.500 g, 1.36 mmol) were placed into a 250 mL single armed round bottom flask. 100 mL of toluene was added to the flask providing a yellow mixture. While stirring, 5 mL of freshly distilled triethylamine was added to the flask via cannula. Then, trimethylsiylylacetlyene (0.334 g, 3.4 mmol) was added to the flask via syringe. The reaction was allowed to stir for 4 hr. The dark red-orange reaction mixture was poured into 100 mL 10% NH_4Cl and the organics were collected. The aqueous layer was extracted with chloroform (2 x 50 mL). The combined organic extracts were washed with 100 mL H_2O. Dried over Na_2SO_4 and filtered. This solution was concentrated via rotary evaporation and subjected to silica gel column chromatography (5:1 hexanes/ethyl acetate) followed by solvent removal to afford a 86% yield of **2.1** (0.447 g, 1.16 mmol) as an orange powder. MP: 127-130°C. ^{1}H NMR ($CDCl_3$, 400MHz, 25°C): δ 0.29 (s, 9H, CH_3), 1.48 (t, 3H, CH_3, $^3J_{HH}$ = 8 Hz), 4.46 (q, 4H, CH_2, $^3J_{HH}$ = 8 Hz), 7.69 (d, 2H, $H^{5,7}$, $^3J_{HH}$ = 12 Hz), 7.87(s, br, 2H, NH_2), 8.99(d, 2H, $H^{4,8}$, $^3J_{HH}$ = 12 Hz) ppm.

II.3.3 Synthesis of 2-amino-6-ethynyl-1,3-diethoxycarbonylazulene (2.2)

2-amino-6-trimethylsiylylacetylene-1,3,-diethoxycarbonylazulene (0.447 g, 1.16 mmol) was placed into a 250 mL round bottom flask. 30 mL of THF was added to dissolve the powder. While stirring, 13.5 ml of freshly distilled N,N'-dimethylformamide was added to the flask followed by the addition of a potassium fluoride/DI H_2O (0.271 g, 4.66 mmol, 2.5 mL) solution. The reaction was allowed to stir for 2 hr. The dark red reaction mixture was poured into 300 mL of DI H_2O. The reacton mixture was extracted with hexanes (3 x 100mL) and dried over Na_2SO_4. This was then filtered and the solvent was removed via rotary evaporation to afford a 70% yield

of **2.2** (0.253 g, 0.813 mmol) as a red-brown powder. MP: 125°C dec. ^{1}H NMR ($CDCl_3$, 400MHz, 25°C): δ 1.50 (t, 3H, CH_3, $^{3}J_{HH}$ = 7 Hz), 3.27 (s, 1H, C*H*), 4.48 (q, 4H, CH_2, $^{3}J_{HH}$ = 7 Hz), 7.70 (d, 2H, $H^{5,7}$, J_{HH} = 11 Hz), 7.90 (s, br, 2H, NH_2), 9.00 (d, 2H, $H^{4,8}$, $^{3}J_{HH}$ = 11 Hz) ppm.

II.3.4 Synthesis of 2,2'-diamino-1,1',3,3'-tetraethoxycarbonyl-6,6'-biazulenylacetylene (2.3)

2-amino-6-bromo-1,3-diethoxycarbonylazulene (0.225 g, 0.615 mmol), 2-amino-6-ethynyl-1,3-diethoxycarbonylazulene (0.201g, 0.646 mmol), triphenylphosphine (0.032 g, 0.123 mmol), copper(I) iodide (0.023 g, 0.123 mmol), and tetrakis(triphenylphosphine)palladium(0) (0.071 g, 0.0615 mmol) were placed into a 250 mL single armed round bottom flask and placed under an argon atmosphere. 150 mL of toluene was added to the flask. While the contents were being stirred, 5 mL of freshly distilled triethylamine was added via cannula. The reaction was allowed to stir for 18 hr. The deep blood red colored mixture was poured into 100 ml 10% NH_4Cl. This mixture was extracted with dichloromethane (3 X 100 mL). Washed with 100 mL DI H_2O. Dried over Na_2SO_4 and filtered. All of the solvent was removed under vacuum using a rotary evaporator and recrystallized from dichloromethane/hexanes to afford a 85% yield of **2.3** (0.311 g, 0.521 mmol) as a brick red powder. ^{1}H NMR ($CDCl_3$, 400MHz, 25°C): δ 1.50 (t, 3H, CH_3, $^{3}J_{HH}$ = 8 Hz), 4.49 (q, 4H, CH_2, $^{3}J_{HH}$ = 8 Hz), 7.77 (d, 2H, $H^{5,7}$, $^{3}J_{HH}$ = 12 Hz), 7.91 (s, br, 2H, NH_2), 9.04 (d, 2H, $H^{4,8}$, $^{3}J_{HH}$ = 12 Hz) ppm. UV-Vis (CH_2Cl_2) λ_{max}(log ε): 505 nm (4.84), 357 nm (4.79), 348 nm (4.77), 250 nm (4.943).

II.3.5 Synthesis of 2,2'-bisformamido-1,1',3,3'-tetraethoxycarbonyl-6,6'-biazulenylacetylene (2.4)

2,2'-diamino-1,1',3,3'-tetraethoxycarbonyl-6,6'-biazulenylacetylene (0.311 g, 0.521 mmol) was placed into a 250 mL round bottom flask and dissolved with 100 mL

dichloromethane. While stirring, formic acid (9.8 mL) and acetic formic anhydride (3.3 mL) were added to the flask. The reaction was allowed to stir for 4hr. The burgundy colored reaction mixture was quenched with 10% Na_2CO_3 and the organic material was dried over Na_2SO_4. The filtrate was filtered and the solvent was removed via rotary evaporation. Recrystallization from dichloromethane/pentane afforded a 77% yield of **2.4** (0.263 g, 0.403 mmol) as a red-brown powder. ^{1}H NMR ($CDCl_3$, 400MHz, 25°C): δ 1.50 (t, 3H, C*H*$_3$, $^3J_{HH}$ = 8 Hz), 4.53 (q, 4H, C*H*$_2$, $^3J_{HH}$ = 8 Hz), 7.93 (d, 2H, $H^{5,7}$, $^3J_{HH}$ = 12 Hz), 8.67 (s, 1H, N*H*), 9.31(d, 2H, $H^{4,8}$, $^3J_{HH}$ = 12 Hz), 10.40 (s, br, 1H, C*H*O) ppm. UV-Vis (CH_2Cl_2) λ_{max}(log ε): 470 nm (4.79), 354 nm (4.80), 348 nm (4.85), 251 nm (4.83), 235 nm (4.82).

II.3.6 Synthesis of 2,2'-diisocyano-1,1',3,3'-tetraethoxycarbonyl-6,6'-biazulenylacetylene (2.5)

2,2'-bisformamido-1,1',3,3'-tetraethoxycarbonyl-6,6'-biazulenylacetylene (0.263 g, 0.403 mmol) was placed into a 250 mL single armed round bottom flask and dissolved in 100 mL of dichloromethane. 0.585 mL of distilled triethylamine was added to the flask and stirred for 10min at 0°C. In a 100 mL single armed round bottom flask, triphosgene (0.251 g, 0.846 mmol) was dissolved with 25 mL of dichloromethane while being cooled to 0°C. The $(COCl_2)_3$/DCM solution was transferred via cannula to the 250 mL flask. The reaction was allowed to stir for 2 hr. The reaction mixture was poured into 250 mL of ice cold water. Collected organic material and dried over Na_2SO_4. The filtrate was filtered and the solvent was removed via rotary evaporation. Recrystallization from dichloromethane/pentane afforded a 54% yield of **2.5** (0.133 g, 0.215 mmol) as a brown powder. Anal. Calcd. for $C_{36}H_{28}N_2O_8$: C: 70.12; H: 4.58; N: 4.54. Found: C: 69.82; H: 4.97; N: 4.10. FTIR (CH_2Cl_2): ν_{CN} = 2124 cm^{-1}; ν_{alkyne} = 2189 cm^{-1}. ^{1}H NMR ($CDCl_3$, 400MHz, 25°C): δ 1.54 (t, 3H, C*H*$_3$, $^3J_{HH}$ = 7 Hz), 4.54 (q,

4H, CH_2, $^3J_{HH}$ = 7 Hz), 8.05 (d, 2H, $H^{5,7}$, $^3J_{HH}$ = 11 Hz), 9.78 (d, 2H, $H^{4,8}$, $^3J_{HH}$ = 11 Hz) ppm. $^{13}C\{^1H\}$ NMR ($CDCl_3$, 125.7MHz, 25°C): δ 14.3 (*C*H_3), 61.4 (*C*H_2), 98.2 (*alkyne C atoms*), 113.9, 131.9, 134.7, 136.1, 139.4, 141.3 (*aromatic C*), 163.2 (*C*O_2R), 178.9 (*C*NR) ppm. UV-Vis (CH_2Cl_2) λ_{max}(log ε): 555 nm (3.80), 444 nm (4.76), 417 nm (4.68), 344 nm (4.79), 244 nm (4.76).

II.3.7 Synthesis of a dinuclear tungsten pentacarbonyl complex featuring 2,2'-diisocyano-1,1',3,3'-tetraethoxycarbonyl-6,6'-biazulenylacetylene (2.6)

[$W(CO)_5$(THF)] was generated according to a literature procedure with the use of $W(CO)_6$ (0.206 g, 0.585 mmol) in 100 mL of THF.[6] Diisocyanide (0.180 g, 0.292 mmol) was dissolved in 50 mL of THF using a 250 mL single armed round bottom flask giving a red-brown color. The Yellow-orange [$W(CO)_5$(THF)] solution was slowly cannulated to the diisocyanide solution over a period of 30 minutes. The reaction was left to stir for 18 hr at room temperature which resulted in a fuschia colored solution. THF was removed in vacuo and dried then sublimed at 40°C to afford a 57% yield of **2.6** (0.210 g, 0.166 mmol) as a dark purple-black microcrystalline powder. FTIR (CH_2Cl_2): ν_{CO} = 1957 vs. 2043 cm^{-1}; ν_{CN} = 2137 cm^{-1} ;ν_{alkyne} = 2184 cm^{-1}. ^1H NMR (CD_2Cl_2, 400MHz, 25°C): δ 1.51 (t, 3H, CH_3, $^3J_{HH}$ = 8 Hz), 4.57 (q, 4H, CH_2, $^3J_{HH}$ = 8 Hz), 8.08 (d, 2H, $H^{5,7}$, $^3J_{HH}$ = 12 Hz), 9.76 (d, 2H, $H^{4,8}$, $^3J_{HH}$ = 12 Hz) ppm. $^{13}C\{^1H\}$ NMR ($CDCl_3$, 125.7MHz, 25°C): δ 14.9 (*C*H_3), 61.4 (*C*H_2), 98.6 (*alkyne C atoms*), 113.9, 132.4, 135.1, 135.6, 138.7, 142.0 (*aromatic C*), 163.2 (*C*O_2R), 165.1 (*C*NR), 194.0 (W *C*O *cis*), 196.2 (W *C*O *trans*) ppm. UV-Vis (CH_2Cl_2) λ_{max}(log ε): 531 nm (4.21).

II.3.8 Synthesis of a mononuclear tungsten pentacarbonyl complex featuring 2,2'-diisocyano-1,1',3,3'-tetraethoxycarbonyl-6,6'-biazulenylacetylene (2.7)

A yellow orange solution of $[W(CO)_5(THF)]$ was generated according to a literature procedure with the use of $W(CO)_6$ (0.024 g, 0.068 mmol) in 50 mL of THF. Diisocyanide (0.167 g, 0.271 mmol) was dissolved in 50 mL of THF using a 250 mL single armed round bottom flask giving a red-brown color. The $[W(CO)_5(THF)]$ solution was slowly cannulated to the diisocyanide solution over a period of 30 minutes. The reaction was left to stir for 40 hr at room temperature giving a dark colored solution. THF was removed via rotary evaporation and dried via a schlenk line yielding a dark powder which was subjected to florisil column chromatography. Three fractions were collected. The first was a minimal amount of the purple dinuclear product, the second was the red violet mononuclear fraction, and the third was unreacted free ligand. Solvent was removed via rotatry evaporation to afford a 20 % yield of **2.7** (0.013 g, 0.0138 mmol) as a dark reddish purple powder. FTIR (CH_2Cl_2): ν_{CO} = 1955 vs. 2045 cm^{-1}: ν_{CN} = 2127, 2140 cm^{-1}(sh) ; ν_{alkyne} = 2188 cm^{-1}. ^1H NMR ($CDCl_3$, 400MHz, 25°C): δ 1.53 (t, 12H, CH_3, $^3J_{HH}$ = 8 Hz), 4.57 (q, 8H, CH_2, $^3J_{HH}$ = 8 Hz), 8.05 (d, 4H, $H^{5,5',7,7'}$, $^3J_{HH}$ = 12 Hz), 9.79 (d, 4H, $H^{4,4',8,8'}$, $^3J_{HH}$ = 12 Hz) ppm. $^{13}C\{^1H\}$ NMR ($CDCl_3$, 125.7MHz, 25°C): δ 14.8, 14.9 (*C*H_3), 61.3, 61.4 (*C*H_2), 98.2, 98.5 (*alkyne C atoms*), 113.8, 113.9, 129.5, 132.4, 134.7, 135.0, 135.6, 135.8, 138.7, 139.4, 141.4, 142.0 (*aromatic C*), 163.2 (*C*O_2R), 165.2 (M*C*NR), 178.9 (*C*NR), 194.0 (W *C*O *cis*), 196.2 (W *C*O *trans*) ppm. UV-Vis (CH_2Cl_2) λ_{max}(log ε): 517 nm (4.17).

II.3.9 Synthesis of [dcpm(Au)$^1_2$bis(1,3-diethoxycarbonyl-2-isocyanoazulene]$^{2+}$([OTF]$^-$)$_2$ (2.8)

Silver triflate (0.060 g, 0.233 mmol) was added to a 100 mL single arm round bottom flask with 25 mL acetone. Bisdicyclohexylphosphinomethanebis(gold(I)chloride), dcpm$(AuCl)_2$, 0.103 g, 0.118 mmol) was added to a separate 100 mL single arm round bottom flask with 25 mL

of dichloromethane. With stirring, the silver trifilate mixture was transferred to the gold(I) mixture via cannula. After 30 minutes, the reaction mixture was cloudy and bluish white in appearence. This was then filtered through a schlenk frit providing a colorless filtrate. The solvent was removed under vacuum yielding a colorless solid residue on the inner walls of the flask. The solid was re-dissolved in 50 ml dichloromethane and 1,3-diethoxycarbonyl-2-isocyanoazulene (0.070 g, 0.236 mmol) in 50 mL dichloromethane was added via cannula. The reaction mixture was stirred for 2 hr. The reaction mixture was then concentrated down via vacuum and the product was crashed out with pentane and dried to afford a 50% yield of **2.8** (0.099 g, 0.058 mmol) as pink crystals. MP: 97-101°C. FTIR (CH_2Cl_2): $\nu_{CN} = 2231$ cm^{-1}.

II.3.10 Synthesis of bis[dcpm(Au)$^1_2$(2,2'-diisocyano-1,1',3,3'-tetraethoxycarbonyl-6,6'-biazulenylacetylene]$^{4+}$([OTF]$^-$)$_4$ (2.9)

Silver triflate (0.050 g, 0.195 mmol) was added to a vial and wrapped in foil. 10 mL of diethyl ether was added to dissolve the silver salt. Bisdicyclohexylphosphinomethanebis(gold(I)chloride), dcpm$(AuCl)_2$, 0.085 g, 0.097 mmol) was added to the vial followed with the addition of 20 ml dichloromethane. The reaction mixture was stirred for 40 minutes. This mixture was then passed through celite and the resulting filtrate was added to a 100 mL round bottom flask which contained 2,2'-diisocyano-1,1',3,3'-tetraethoxycarbonyl-6,6'-biazulenylacetylene (0.060 g, 0.097 mmol) dissolved in 25 mL dichloromethane. The reaction mixture was stirred for 2 hr. the solvent was removed via rotary evaporation to afford a 78% yield of **2.9** (0.131 g, 0.038 mmol) as a brown powder. FTIR (CH_2Cl_2): $\nu_{CN} = 2233$ cm^{-1}.

II.4. Results and Discussion

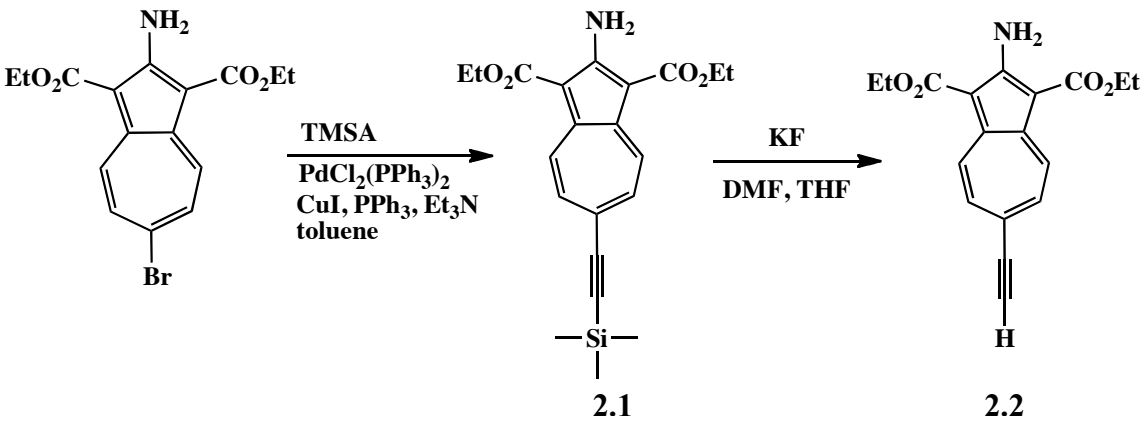

Scheme II.3. Synthesis of precursors for the 6,6'-biazulenylacetylene chemistry

Synthesis begins with the 2-amino-6-bromoazulene which was in itself prepared following a modified prep of the original Nozoe procedure.[30] In order to couple the molecules via Sonogashira conditions, 10 mol% palladium catalyst with 20 mol% of copper iodide and triphenylphosphine were added with the halogenated aminoazulene and dissolved in toluene. Triethylamine and trimethylsiylylacetylene were then added to commence the reaction. This reaction is highly reproducible with an 86% yield. This orange powder (compound **2.1**) is then dissolved in minimal tetrahydrofuran and subjected to potassium fluoride and N,N'-dimethylformamide resulting in the terminal alkyne (compound **2.2**) with a yield of 70%. Purification of this red-brown powder is best done via recrystallization. Compound **2.2** is an important piece for construction of the biazulenyl motif utilizing an acetylene spacer connected through the 6 and 6' carbon position of the azulene rings.

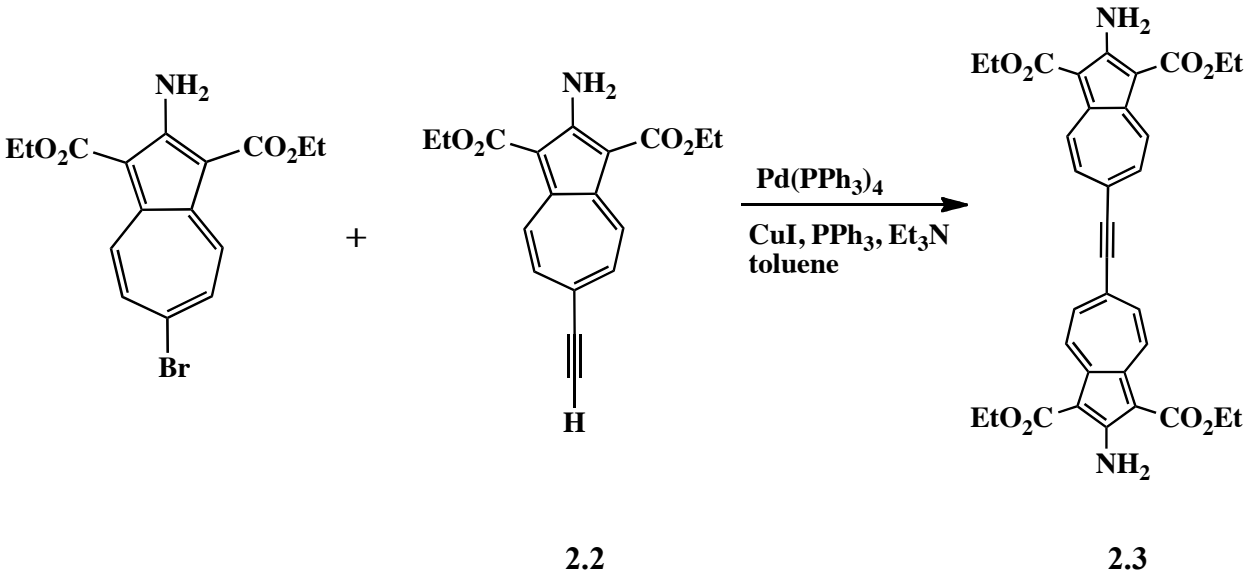

2.2 **2.3**

Scheme II.4. Synthesis of the 2,2'-diamino-6,6'-biazulenylaceylene scaffold.

10 mol% palladium catalyst in the presence of 20 mol% copper iodide and 20 mol% triphenylphosphine were added to a flask with **2.2** and 2-amino-6-bromoazulene. After 18 hours, the reaction was worked up and 85% of brick red powder (Compound **2.3**) was obtained after recrystallization from dichloromethane/hexanes. Numerous purification attempts were initially carried out in the early stages of optimization. All attempts in purification of compound **2.3** using silica gel column chromatography led to the loss of the brick red product on the column. Thus, recrystallization proved to be the best method for purification. It also proved to be important for this reaction to be conducted under strict anaerobic conditions to arrive to a purely coupled material. Homo coupling (two acetylene bridges) was observed when the reaction was carried out in ambient conditions while being exposed to air consequently resulting in an inseparable mixture. This was seen by Ito and others in 2001.[9]

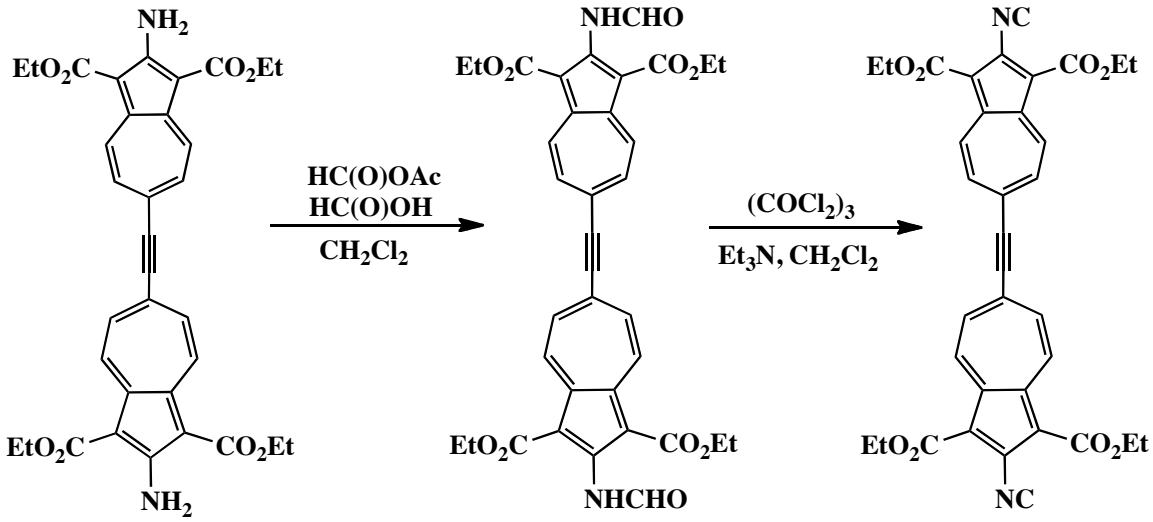

2.3 **2.4** **2.5**

Scheme II.5. Synthesis of the 2,2'-diisocyano-6,6'-biazulenylacetylene linker.

Compound **2.3** was formylated using excess acetic-formic anhydride and formic acid for 4 hours. Gentle heating could also be used to help speed up the reaction if desired. Another acceptable method for formylation involved the in-situ preparation of acetic-formic anhydride. After 4 hours, red-brown powder (Compound **2.4**) was prepared in a 77% yield. Purification was completed via recrystallization from dichloromethane/pentane.

Dehydration of compound **2.4** was carried out using triphosgene and triethylamine over the course of 2 hours. Washing the reaction mixture with excess water following completion proved to be critical for getting rid of triethylammonium salts. Brown powder (Compound **2.5**) was prepared in a yield of 54%. Purification is best done via recrystallization from dichloromethane/pentane.

Table II.1. ^{1}H NMR data in ppm of selected azulenic based compounds in $CDCl_3$ and/or CD_2Cl_2 at 25°C.[3,30]

Compound	4/8, 4'/8'	5/7, 5'/7'	CH_2	CH_3
$^{2}H_2NAzBr^{6}E_2$	8.78	7.77	4.45	1.47
$^{2}CNAzNC^{6}E_2$	9.80	7.79	4.53	1.52
$^{2}H_2N^{6,6'}(Az)_2^{2'}H_2NE_4$	9.17	7.78	4.47	1.48
$^{2}NHCHO^{6,6'}(Az)_2^{2'}NHCHOE_4$	9.50	7.97	4.53	1.50
$^{2}CN^{6,6'}(Az)_2^{2'}CNE_4$	9.93	8.03	4.55	1.54
2.1	8.99	7.69	4.46	1.48
2.2	9.00	7.70	4.48	1.50
2.3	9.04	7.77	4.49	1.50
2.4	9.31	7.93	4.53	1.50
2.5	9.78	8.05	4.54	1.54

^{1}H NMR was an effective method of characterization. Table II.1 summarizes NMR data for the compounds **2.1** through **2.5** and for a series of other relevant azulenic compounds. This data clearly shows that the functional group at the terminal ends of the azulenic framework has an influence on the chemical shifts of the azulenic ring. Evidence for this claim is seen while analyzing the chemical shifts for compounds **2.3** through **2.5**. There is an increase of 0.74ppm for $H^{4,8/4',8'}$ when going from the diamino to the diisocyanide. Furthermore, a 0.28 ppm shift downfield is observed for $H^{5,7/5',7'}$ when converting to the diisocyanide. This downfield shift is indicative of a deshielding effect upon changing the functionality at the 2 and 2' positions on the azulenic ring. This effect is felt, albeit slightly, in the diethyl ester region as well. This offers further support for an extended conjugated π system for these compounds. A similar relationship was observed for the 6,6'-biazulenyl analogue.[3]

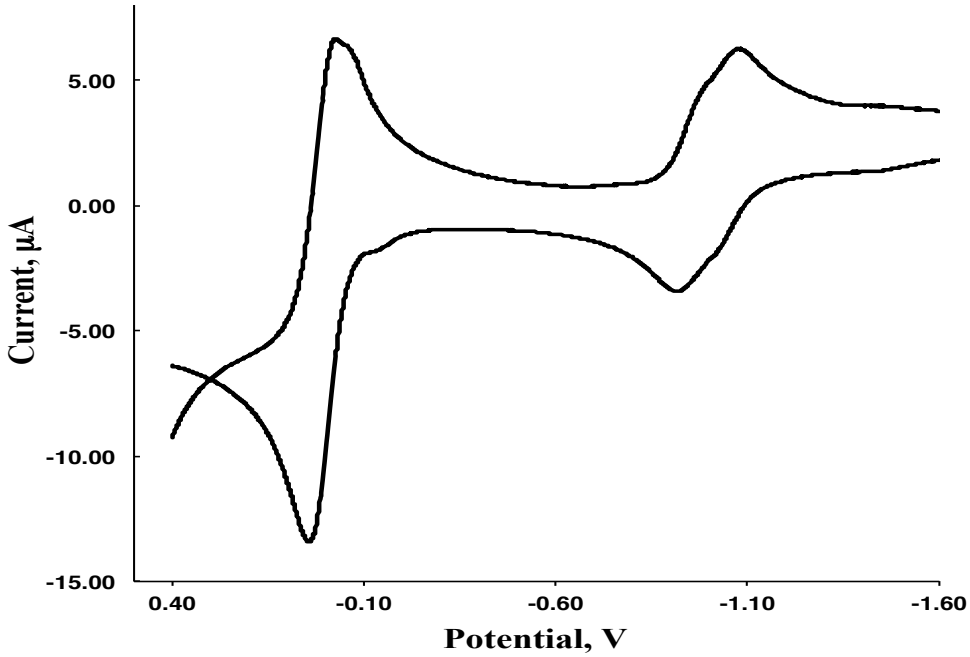

Figure II.3. Cyclic voltammogram of 2.5 in CH_2Cl_2 with an internal FcH/FcH^+ ref. at a scan rate of 50mV/sec.

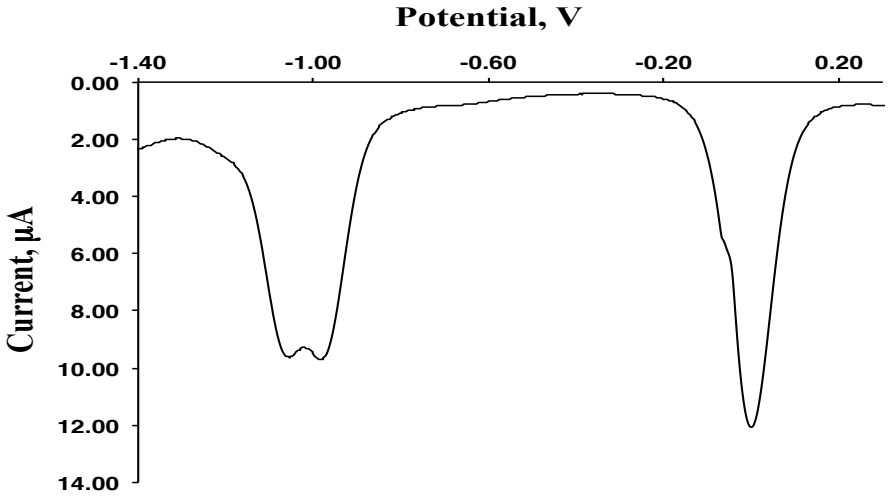

Figure II.4. Differential pulse voltammogram of 2.5 in CH_2Cl_2 with an internal FcH/FcH^+ ref.

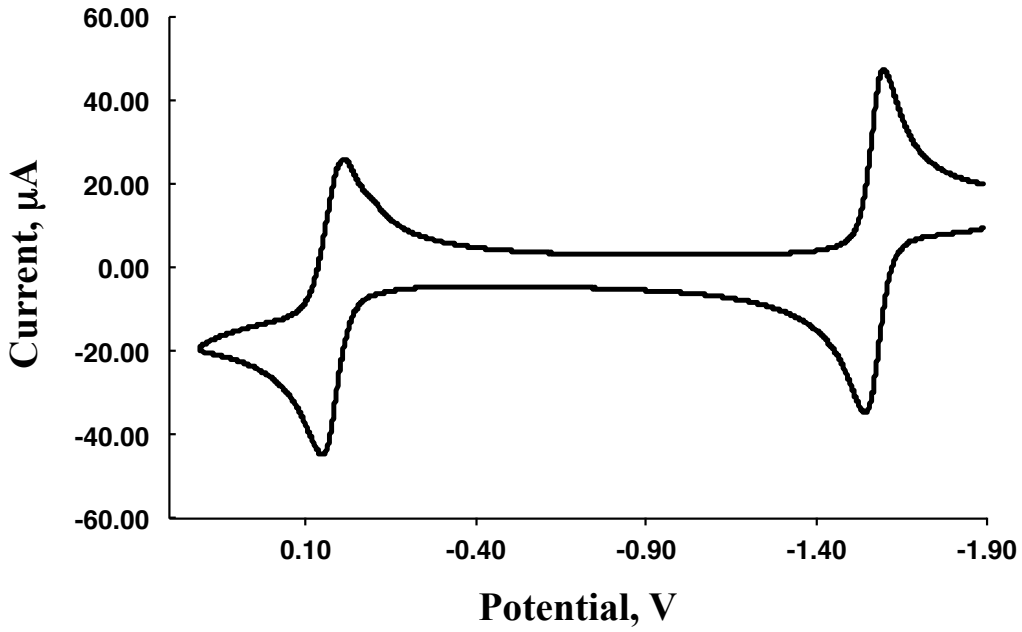

Figure II.5. Cyclic voltammogram of 2.3 in CH_2Cl_2 with an internal FcH/FcH^+ ref. at a scan rate of 500mV/sec.

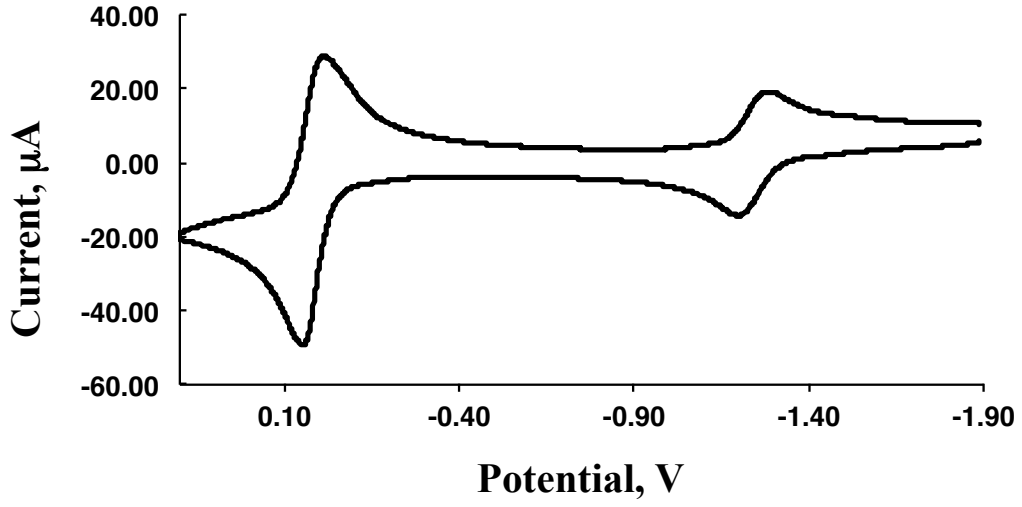

Figure II.6. Cyclic voltammogram of 2.4 in CH_2Cl_2 with an internal FcH/FcH^+ ref. at a scan rate of 500mV/sec.

Table II.2. Reduction and oxidation potentials of 1.3, 1.6, and selected compounds from the literature in CH_2Cl_2 versus FcH/FcH^+ in volts. [a]Irreversible.[3,9,30]

Compound	$E_{1/2\ (red1,\ red2)}$	$E_{1/2,\ ox\ 1}$
$^{2}CNAzE_2$	-1.55[a]	-0.10[a]
$^{2}CN^{6,6'}(Az)_2{}^{2'}CNE_4$	-1.02	
$^{6,6'}BiAzE_4$ (w/ alkyne spacer)	-0.96, -1.15	
2.3	-1.585	
2.4	-1.265	
2.5 F	-0.982, -1.056	

Figures II.3 through II.6 feature cyclic and differential pulse voltammograms for compounds **2.3**, **2.4**, and **2.5** acquired in dichloromethane where ferrocene was used as an internal standard. CV and DPV data for **2.5** indicate that two redox processes occur. This data suggests a stable stepwise two-electron reduction of the biazulenic π system as noted by two distinct reversible redox potentials of -0.982 and -1.056V on the electrochemical timescale. Precursors (**2.3** and **2.4**) exhibit two electron processes as well but they occur at identical potentials. The more negative redox potentials for these precursors indicate that electron donating groups, such as amines, at the 2 and 2' positions make the biazulene ring more difficult to reduce. This is due to the stabilizing isocyanide groups decreasing the band gap of the biazulene and allowing for the easier addition of electrons into the LUMO. Figure II.7 illustrates

a simple Hückel calculation for the LUMO of compound **2.5** showing its extended conjugated π-system. Figure II.8 shows a possible illustration for the suspected closed shell dianion of **2.5** based on electrochemical data.

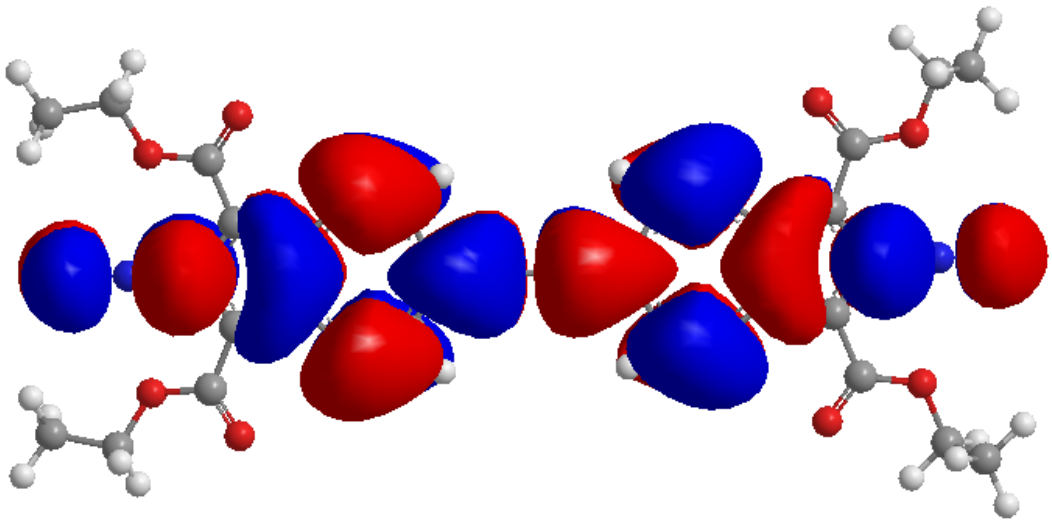

Figure II.7. LUMO of 2.5 using a simple Hückel calculation.

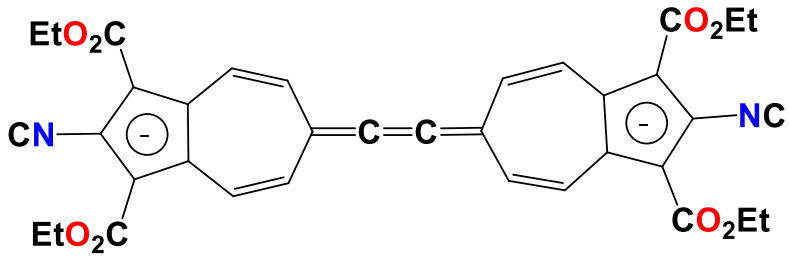

Figure II.8. Potential representation of the closed shell dianion for 2.5.

Electronic spectra were obtained to determine the effect of substituents on the 2 and 2' positions of the 6,6'-biazulenylacetylene framework (Table II.3). The data depicted in the table are representative of the believed S_0 to S_1 transitions for each listed compound. The LUMO has orbital density at the 2-position unlike the HOMO; thus, varying the nature of substituent at the 2-position should only effect the LUMO.[3] The λ_{max} value for a relatively weak S_0 to S_1 transition in the electronic spectra of compounds **2.3** through **2.5** in dichloromethane increases upon progressing from **2.3** to **2.5**. This trend parallels the order of decreasing electron donating/increasing electron withdrawing strength of the groups at positions 2,2' of the 6,6'-biazulenylacetylene and also correlates with the chemistry for the 6,6'-biazulenyl analogoue.[3] Energy of the more intense band (S_0 to S_2) increases in reverse order where **2.5** < **2.4** < **2.3**. This indicates that the choice of substituent at the 2,2' positions provide a way to tune both the S_0 to S_1 and S_0 to S_2 transitions.[3]

Table II.3. Electronic transititons for azulenic compounds in CH_2Cl_2 and pentane.[34]

Compound	λ_{max} (nm)	Energy of Transition (cm^{-1})
Azulene	575	17,391
^{2}CNAz	560	17,857
^{2}CNAzE_2	522	19,157
^{2}CNAzE_2NC^6	535	18,892
6,6'-BiAzE_4	592	16,892
^{2}CN(AzE_2)$_2$NC$^{2'}$	531	18,832
6,6'-BiAzE_4 w/ alkyne bridge	551	18,149
2.3	505 (shoulder)	19,802
2.5	555	18,018

Coordination chemistry of compound **2.5** was initially examined with tungsten pentacarbonyl. The resulting bis and mono tungsten complexes, **2.6** and **2.7** respectively, provided evidence for metal to ligand charge transfer (MLCT). Previously, the Barybin group reported on other azulenic systems featuring this type of MLCT. The 2,6-diisocyanide published in 2006 shows a great energy of binucleation after complexation of both ends of the diisocyanide. This binucleation energy indicates a relatively large involvement of the aromatic π-system compared to a similar benzenoid-based system published by Bennett.[36]

Preparation of the bistungsten complex (Figure II.9) was performed using a tungsten pentacarbonyl THF adduct prepared from tungsten hexacarbonyl following an established preparation.[35] These reactions were treated as air sensitive and followed via IR using dichloromethane (Figure II.10). IR is a powerful tool for characterization of the organometallic complexes since a change of symmetry around the metal center causes obvious shifts in the stretching frequencies of CO's as well as isocyanide, due to σ-donation and π-backbonding. For instance, the free unbound isocyanide has a stretch of 2124 cm^{-1}, whereas, compound **2.6** has an isocyanide stretch of 2137 cm^{-1}. **2.6** also has carbonyl stretches of 1957 and 2043 cm^{-1}. Complexation provided 57% of purple powder. A MLCT band for **2.6** was observed at 531nm.

The synthesis of the monotungsten analogue (compound **2.7,** Figure II.9) was more difficult to isolate than the bistungsten complex. In order to prepare the monocomplex, an excess of free ligand (4:1) and slow transfer of all reagents is required.

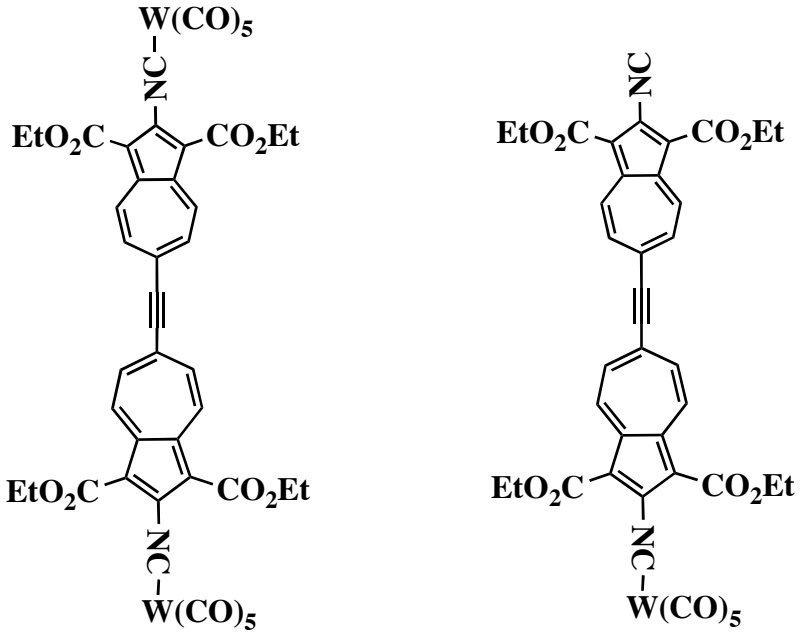

Figure II.9. Coordination of the diisocyanide with tungsten pentacarbonyl.

The most difficult step of this synthetic pathway was the purification step. For instance, column chromatography was a method tried on several occasions. A good amount of material stuck to the column during these trials. The best yield using this method to date is 20% of reddish-purple powder (**2.7**). IR indicated that compound **2.7** has two isocyanide stretches of 2127 cm^{-1} and 2140 cm^{-1} and carbonyl stretches of 1955 and 2045 cm^{-1} (Figure II.11). A MLCT band for **2.7** was observed at 517nm.

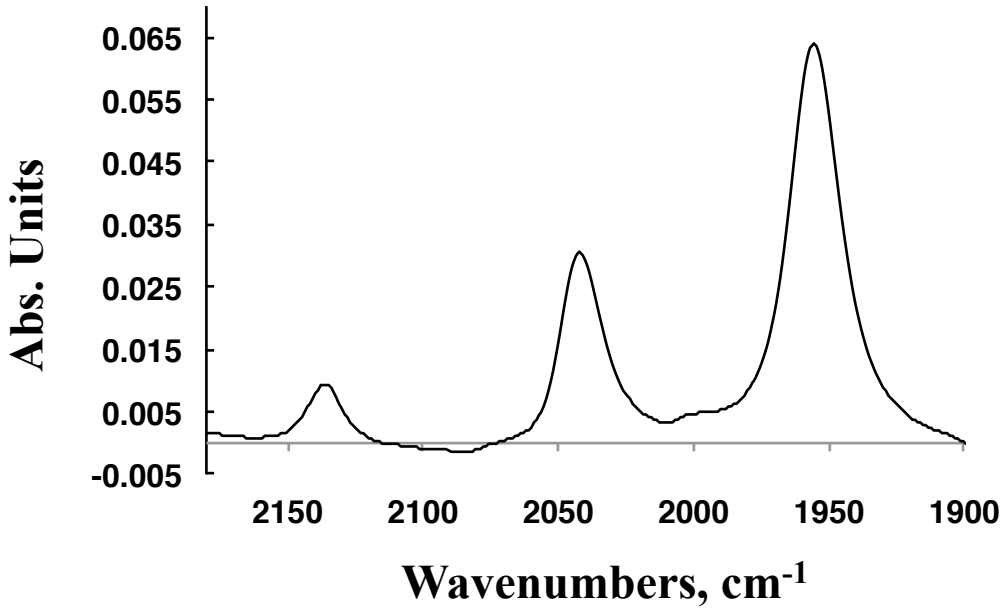

Figure II.10. FTIR of compound 2.6 in CH_2Cl_2 at 25°C.

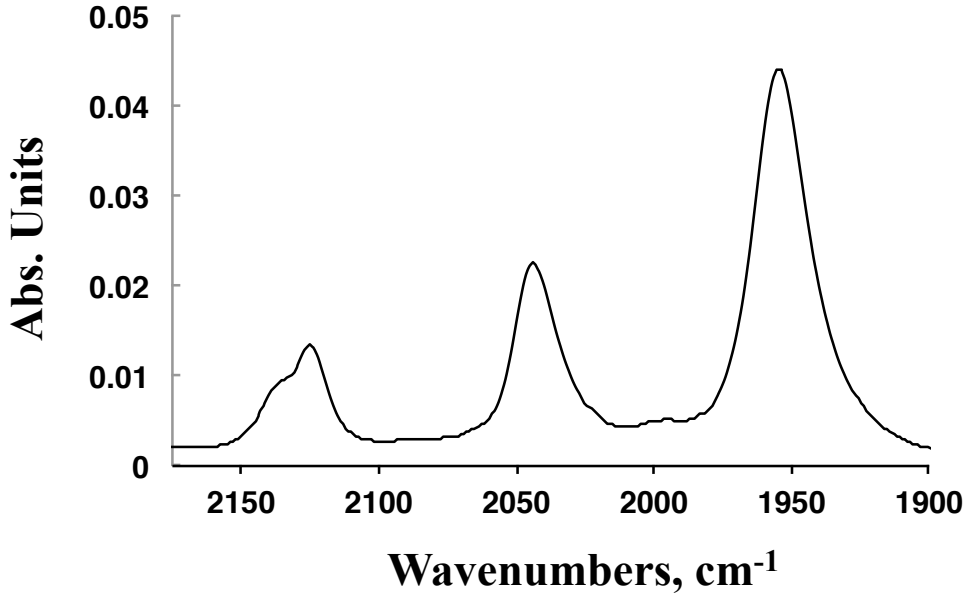

Figure II.11. FTIR of compound 2.7 in CH_2Cl_2 at 25°C.

The measured metal to bridge charge transfer (MBCT) depicts the ability of electronic communication of a given substrate bridged by metal termini. The MBCT for compound **2.6** was 18,832 cm^{-1} (531nm). Compound **2.7** had a metal to bridge charge transfer of 19,342.4 cm^{-1} (517nm). The energy of binucleation, which is the measured difference in charge transfer maxima, in going from **2.6** to **2.7** was calculated to be 510 cm^{-1}. This suggests that the effect of binucleation is not as great as seen in the 2,6-diisocyanoazulene case where the complexation was occurring at the 2 and 6 positions on the azulene ring. Both of these diisocyanobiazulene complexes are conjugated due to good orbital overlap, therefore, it is not surprising to observe red shifted MBCT bands for the complexes. Table II.4 showcases some relevant energies of binucleation for select aromatic compounds.

Table II.4. MBCT and binucleation energies for selected compounds conducted in CH_2Cl_2.[3, 30, 36]

Compound	E (MBCT) (cm^{-1})	$\Delta^{Binucleation}$ (cm^{-1})
$((OC)_5W)CNC_6H_4NC(W(CO)_5)$	27,027	1,221
$((OC)_5W)^2CNAzNC^6(W(CO)_5)$	19,417	2,042
$((OC)_5W)^2CN(AzE_2)_2NC^2(W(CO)_5)$	20,161	?
2.6	18,832.4	510

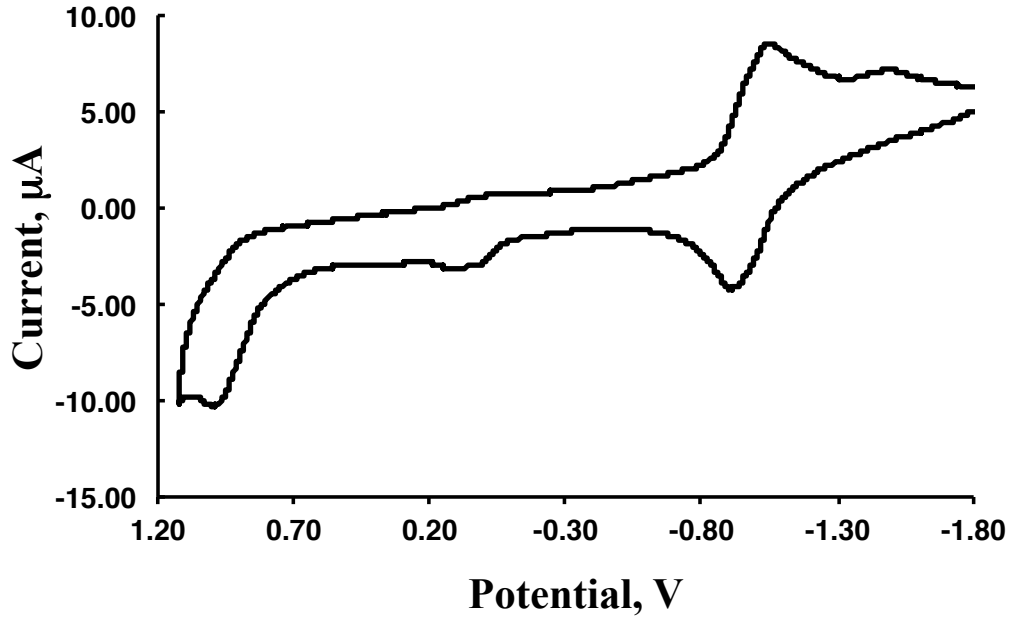

Figure II.12. Cyclic voltammogram of 2.6 in CH_2Cl_2 with an internal FcH/FcH^+ ref. at a scan rate of 100mV/sec.

Cyclic voltammetry was performed on compound **2.6** using a scan rate of 100 mV/sec in dichloromethane (Figure II.12). This figure illustrates a stepwise reversible two-electron reduction process featuring an $E_{1/2}$ value of -0.98 V and an irreversible oxidative half wave at 1.00V attributed to tungsten oxidation. Reduction of **2.6** occurs at almost the same exact potential as the first reduction in compound **2.5**. The two-electron reductive process for compound **2.6** and that its redox properties are fairly close to that seen in compound **2.**5 seems to indicate the LUMO is mostly bridge-based. This potential is almost the same as the analogous bistungsten complex from Dr. Tiffany Maher's electrochemical experiment for the 2,2'-diisocyano-6,6'-biazulenyl.[3]

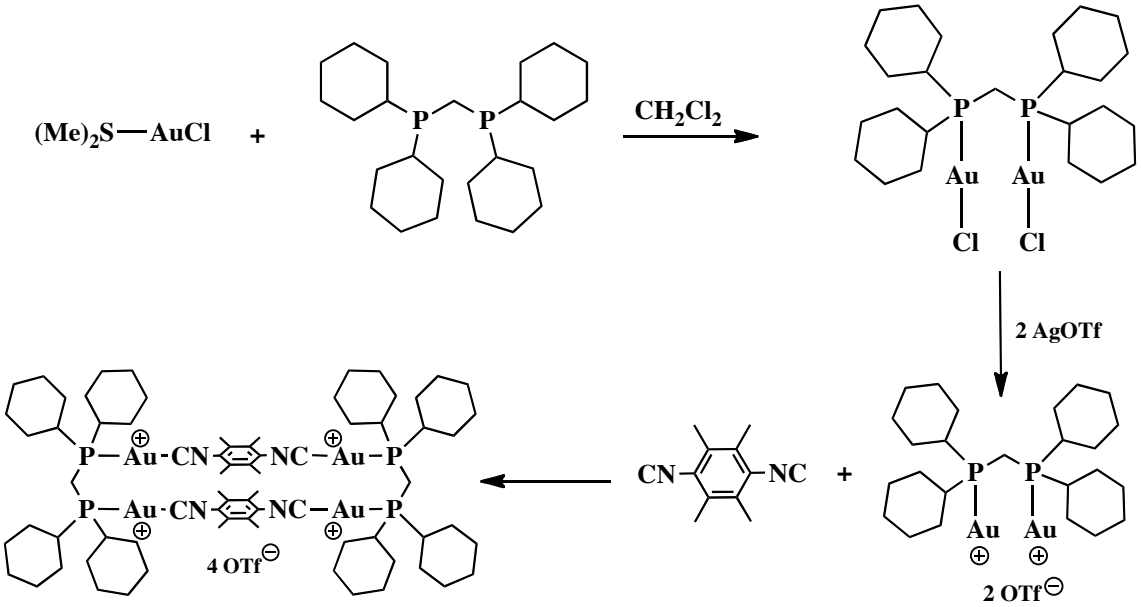

Scheme II.6. Synthesis of the 1,4-diisocyanodurene tetragold(I) rectangle.[39]

A keen interest of researchers has involved the design and study of gold complexes for rheumatoid arthritis. Over the past couple of decades, an interest in the design of organogold complexes as potential electronic devices has taken shape due to the interesting electronic properties associated with the aurophilic, or gold-gold, interactions.[15-28,32] These interactions are typically 3 Å in length and the strength is comparable to the strength of a hydrogen bond. Gold(I) complexes have shown the ability for emission, which is intriguing for the design of devices.[15-28] Emission studies have begun to carry over to Au(I) rectangles that would force aurophilic interactions. It is of interest to design an organogold(I) rectangle featuring the 2,2'-diisocyano-6,6'-biazulenylacetylene linker.

Scheme II.6 illustrates a synthetic route from Puddephatt and coworkers.[32] This was the first tetragold(I) rectangle to be published and the crystal structure provided evidence for aurophilic interactions. The first step involved making the gold(I) synthon.

This was followed by methathesis with silver triflate and followed by coordination with the diisocyanodurene. Emission studies have not been reported to the best of the author's knowledge for this complex. Therefore, the diisocyanodurene complex offered precedence for the development of organogold(I) chemistry with non-benzenoids developed by Barybin and coworkers (Scheme II.7, Deplazes).[33] This was one of the few known examples featuring a 1,1'-diisocyanoferrocene coordinated to gold in an organometallic architecture.

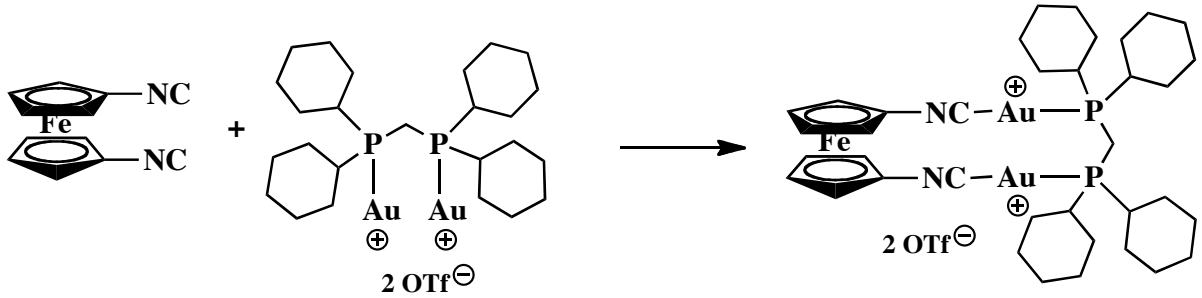

Scheme II.7. Synthesis of the 1,1'-diisocyanoferrocene digold(I) rectangle.[33]

The first azulenic-based gold(I) rectangles were prepared. Synthesis of compound **2.8** was conducted using a modified procedure of Puddephatt's original preparation for the 1,4-diisocyanodurene (Scheme II.8). $Dcpm(AuCl)_2$ (dcpm = dicyclohexylphosphinomethane) was stirred with silver triflate in the presence of dichloromethane for 30 minutes to prepare the intermediate using metathesis. The near colorless isolated intermediate was mixed with a solution of the isocyanide for approximately 2 hours. The resulting pink crystalline material was isolated in a yield of 50% and characterized by IR and X-ray crystallography.

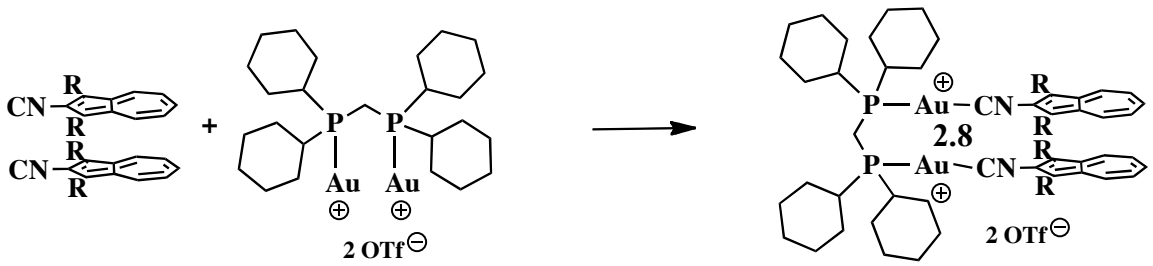

R = CO_2Et

Scheme II.8. Synthesis of compound 2.8.

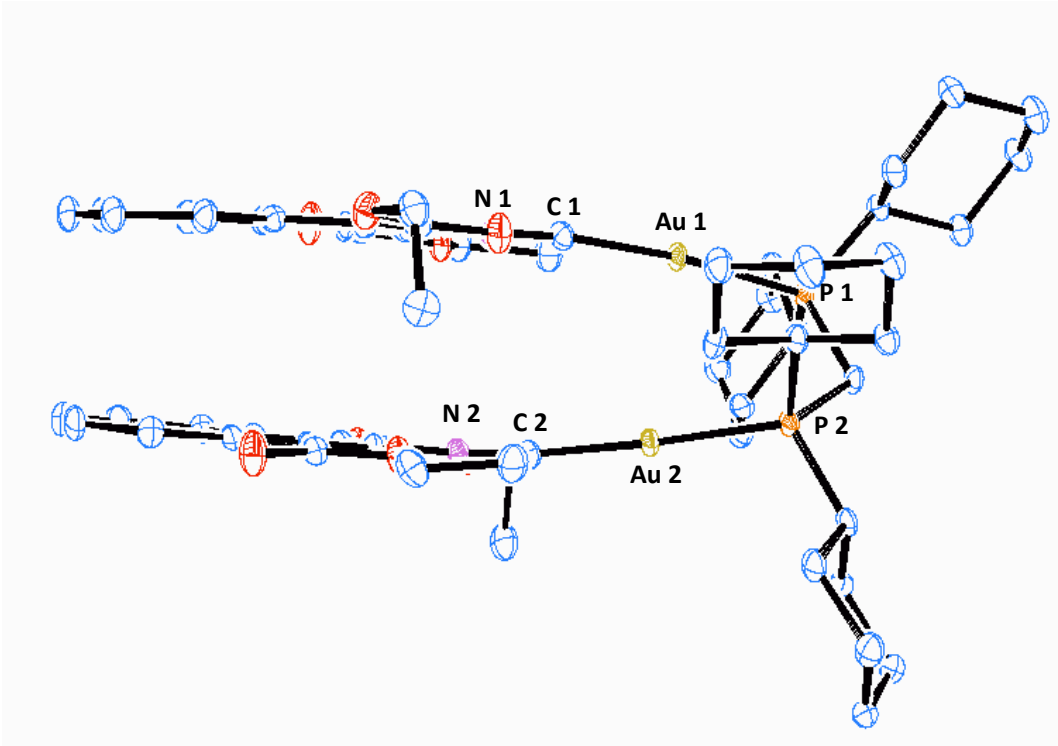

Figure II.13. X-ray structure of compound 2.8.

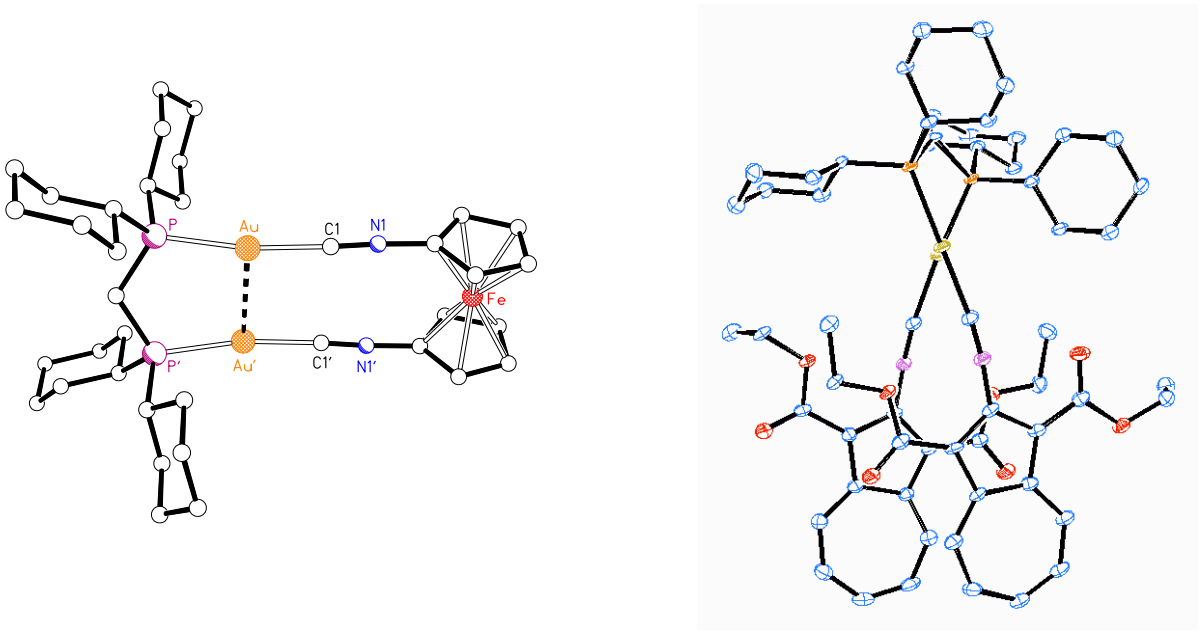

Figure II.14. X-ray structure of the 1,1'-diisocyanoferrocenyl gold rectangle and compound 2.8.[33]

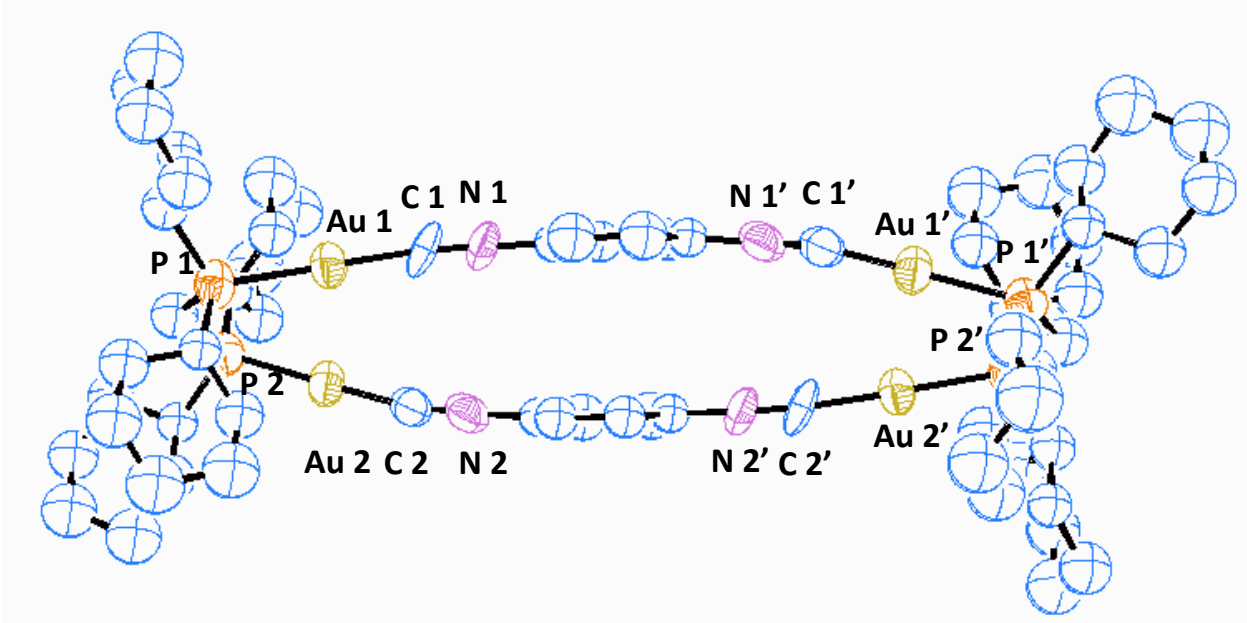

Figure II.15. X-ray structure of Puddephatt's tetragold(I) rectangle.[32]

A single crystal of compound **2.8** was grown from diffusion of dichloromethane/pentane at 4°C over the period of a few days. X-ray diffraction provided the first crystal structure of an azulenic based organogold(I) dinuclear complex. An illustration is depicted in Figure II.13 and compared with two other compounds featured in Figures II.14 and II.15. Interestingly, compound **2.8** features an aurophilic interaction of 3.062 Å. This type of interaction was also seen in the 1,1'-diisocyanoferrocene complex (3.047 Å) shown in Figure II.14 and Puddephatt's gold rectangle (3.133 Å) featured in Figure II.15. Excitingly, the aurophilic interaction remains intact for compound **2.8** even though it has an interplanar azulene angle of 3° where the azulene rings do not directly lie on top of one another. This is a reasonable result considering the natural repulsion that would occur having two azulene molecules oriented on top of one another in the same direction. Table II.5 summarizes some of the crystallographic results.

Table II.5. Selected bond distances and/or angles from X-ray diffraction.[33]

	2.8	[1,1'-$Fc(NC)_2$dcpmAu_2][OTf$^-$]$_2$	[$(CNC_6H_4NC)_2$(dcpmAu_2)$_2$][OTf$^-$]$_4$
Au-Au (Å)	3.062	3.047	3.133
P-P (Å)	3.096	3.155	3.214
C-C (Å)	3.541	3.236	3.557
N-N (Å)	3.709	3.281	3.632
P-Au-C (°)	174	169	171
Au-C-N (°)	172	174	171
Interplanar angle (°)	3	1.5	

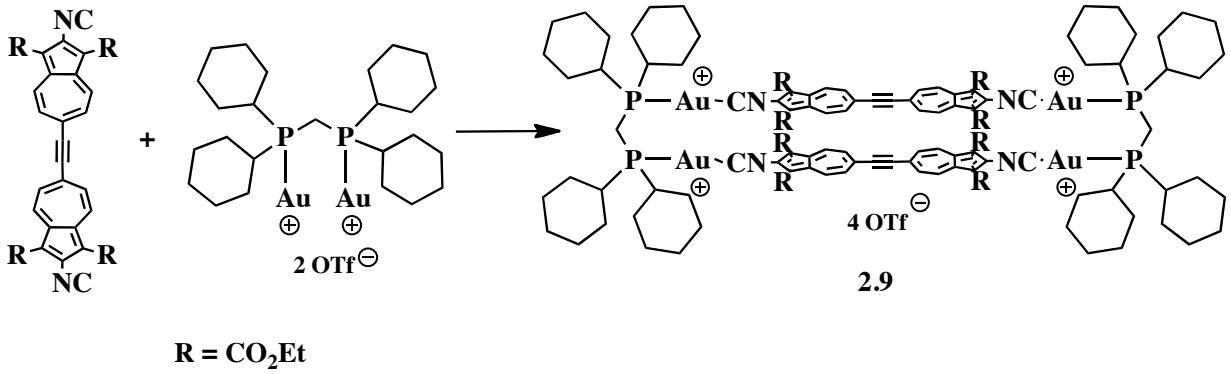

Scheme II.9. Synthesis of compound 2.9.

The synthesis of compound **2.9** began with the mixing of 2,2'-diisocyano-6,6'-biazulenylacetylene with the digold(I) precursor (Scheme II.9). This reaction was completed in 2 hours yielding brown powder in a 78% yield. IR proved to be an effective method of characterization. Compound **2.9** had an IR stretch of 2231 cm^{-1}, which is indicative of sigma donation from the isocyanide to the gold(I) center.

Emission experiments were conducted for several complexes. These studies were done with a fluorimeter at room temperature using distilled dichloromethane as a solvent (table II.6). Four of the five complexes listed in table II.6 exhibited emissive properties after being excited at all of the electronic transitions for the given compound. Compound **2.8** was the only one that did not exhibit emission in solution. To the best of the author's knowledge, the compounds prepared from published preparations have yet to provide documented emission data in the literature.

Compound **2.9** was the first to be studied and showed an emission of 596 nm. This is a considerable red shift when considering excitation was at 297 nm. To help gain an understanding for this phenomenon, a few other complexes were studied. After the study, it was

Table II.6. Emission data of selected gold-gold based compounds in CH_2Cl_2 at 24°C.

Compound	$\lambda_{excitation}$ (nm)	$\lambda_{emission}$ (nm)
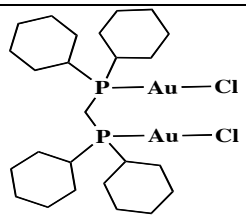	247	495
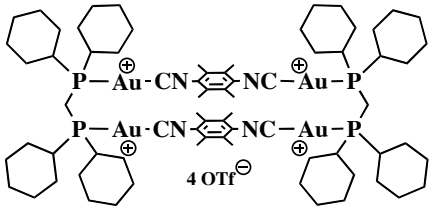	266	532
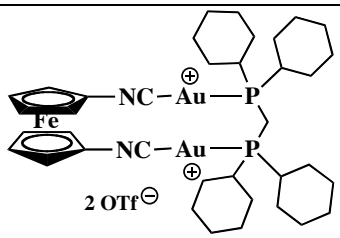	247	495
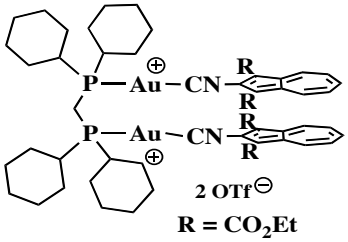		No emission observed
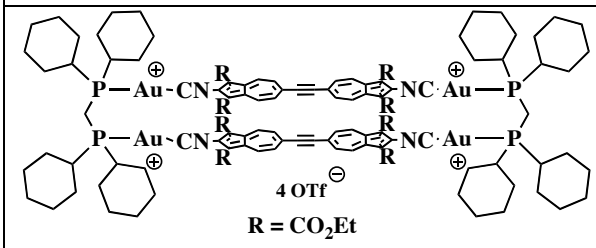	297	596

determined that the aurophilic interaction plays a strong part in the luminescence of the complexes. These aurophilic interactions are intramolecular in nature and allow for the observed σ to σ* transitions.[20] The same type of transition may play a role for some of the other gold ring compounds from table II.6. This result for **2.9** matches up well with the gold rectangle featuring 1,4-diisocyanodurene which had an emission of 532 nm.

Self assembled monolayers featuring coordination to Au(111) surfaces were completed for compound **2.5** and for the 2,2'-diisocyano-6,6'-biazulenyl analogue by Brad Neal and Dr. Tiffany Maher.[3] The results for **2.5** correlate with those of the analogue (Figure II.16). From Figure II.16, compound **2.5** (left) indicates favorable formation of the SAM based on the experimental thickness of 27(3) Å measurement

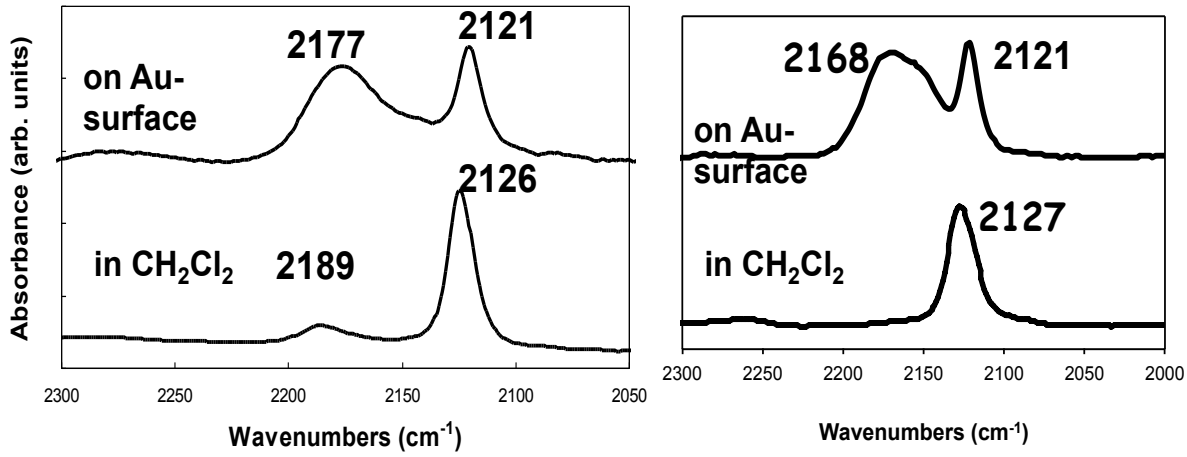

Figure II.16. SAM of 6,6'-biazulenyl ligands on Au(111). Left: SAM of compound 2.5. Right: SAM of 2,2'-diisocyano-6,6'-biazulenyl.[3]

when compared to the calculated theoretical height of 23 Å. The formation of the SAM can be followed by IR and spectra from the gold surface can be compared with that of the solution. For instance, the isocyanide stretch of 2126 cm^{-1} shifts to 2177 cm^{-1} being

higher in energy upon binding to the gold surface. The alkyne stretch of 2189 cm^{-1} falls underneath the broad stretch for the gold isocyanide interaction. Remarkably, the SAM appears to be stable at ambient conditions and stands upright in a linear fashion while being bound to the gold surface making it a good candidate for further studies on the gold surface.

II.5. Conclusions and Outlook

2,2'-diisocyano-1,1',3,3'-tetraethoxycarbonyl-6,6'-biazulenylacetylene ligand was prepared in a reasonable yield via a novel synthetic pathway and characterization methods offer support for its formation. Cyclic voltammetry experiments were performed for the diisocyanide as well as for the diamino and bisformamide ligand precursors. Results from these experiments indicated a reversible stepwise two-electron reduction of the biazulenic π-system. A potential resonance structure for the proposed coplanar diamagnetic biazulenide dianion was illustrated.

Coordination chemistry involving the use of electron rich tungsten pentacarbonyl units with the diisocyanide to prepare bis and monotungsten complexes was presented. Electronic absorption data suggested that the diisocyanide is involved in metal-to-bridge charge-transfer when complexed to tungsten pentacarbonyl.

Di and tetragold(I) complexes featuring a dcpm gold(I) backbone were made using isocyano bridging ligands. A crystal structure of the first gold half ring featuring 1,3-diethoxycarbonyl-2-isocyanoazulene and the dcpm gold(I) backbone was documented and showed a coplanar angle of 3° for the azulene motifs. Four of the gold complexes presented in this chapter were emissive during the solution-based photoluminescence experiments. A stable SAM featuring the diisocyanide was prepared on a Au(111) surface.

Future work should involve the pursuit of growing a crystal suitable for X-ray diffraction. This is of the utmost importance where it will help definitively prove the linear coplanar diisocyanide structure and would be the first of its kind. Based on the electrochemical results from this chapter, chemical reduction of the diisocyanide should be investigated. It would be expected that the cyclopentadienyl rings of azulene would partake in the reduction allowing for the possibility of η^5 complexes. Solubility of such complexes may be limited. Continuation of

the coordination chemistry featuring this ligand should be addressed. For instance, the monotungsten diisocyanide complex should be used to prepare a SAM since this complex would have a capped isocyanide hand and serve as an IR handle. Also, more gold complexes should be made featuring different backbones to determine its effect on emission. Lastly, metal organic frameworks could be prepared using the ligand in order to take advantage of it as a symmetrical bridge.

II.6 References

1) Barybin, M. V. *Coordination Chemistry Reviews*. **2010**, *254*, 1240.

2) DuBose, D. L.; Robinson, R. E.; Holovics, T. C.; Moody, D. R.; Weintrob, E. C.; Berrie, C. L.; Barybin, M. V. *Langmuir*. **2006**, *22*, 4599.

3) Maher, T. R.; Spaeth, A. D.; Neal, B. M.; Berrie, C. L.; Thompson, W. H.; Day V. W.; Barybin, M. V. *Journal of the American Chemical Society*, **2010**. 132, 15924.

4) Shoji, T.; Ito, S.; Toyota, K.; Yasunami, M.; Morita, N. *Tetrahedron Letters*. **2007**, *48*, 4999.

5) Razus, A. *Journal of the Chemical Society, Perkin Transactions 1*. **2000**, 981.

6) Hanke, M.; Jutz, C. *Synthesis*. **1980**, 31.

7) Hafner, K.; Meinhardt, K. P. *Organic Synthesis*. **1984**, *62*, 134.

8) Kurotobi, K.; Tabata, H.; Miyauchi, M.; Murafuji, T.; Sugihara, Y. *Synthesis*. **2002**, 1013.

9) Ito, S.; Inabe, H.; Okujima, T.; Morita, N.; Watanabe, M.; Harada, N.; Imafuku, K. *Journal of Organic Chemistry*. **2001**, *66*, 7090.

10) Huenig, S.; Ort, B. *Liebigs Annalen der Chemie*. **1984**, 1959.

11) Huenig, S.; Ort, B.; Hanke, M.; Jutz, C.; Morita, T.; Takase, K.; Fukazawa, Y.; Aoyagi, M.; Ito, S. *Liebigs Annalen der Chemie*. **1984**, 1952.

12) Ito, S.; Inabe, H.; Okujima, T.; Morita, N.; Watanabe, M.; Imafuku, K. *Tetrahedron Letters*. **2000**, *41*, 8343.

13) Ito, S.; Ando, M.; Nomura, A.; Morita, N.; Kabuto, C.; Mukai, H.; Ohta, K.; Kawakami, J.; Yoshizawa, A.; Tajiri, A. *Journal of Organic Chemistry*. **2005**, *70*, 3939.

14) Ito, S.; Okujima, T.; Morita, N. *Journal of the Chemical Society, Perkin Transactions 1*. **2002**, 1896.

15) King, C.; Khan, M. N. I., Staples, R. J.; Fackler, Jr, J. P. *Inorganic Chemistry*. **1992**, *31*, 3236.

16) Jones, W. B.; Yuan, J.; Narayanaswamy, R.; Young, M. A.; Elder, R. C.; Bruce, A. E.; Bruce, M. R. M. *Inorganic Chemistry*. **1995**, *34*, 1996.

17) Wong, W-Y.; Ho, C-L. *Coordination Chemistry Reviews*. **2006**, *250*, 2627.

18) Yam, V. W-W.; Choi, S. W-K.; Cheung, K-K. *Organometallics.* **1996**, *15*, 1734.

19) Yam, V. W-W,; Lo, K. K-W. *Chemical Society Reviews*. **1999**, *28*, 323.

20) Irwin, M. J.; Jia, G.; Payne, N. C.; Puddephatt, R. J. *Organometallics*. **1996**, *15*, 51.

21) Perreault, D.; Drouin, M.; Michel, A.; Harvey, P. D. *Inorganic Chemistry*. **1991**, *30*, 4.

22) Assefa, Z.; Staples, R. J.; Fackler, Jr., J. P. *Inorganic Chemistry*. **1994**, *33*, 2790.

23) King, C.; Wang, J-C.; Khan, M. N. I.; Fackler, Jr., J. P. *Inorganic Chemistry*. **1989**, *28*, 2145.

24) Shieh, S-J.; Hong, X.; Peng, S-M.; Che, C-M. *Journal of the Chemical Society, Dalton Transactions*. **1994**, 3067.

25) Paek, J. H.; Song, K. H.; Jung, I.; Kang, S. O.; Ko, J. *Inorganic Chemistry*. **2007**, *46*, 2787.

26) Tiekink, E. R. T.; Kang, J-G. *Coordination Chemistry Reviews*. **2009**, *253*, 1627.

27) Pyykko, P. *Angewandte Chemie, International Edition*. **2004**, *43*, 4412.

28) Scherbaum, F.; Grohmann, A.; Huber, B.; Kruger, C.; Schmidbaur, H. *Angewandte Chemie, International Edition*. **1988**, *27*, 1544.

29) Connely, N. G.; Geiger, W. E. *Chemical Reviews*. **1996**, *96*, 877.

30) Holovics, T. H.; Robinson, R. E.; Weintrob, E. C.; Toriyama, M.; Lushington, G. H.; Barybin, M. V. *Journal of the American Chemical Society*. **2006**, *128*, 2300.

31) Krimen, L. I. *Organic Synthesis*. **1970**, *50*, 1.

32) Irwin, M. J.; Rendina, L. M.; Vittal, J. J.; Puddephatt, R. J. *Chemical Communications*. **1996**, 1281.

33) Deplazes, S. F. "Ligand Design, Coordination, and Electrochemistry of Non-benzenoid Isocyanides." The University of Kansas, 2007. UMI, Ann Arbor, MI.

34) Maher, T. R. *Design of Novel Electron-Rich Organometallic Frameworks Involving Metal-Isocyanide Junctions*. **2009**, UMI: Ann Arbor.

35) Herrmann, W. A.; Zybill, C. In *Synthetic Methods of Organometallic and*

Inorganic Chemistry; Herrmann, W. A.; Salzer, A., eds; Thieme: Stuttgart, **1996**, *1*, 117.

36) Grubisha, D. S.; Rommel, J. S.; Lane, T. M.; Tysoe, W. T.; Bennett, D. W. *Inorganic Chemistry*. **1992**, *31*, 5022.

CHAPTER III

III. Regioselective Monofunctionalization of the 2,2'-Biazulenyl Scaffold: Chemistry of the 6-Isocyano-2,2'-biazulenyl Ligand

III.1. Introduction

Bicyclo[5.3.0]decapentaene, known as azulene, was not recognized for its nonbenzenoid character until the mid 1930s.[1,2] This polar, blue-colored compound is isomeric with naphthalene and has a dipole moment of 1.08 Debye (Figure III.1).

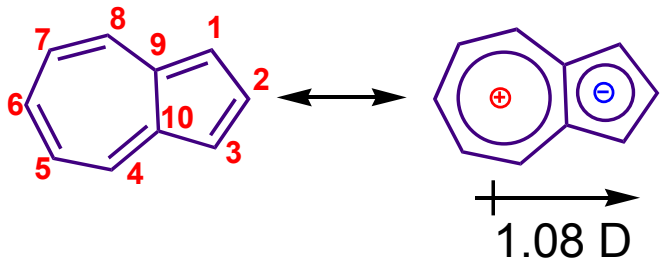

Figure III.1. Azulene: atom numbering scheme and the resonance form emphasizing its polar nature.

The polar nature of azulene and the remarkably low aromatic delocalization energy associated with its π-system (Figure III.2)[3] make this nonbenzenoid aromatic scaffold an attractive building block for the design of electronic and optical materials.[4]

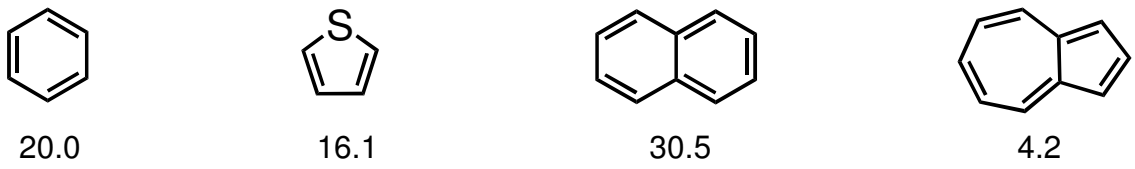

Figure III.2. Aromatic delocalization energies for select aromatics in kcal/mol.[3]

Many functionalized azulenes have been synthetically accessible, albeit usually in small quantities, for over fifty years thanks to the pioneering efforts of Haftner and Nozoe.[5,6] New

azulenic derivatives featuring isocyanide substituents have recently emerged and are being considered as molecular building blocks for charge delocalization and transport at the nanoscale.[7,8]

Treboux and coworkers theorized that the linear 2,6-azulenic motif could serve as an effective charge transport mediator between electron reservoirs and even function as a "molecular switch" due to its structural asymmetry (Figure III.3).[9] The first experimental reports on such systems are credited to the groups of Barybin and Chisholm.[7,10-12]

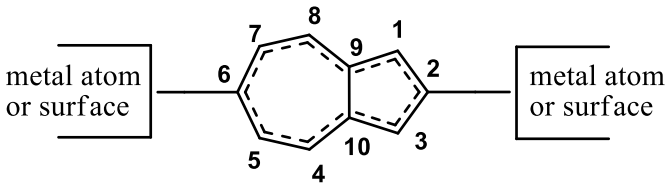

Figure III.3. The hypothetical 2,6-azulenic linker.[9]

The first examples of azulenic self assembled monolayer (SAMs) films were reported by Barybin, Berrie and co-workers in 2006.[13] These were formed by the adsorption of various isocyanoazulene derivatives on the gold(111) metal surface. The π-conducting isocyanide junctions serve as effective "alligator clips" to couple (both structurally and electronically) the azulenic scaffolds to the metal surface. Such one molecule-thick films are of keen interest to researchers in the field of molecular electronics.[13]

Adsorption of isocyanoarenes to the Au(111) surface occurs in the terminal upright fashion (i.e., nearly parallel to the surface normal) as suggested by infrared and ellipsometric analyses of aryl isocyanide SAMs.[13-15] Optical ellipsometry is a technique that allows estimating thickness of a film formed above the substrate surface. It has been recently demonstrated that a

number of isocyanoazulenic SAMs on Au(111) appear to have enhanced stability in air as compared to SAMs of benzenoid isocyanoarenes.[13]

The chemistry of linear π-bridges containing more than one azulenic unit was introduced in Chapter II of this Thesis. Three linear biazulenyl scaffolds can be envisioned that differ from each other by connectivity of the azulenic units through carbon atoms 2,2', 6,6', or 2,6' (Figure III.4).

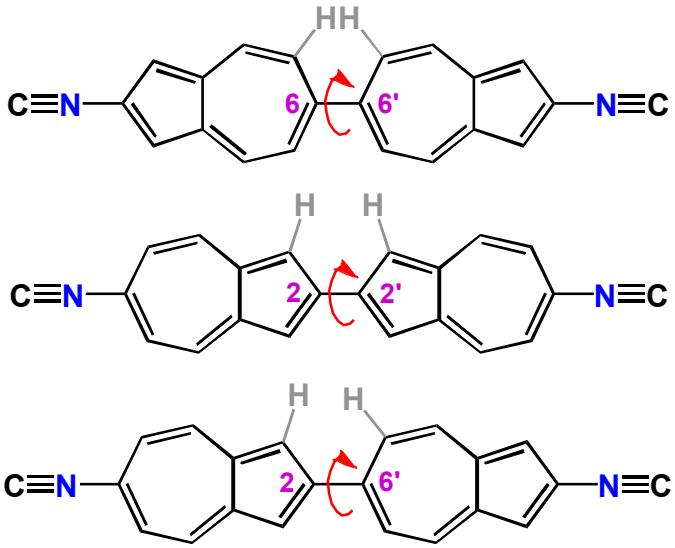

Figure III.4. Three possible linear diisocyanobiazulene frameworks.

The isocyanide-terminated linear biazulenyl linkers would feature quite different azulene-azulene interplanar angles, depending on the connectivity of the azulenic moieties (Figure III.4). Of the three possibilities, the 2,2'-coupled biazulenic framework should experience the lowest H-H repulsion in the vicinity of the central C-C bond. In fact, a gas-phase DFT study of the hypothetical 6,6'-diisocyano-2,2'-biazulenyl linker predicted the azulenyl-azulenyl dihedral angle to be less than 5°, while the interplanar angle in the crystallographically characterized 2,2'-biazulenyl is a perfect 0° (T. R. Maher, Ph.D. Thesis, The University of Kansas, 2009).

Thus, the 2,2'-biazulenic bridge would provide the highest extent of π-conjugation within the linker.

The synthesis of 2,2'-biazulene was first reported by Morita and Takase in 1982 and involves the Ulmann coupling of 2-haloazulene derivatives.[16] High temperatures are needed for this process, which employs highly activated copper metal, to proceed. Reasonable yields were reported by Morita and Takase for accessing 1,1',3,3'-tetra(ethoxycarbonyl)-2,2'-biazulene. All four ester functionalities can be efficiently removed to afford the unsubstituted 2,2'-biazulene.[16]

Surprisingly, the reactivity of 2,2'-biazulene has not been explored at all since the publication of its synthesis nearly 30 years ago, which may be associated with the relatively difficult synthetic access of the compound. In 2001, Makosza and coworkers published a convenient selective method for the amination of azulene and a few of its derivatives at carbon atom 6 using aminotriazole.[17] This report inspired our efforts to access the first functionalized 2,2'-biazulenes.

Dr. Tiffany Maher, a former graduate student in the Barybin group, attempted double functionalization of the 2,2'-biazulenyl scaffold at 6 and 6' positions with the amino groups in hope to subsequently convert these substituents into the isocyano groups.[18] Her efforts in this regard suggested that only one amino group can be installed at best, perhaps, because the 6'-position of the 2,2'-biazulenyl scaffold becomes deactivated toward nucleophilic substitution upon introduction of the electron-donating $-NH_2$ substituent at the opposite end of the molecule (position 6). Amination attempts were carried out on both the unsubstituted 2,2'-biazulene and its 1,1'-3,3'-tetra(ethoxycarbonyl) derivative. Only the "parent" 2,2'-biazulene appeared to undergo reasonably clean amination, which occurred exclusively at the 6-position. Dr. Maher was also able to isolate very small quantities of what appeared to be 6-isocyano-2,2'-biazulene

and obtain FTIR and elemental analysis evidence consistent with this formulation. However, the preliminary syntheses of both 6-formamido-2,2'-biazulene and 6-isocyano-2,2'-biazulene proved to be poorly reproducible at best and the unambiguous characterization of these compounds was yet to be accomplished.

III.2. Work Described in Chapter III

In Chapter III, highly reproducible, optimized regioselective syntheses of 6-amino-, 6-formamido-, and 6-isocyano-2,2'-biazulenes are reported. Preliminary X-ray crystallographic characterization of 6-amino-2,2'-biazulene is presented. The redox behavior of the above novel derivatives of 2,2'-biazulene, addressed by cyclic voltammetry, is described. In addition, interaction of 6-isocyano-2,2'-biazulene with the Au(111) surface to form the first 2,2'-biazulenic SAMs anchored to the metal via the isocyanide junctions is discussed.

III.3. Experimental Section

III.3.1 General Procedures and Starting Materials

Unless specified otherwise, all operations were performed under an argon atmosphere of 99.5% argon further purified by passage through columns of activated BASF catalyst and molecular sieves. All connections involving the gas purification systems were made of glass, metal, or other materials impermeable to air. Solutions were transferred via stainless steel cannulas whenever possible. Standard Schlenk techniques were employed with a double manifold vacuum line. CH_2Cl_2 and Et_3N were distilled over CaH_2. THF and Toluene were distilled over Na/benzophenone. Following purification, all distilled solvents were stored under argon.

Solution infrared spectra were recorded on a PerkinElmer Spectrum 100 FTIR spectrometer with samples sealed in 0.1mm gas tight NaCl cells. NMR samples were analyzed using Bruker DRX-400 and Bruker Avance 500 spectrometers. ^{1}H and ^{13}C chemical shifts are given with reference to residual ^{1}H and ^{13}C solvent resonances relative to Me_4Si. UV-vis spectra were recorded in CH_2Cl_2 at 24°C using a CARY 100 spectrophotometer.

Cyclic voltammetric (CV) and differential pulse voltammetric (DPV) experiments on 2 x 10^{-3}M solutions of selected compounds in CH_2Cl_2 were conducted at room temperature using an EPSILON (Bioanalytical Systems, INC., West Lafayette, IN) electrochemical workstation. The electrochemical cell was placed in an argon-filled Vacuum Atmospheres dry-box. Tetrabutylammonium hexafluorophosphate (0.1 M solution in CH_2Cl_2) was used as the supporting electrolyte. CV data was recorded at room temperature using a three component system consisting of a platinum working electrode, platinum wire auxillary electrode, and a glass encased non-aqueous silver/silver chloride reference electrode. The reference Ag/Ag^{+} electrode

was monitored with the ferrocenium/ferrocene couple. IR compensation was achieved prior to each CV scan by measuring the uncompensated solution resistance followed by incremental compensation and circuit stability testing. Background CV scans of the electrolyte solution were recorded before adding the analytes. The half-wave potentials ($E_{1/2}$) were determined as averages of the cathodic and anodic peak potentials of reversible couples and are referenced to the external FcH^+/FcH couple.[19] Elemental analysis was carried out by Chemisar/Guelph Chemical Laboratories Ltd, Ontario, Canada.

All work related to self-assembled monolayer formation and characterization (SAMs) was conducted by Mr. Brad M. Neal.

2,2'-Biazulene[16] and acetic-formic anhydride[20] were prepared according to literature procedures. Other reagents were obtained from commercial sources and used as received. Preliminary syntheses and limited characterization of compounds **3.1**, **3.2**, and **3.3** were originally described by Dr. Tiffany Maher, a former member of the Barybin group (T. R. Maher, Ph.D. Thesis, The University of Kansas, 2009).[18]

III. 3.2 Synthesis of 6-amino-2,2'-biazulene (3.1)

A solution of potassium tert-butoxide (1.36 g, 12.1 mmol) in 50 mL of DMSO was added via cannula to a solution of 2,2'-biazulene (0.510 g, 2.01 mmol) and 4-amino-1,2,4-triazole (0.506 g, 6.02 mmol) in 25 mL DMSO at room temperature. The reaction mixture was vigorously stirred for 5 hrs and then poured into 300 mL. The resulting solution was stirred for 10 minutes and then extracted with dichloromethane (5×75 mL). The organic fractions were combined and washed with water (5×100 mL). All solvent was removed via rotary evaporation and the residue was recrystallized from dichloromethane/pentane affording a 74% yield of **3.1** (0.400 g, 1.49 mmol) as a red-brown powder. MP: 152-155°C dec. HRMS (ES+, m/z) calc. for $C_{20}H_{16}N$: 270.1283, found: 270.1271.[18] ^{1}H NMR (Acetone-d^6, 400MHz, 25°C): δ 6.52 (s, br, 2H, NH_2), 6.55 (d, 2H, $H^{5,7}$, $^3J_{HH}$ = 8 Hz), 7.13(t, 2H, $H^{5',7'}$, $^3J_{HH}$ = 10 Hz), 7.43 (t, 1H, $H^{6'}$, $^3J_{HH}$ = 10 Hz), 7.51(s, 2H, $H^{1,3}$), 7.74(s, 2H, $H^{1',3'}$), 7.92(d, 2H, $H^{4,8}$, $^3J_{HH}$ = 12 Hz), 8.21(d, 2H, $H^{4',8'}$, $^3J_{HH}$ = 12 Hz) ppm.

III.3.3. Synthesis of 6-formamido-2,2'-biazulene (3.2)

Under argon atmosphere, formic acid (0.24 g, 5.2 mmol, 0.29 mL) was added to a 1 mL flask containing acetic anhydride (0.43 g, 4.2 mmol, 0.40 mL) cooled to 0 °C and equipped with a microscale reflux condenser and a magnetic stir bar. The resulting mixture was heated to 60 °C and stirred at this temperature for 3 hrs to form acetic-formic anhydride. The mixed anhydride was then cooled to room temperature and transferred with 5 mL of dichloromethane into a 100 mL single arm round bottom flask under argon. A red-orange solution of 6-amino-2,2'-biazulene (0.273 g, 1.01 mmol) in 50 mL of THF was transferred via cannula to the above solution of mixed anhydride with stirring. After one hour of stirring at room temperature, the color of the reaction mixture changed to cherry-red. The mixture was stirred for an additional 17

hrs while gradually turning green-brown. Then, the reaction mixture was poured into 50 mL of water to crash out the product. The solid was filtered off and washed with diethyl ether (2×100 mL). After drying at 10^{-2} Torr, **3.2** (0.225 g, 0.757 mmol) was isolated in a 75% yield as a forest green powder. MP: 125°C dec. This product is very poorly soluble or insoluble in most organic solvents.

III.3.4 Synthesis of 6-isocyano-2,2'-biazulene (3.3)

6- formamido-2,2'-biazulene (0.200 g, 0.674 mmol) was added to a 250 ml single arm round bottom flask using 75 ml THF. Triethylamine (0.341 g, 3.37 mmol, 0.470 mL) was added to a suspension of 6- formamido-2,2'-biazulene (0.200 g, 0.674 mmol) in 75 mL of THF and the resulting mixture was frozen using a liquid nitrogen bath. A solution of triphosgene (0.220 g, 0.741 mmol) in 30 mL of THF was added via cannula to the above frozen mixture over a period of 30 minutes. This reaction mixture was allowed to warm to room temperature and stirred for 6 hrs. Then, it was poured into 100 mL of water. After stirring for 10 minutes, the quenched reaction mixture was extracted with dichloromethane (5×50 mL) and the combined extracts were dried over anhydrous Na_2SO_4. The drying agent was filtered off and all solvent was removed from the filtrate by means of rotary evaporation under vacuum. The residue was recrystallized from dichloromethane/pentane to afford a 54% yield of **3.3** (0.102 g, 0.366 mmol) as a lime-green powder. FTIR (CH_2Cl_2): ν_{CN} 2115 cm^{-1}. ^1H NMR (THF-d^8, 400 MHz, 25 °C): δ 7.22 (m, 4H, $H^{5,7}/H^{5',7'}$, $^3J_{HH}$ = 8 Hz), 7.51 (t, 1H, $H^{6'}$, $^3J_{HH}$ = 8 Hz), 7.90 (s, 2H, $H^{1',3'}$), 8.01 (s, 2H, $H^{1,3}$), 8.27 (d, 2H, $H^{4',8'}$, $^3J_{HH}$ = 8 Hz), 8.31(d, 2H, $H^{4,8}$, $^3J_{HH}$ = 8 Hz) ppm.

III.4. Results and Discussion

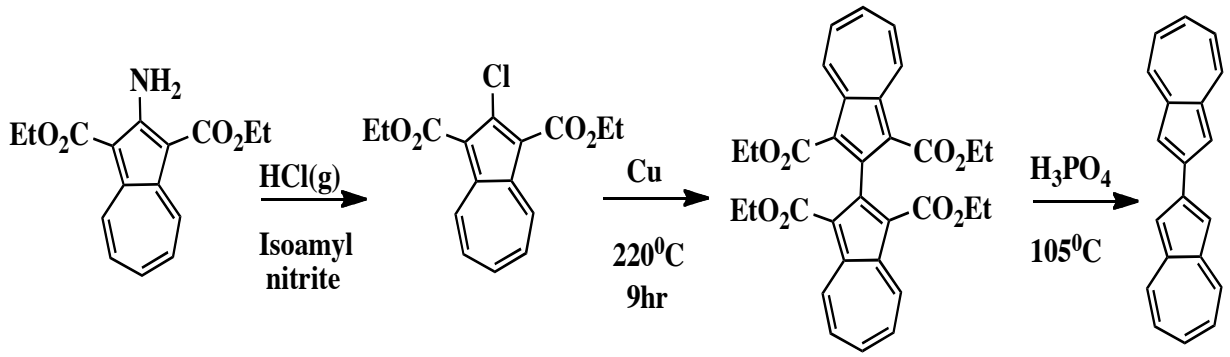

Scheme III.1. Synthesis of 2,2'-biazulene.[16]

The synthesis of 2,2'-biazulene was performed following a slightly modified procedure of Morita and Takase (Scheme III.1).[16] 2-Amino-1,3 di(ethoxycarbonyl)azulene was chlorinated in the presence of HCl(g) and isoamyl nitrite for a 97% yield of red crystals having a melting point of 70°C after recrystallization from ethanol. 2-Chloro-1,3-di(ethoxycarbonyl)azulene was then mixed with activated copper and the mixture was heated at 220°C to effect Ulmann coupling of the azulenic moieties.[16] After 9 hours of heating and subsequent workup of the reaction mixture, long purple needles of 1,1',3,3'-tetra(ethoxycarbonyl)-2,2'-biazulene were isolated in 62% yield. Treatment of this compound with H_3PO_4 at 105 °C effected clean de-esterification to give green microcrystals of 2,2'-biazulene in an 80% isolated yield.

Attempts to functionalize the 2,2'-biazulene scaffold with (an) amino group(s) were conducted using 4-amino-1,2,4-triazole, methoxyamine hydrochloride, or trimethyl hydrazinium iodide in the presence of potassium tert-butoxide and dimethyl sulfoxide.[17] All of these reagents have previously been shown to aminate azulene with varied efficiencies and regioselectivities.[17] Notably, the best yields of 6-aminoazulene have been obtained by employing 4-amino-1,2,4-

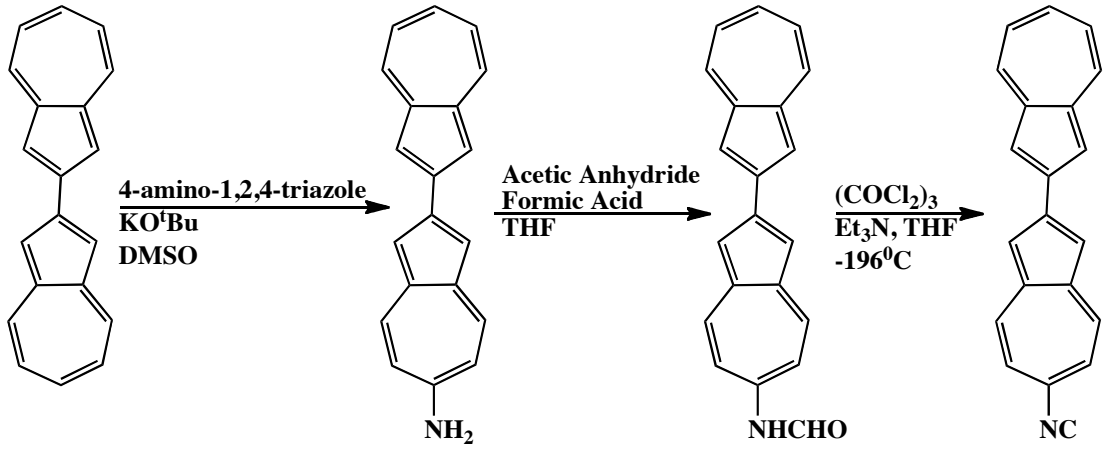

Scheme III.2. Synthesis of the 6-isocyano-2,2'-biazulene.

triazole as the aminating agent in the presence of a large excess of potassium tert-butoxide.[17]

Treatment of 2,2'-biazulene with excess 4-amino-1,2,4-triazole and a large excess of potassium tert-butoxide in dimethyl sulfoxide afforded a dark red-orange mixture. Following a somewhat laborious workup and recrystallization, red-brown microcrystalline 6-amino-2,2'-biazulene (**3.1**) was isolated in a 74% yield. Remarkably, only mono-amination of the 2,2-biazulenic framework exclusively at position 6 was observed. The ^{1}H NMR resonance for the NH_2 hydrogen atoms of **3.1** occurs at 6.52 ppm in acetone-d^6. This value is nearly 2 ppm downfield compared to δ(NH_2) observed for 6-aminoazulene in $CDCl_3$ (4.55 ppm), which probably indicates a more planar (or less pyramidal) geometry of the nitrogen atom in **3.1**. A resonance form of **3.1** featuring the sp^2-hybridized nitrogen atom is shown in Figure III.5. It appears that attaching the electron-donating NH_2 group at the 6-position of the 2,2'-biazulenyl framework completely shuts down the nucleophilic substitution reactivity at the other end of the molecule, i.e., at the 6'-position.

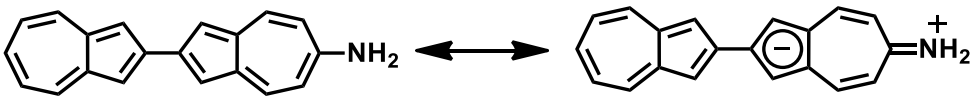

Figure III.5. Neutral and zwitterionic resonance forms of compound 3.1.

Combining **3.1** with acetic-formic anhydride, carefully prepared *in situ* by the recent method of Figueroa *et al*,[20] in THF afforded a very poorly soluble forest green powder of 6-formamido-2,2'-biazulene (**3.2**) in a 75% yield.

Multiple attempts to optimize the dehydration of formamide **3.2** have led to the following rather unusual synthetic protocol. A green suspension of **3.2** and excess triethylamine in THF needs to be frozen using a liquid nitrogen bath (*ca.* -196 °C) and then slowly treated with triphosgene dissolved in THF. After thawing and warming up to room temperature, the reaction mixture should be stirred for 6 hrs. Quenching of the mixture with water to remove any salt by-products followed by a simple reaction workup affords air-stable 6-isocyano-2,2'-biazulene (**3.3**) as a lime-green powder in a 54% yield(Scheme III.2).

The IR spectrum of **3.3** in CH_2Cl_2 features a prominent band at 2115 cm^{-1}, which is a signature of the isocyano group. In fact, the energy of this ν_{CN} band is practically identical to those documented by the Barybin group for other 6-isocyanoazulene derivatives (Table III.1). Interestingly, all 6-isocyanoazulene derivatives isolated to date exhibit ν_{CN} which is about 10 cm^{-1} lower in energy compared to any 2-isocyanoazulenes. This can be explained by the fact that the seven-membered ring of the azulenic moiety carries a partially positive charge and, hence, is electron-withdrawing with respect to the isocyano group. In addition, one can envision a minor

"cyclopentadienide"-like resonance form as illustrated for the case of **3.3** in Figure III.6, which features a reduced C-NR bond order.

Table III.1. Isocyanide stretching frequencies for selected isocyanoazulene derivatives.[13]

Compound	ν_{NC} (cm^{-1})
2-isocyanoazulene	2127
6-isocyanoazulene	2117
6-isocyano-1,3-dibromoazulene	2115
6-isocyano-1,3-di(ethoxycarbonyl)azulene	2115
2,6-diisocyano-1,3-di(ethoxycarbonyl)azulene[6]	2116, 2125
2-formamido-6-isocyano-1,3-di(ethoxycarbonyl)azulene	2116
3.3	2115

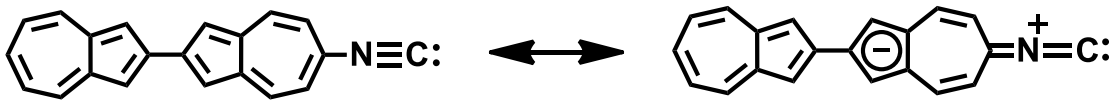

Figure III.6. Neutral and zwitterionic resonance forms of compound 3.3.

The redox properties of biazulenylamine **3.1** were assessed by cyclic voltammetry and differential pulse voltammetry (Figures III.7 and III.8). The CV and DPV profiles of **3.1** clearly indicate a *stepwise* two-electron reduction with both steps being reversible on the electrochemical timescale.

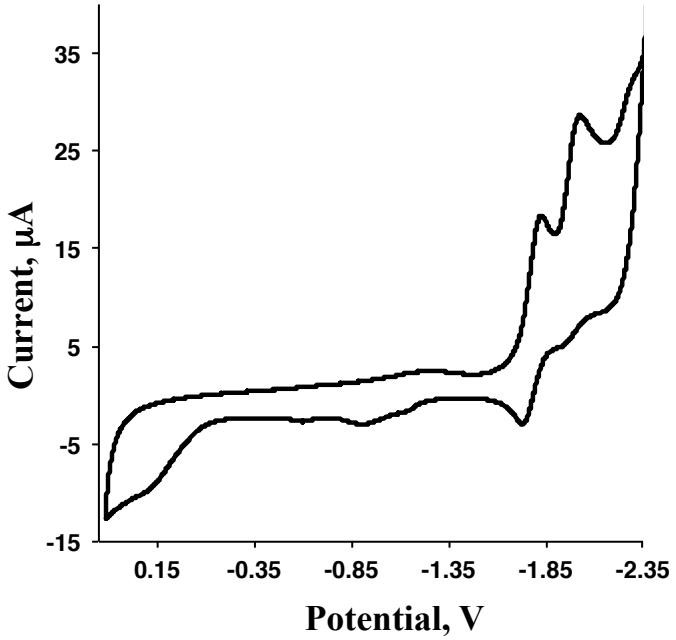

Figure III.7. Cyclic voltammogram of 3.1 in CH_2Cl_2 versus FcH/FcH^+. Scan rate = 100mV/sec.

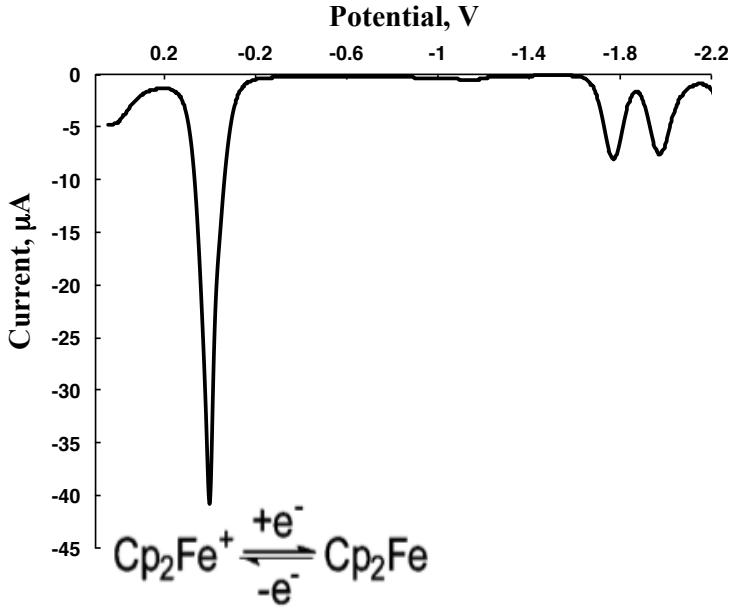

Figure III.8. Differential pulse voltammogram of 3.1 in CH_2Cl_2 with internal FcH/FcH^+ reference.

Table III.2 compares the redox properties of **3.1** and **3.3** with those of several other azulenic derivatives. From this table it is clear that **3.1** is harder while **3.3** is easier to reduce than the "parent" 2,2'-biazulene. This is consistent with the electron-donating nature of the amino group and the electron-withdrawing nature of the isocyano substituent. Also, attaching the 2-azulenyl moiety at the 2 position of 6-isocyanoazulene to give **3.3** makes the reduction potential less negative by virtue of significantly extending the conjugated π-system of the molecule.

Table III.2. Half-wave redox potentials for 3.1, 3.3, and several other azulenic derivatives in CH_2Cl_2 versus FcH/FcH^+.[8,18,21]

Compound	$E_{1/2, red1}$	$E_{1/2, red2}$
6-isocyanoazulene	-1.75	not observed
1,1',3,3'-tetra(ethoxycarbonyl)-2,2'-biazulene	-1.82	-2.14
2,2'-biazulene	-1.63	irreversible
3.1	-1.80	-2.00
3.3	-1.54	irreversible

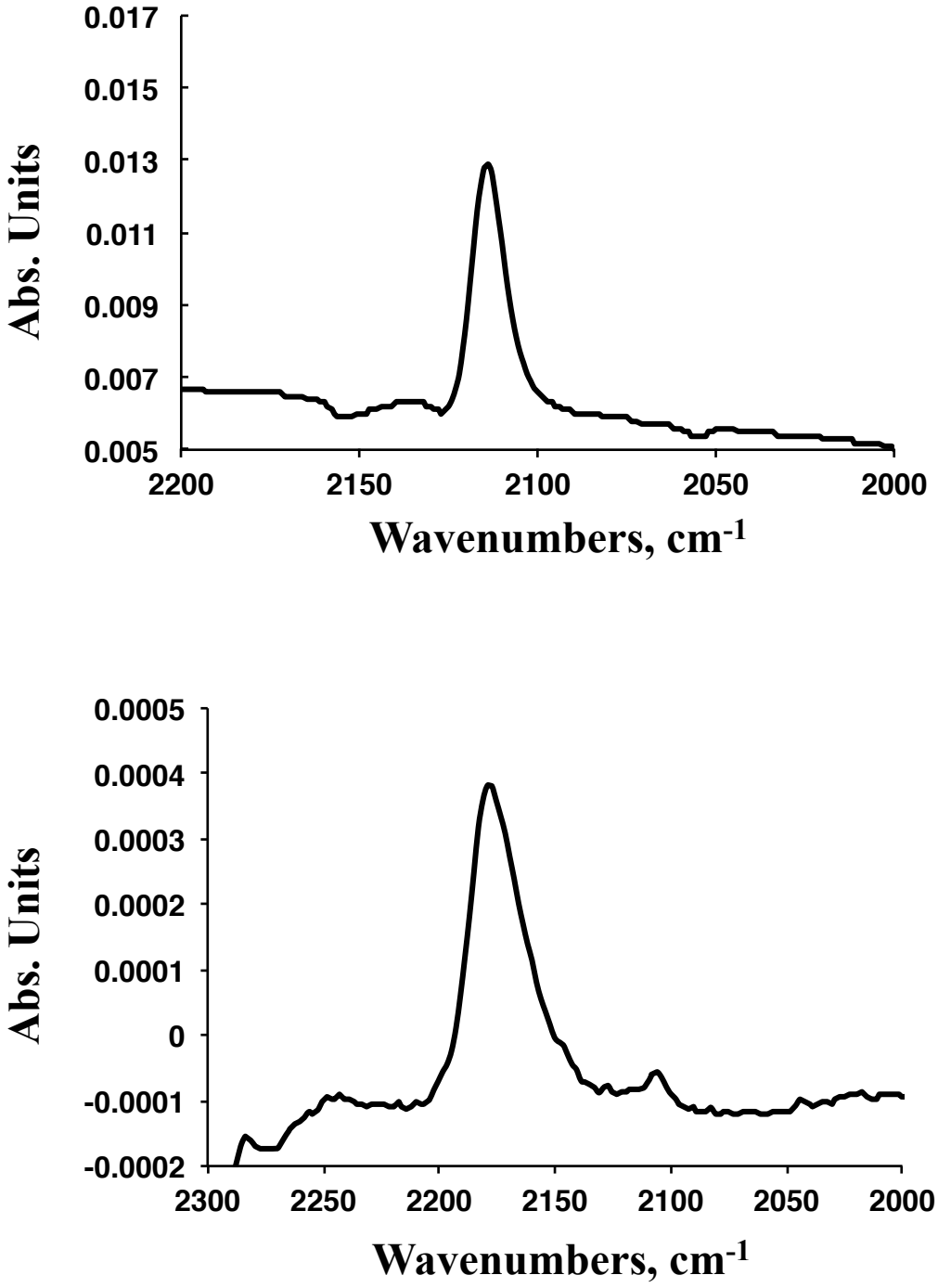

Figure III.9. Top: FTIR spectrum of 3.3 in CH_2Cl_2. Bottom: FTIR spectrum of 3.3 absorbed on Au(111).

Exposure of a Au(111) substrate to a solution of isocyanide **3.3** leads to the formation of a 2,2'-biazulenic film on the gold surface. The ellipsometric thickness of this film measured by Mr. Brad Neal is 25 Å, whereas the calculated thickness assuming the terminal upright coordination of the molecule to the gold surface through the isocyano group is only 16.5 Å. This discrepancy could arise from neglecting absorption of **3.3** at 632.4 nm (HeNe laser used in the experiment) and/or multilayer rather than monolayer formation due to some physisorbed molecules of **3.3**. Figure III.9 illustrates that the adsorption of **3.3** to the gold surface results in the shift of the ν_{CN} band from 2115 cm^{-1} to 2175 cm^{-1}. The latter ν_{CN} energy is typical for isocyanoazulenes adsorbed on Au(111) in the terminal upright fashion.[13,22] Importantly, the surface FTIR spectrum of **3.3** exhibits only one isocyanide environment (corresponding to the isocyanide group bound to gold). While the lack of any features in this spectrum that might correspond to the uncoordinated or "free" isocyanide group does not completely discount the possibility of a multilayer formation, it certainly suggests that such an arrangement is not likely.

A small twinned crystal of 6-amino-2,2'-biazulene was grown by slow evaporation of its solution in acetone. Preliminary X-ray analysis of **3.1** indicated that the two azulenic moieties in this compound are essentially coplanar (Figure III.10). The torsion angle of < 2° observed for **3.1** is very similar to that in the unsubstituted 2,2'-biazulene.[18] The central C-C bond length, C2-C12, of 1.440(13) Å compares well to the corresponding value of 1.455(4) Å documented for the unsubstituted 2,2-biazulene. The overall length of the molecule from N2 to H16 is about 1.42 nm.

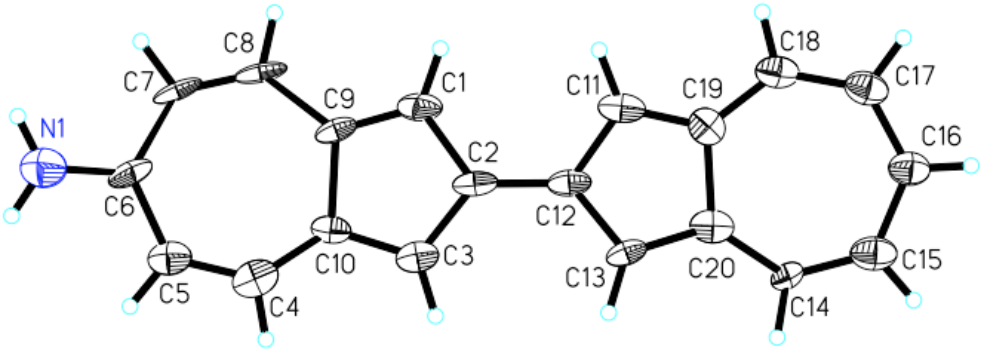

Figure III.10. Preliminary X-ray crystal structure of compound 3.1.

III.5. Conclusions and Outlook

The highly regioselective, optimized mono-amination of 2,2'-biazulene described herein constitutes the only example of direct derivatization of the 2,2'-biazulenic framework. This fully characterized aminobiazulene undergoes stepwise, reversible 2-electron reduction and functions as a convenient precursor to 6-isocyano-2,2'-biazulene, which can be reproducibly prepared in a moderate yield.

The latter compound was employed to form the first self-assembled monolayer films of 2,2'-biazulene. The isocyanide group serves as an effective "alligator clip" that couples the biazulenic framework to the gold surface and orients the molecule approximately parallel to the metal surface normal.

Future efforts will involve completing structural characterization of all monofunctionalized 2,2'-biazulenes reported in this Chapter and developing strategies for accessing hitherto unknown 6,6'-diisocyano-2,2'-biazulene, which would be a very intriguing linear linker relevant to molecular electronics applications. Complexation of **3.3** to the Cr(I) center to give a homoleptic octahedral low-spin d^5 adduct will allow studying unpaired electron spin delocalization within the 2,2'-biazulenic framework by ^{1}H, ^{13}C, and ^{14}N NMR.

III.6 References

1) Hansen, H. J. *Chimia*. **1996**, *50*, 489.
2) Hansen, H. J. *Chimia*. **1997**, *51*, 147.
3) Dewar, M. J. S. *The Molecular Orbital Theory of Organic Chemistry,* McGraw-Hill: New York, 1969.
4) Redl, F. X.; Kothe, O.; Rockl, K.; Bauer, W.; Daub, J. *Macromolecular Chemistry and Physics*. **2000**, *201*, 2091.
5) Nozoe, T.; Matsumura, S.; Murase, Y.; Seto, S. *Chemistry and Industry*. **1955**, 1257.
6) Hafner, K.; Meinhardt, K. P. *Organic Synthesis*. **1984**, *62*, 134.
7) Holovics, T. C.; Robinson, R. E.; Weintrob, E. C.; Toriyama, M.; Lushington, G. H.; Barybin, M. V. *Journal of the American Chemical Society*. **2006**, *128*, 2300.
8) Robinson, R. E.; Holovics, T. C.; Deplazes, S. F.; Powell, D. R.; Lushington, G. H.; Thompson, W. H.; Barybin, M. V. *Organometallics*. **2005**, *24*, 2386.
9) Treboux, G.; Lapstun, P.; Silverbrook, K. *Journal of Physical Chemistry B*. **1998**, *102*, 8978.
10) Barybin, M. V.; Chisholm, M. H.; Dalal, N. S.; Holovics, T. C.; Patmore, N. J.; Robinson, R. E.; Zipse, D. J. *Journal of the American Chemical Society*. **2005**, *127*, 15182.
11) Barybin, M. V.; Chisholm, M. H.; Patmore, N. J.; Robinson, R. E.; Singh, N. *Chemical Communications*. **2007**, 3652.
12) Alberding, B. G.; Barybin, M. V.; Chisholm, M. H.; Gustafson, T. L.; Reed, C. R.; Robinson, R. E.; Patmore, N. J.; Singh, N.; Turro, C. *Journal of the Chemical Society, Dalton Transactions*. **2010**, *39*, 1979.

13) DuBose, D. L.; Robinson, R. E.; Holovics, T. C.; Moody, D. R.; Weintrob, E. C.; Berrie, C. L.; Barybin, M. V. *Langmuir*. **2006**, *22*, 4599.

14) Henderson, J. I.; Feng, S.; Bein, T.; Kubiak, C. P. *Langmuir*. **2000**, *16*, 6183.

15) Clot, O.; Wolf, M. O. *Langmuir*. **1999**, *15*, 8549.

16) Morita, T.; Takase, K. *Bulletin of the Chemical Society of Japan*. **1982**, *55*, 1144.

17) Makosza, M.; Osinski, P. W.; Ostrowski, S. *Polish Journal of Chemistry*. **2001**, *75*, 275.

18) Maher, T. R. *Design of Novel Electron-Rich Organometallic Frameworks Involving Metal-Isocyanide Junctions*. **2009**, UMI: Ann Arbor.

19) Connelly, N. G.; Geiger, W. E. *Chemical Reviews*. **1996**, *96*, 877.

20) Ditri, T. B.; Fox, B. J.; Moore, C. E.; Rheingold, A. L.; Figueroa, J. S. *Inorganic Chemistry*. **2009**, *48*, 8362.

21) Huenig, S.; Ort, B. *Liebigs Annalen der Chemie*. **1984**, 1959.

22) Maher, T. R.; Spaeth, A. D.; Neal, B. M.; Berrie, C. L.; Thompson, W. H.; Day V. W.; Barybin, M. V. *Journal of the American Chemical Society*, **2010**, *132*, 15924

CHAPTER IV

IV. Synthesis, Properties and Complexation of *($_p$S)*-1-Isocyano-2-methylferrocene, the First Planar-chiral Isocyanide Ligand

(based on McGinnis, D. M.; Deplazes, S. F.; Barybin, M. V. *Journal of Organometallic Chemistry* **2011,** *in press* (web version published 05/27/11, doi:10.1016/j.jorganchem.2011.05.010)

IV.1. Introduction

Isocyanides, RN≡C, incorporating chiral substituents R are found in the structures of numerous natural products[1] and constitute important building blocks in contemporary polymer chemistry[2] and materials science.[2,3] To the best of this Thesis author's knowledge, all synthetic and naturally occurring organic isocyanides known to date exhibit *central* chirality. Recent progress in the chemistry of η^5-stabilized organometallic isocyanocyclopentadienides,[4] such as isocyanoferrocene (FcNC, Fc = ferrocenyl group), has created an opportunity to pursue a new class of chiral isocyanide compounds featuring *planar*-chiral substituents immediately attached to the isocyano functionality. Substances of this type are particularly intriguing given the vast and ever-growing role of planar chiral metallocene-based organometallics in synthesis, catalysis, and materials applications.[5] Notably, a few *central* chiral isocyanide compounds incorporating the ferrocenyl moiety are known.[6,7]

IV.2. Work Described in Chapter IV

In this Chapter, the synthesis and properties of the first planar-chiral isocyanide ligand, namely *($_p$S)*-1-isocyano-2-methylferrocene, as well as those of its crystallographically characterized *bis* adduct with PdI_2 are described. Redox behavior of several new planar-chiral ferrocene-based compounds is discussed. This Chapter constitutes an important revision/expansion of the original work of Dr. Stephan F. Deplazes (Ph.D. 2007), a former graduate student in the Barybin group.

IV.3. Experimental Section

IV.3.1 General Procedures and Starting Materials

Unless specified otherwise, synthetic operations were performed under an atmosphere of 99.5% argon purified by passage through columns of activated BASF catalyst and molecular sieves. Standard Schlenk techniques were employed with a double manifold vacuum line. Solvents, including deuterated solvents, were freed of impurities by standard procedures and stored under argon.[8]

Solution infrared spectra were recorded on a PerkinElmer Spectrum 100 FTIR spectrometer with samples sealed in 0.1 mm gas-tight NaCl cells. NMR samples were analyzed on a Bruker Avance 400 spectrometer. ^{1}H and ^{13}C NMR chemical shifts are given with reference to residual ^{1}H solvent resonances relative to $SiMe_4$. Chiral HPLC was performed using a Chiralpak OD column (0.46 cm × 25 cm, Dancel Chemical Ind., LTD) installed on a Shimadzu LC-10AD HPLC with a Shimadzu SPD-10 VP UV-Vis Detector. Optical rotation data were obtained using an AUTOPOL IV polarimeter (Rudolf Research Analytical). High resolution mass-spectral (HRMS) analyses were performed in the MS laboratory of the University of Kansas. Elemental analyses were carried out by Desert Analytics (currently Columbia Analytical Services), Tucson, Arizona. Melting points are uncorrected and were determined for samples in sealed capillary tubes.

Cyclic voltammetry (CV) experiments on *ca.* 2×10^{-3} M solutions of **4.2**, **4.3**, **4.4** were conducted using an EPSILON (Bioanalytical Systems INC., West Lafayette, IN) electrochemical workstation. The electrochemical cell was placed in an argon-filled Vacuum Atmospheres dry-box. Tetrabutylammonium hexafluorophosphate (0.1 M solution in CH_2Cl_2) was used as a supporting electrolyte. Cyclic voltammograms were recorded at 22 ± 2 °C using a three

component system consisting of a platinum (for **4.4**) or a glassy carbon (for **4.2** and **4.3**) working electrode, a platinum wire auxiliary electrode, and a glass encased non-aqueous silver/silver chloride reference electrode. The reference Ag/Ag^+ electrode was monitored with the internal Cp_2Co^+/Cp_2Co ($E_{1/2}$ = -1.33 V vs. Cp_2Fe^+/Cp_2Fe in CH_2Cl_2) couple for **4.2, 4.3** and isocyanoferrocene and with the external Cp_2Fe^+/Cp_2 couple for **4.4**.[9] IR compensation was achieved before each CV run by measuring the uncompensated solution resistance followed by incremental compensation and circuit stability testing. Background cyclic voltammograms of the electrolyte solution were recorded before addition of the analytes. The half-wave potentials ($E_{1/2}$), referenced to the Cp_2Fe^+/Cp_2Fe couple, were determined as averages of the cathodic and anodic peak potentials of reversible couples. The X-ray crystallographic analysis of compound **4.4** was performed by Dr. Douglas Powell.

Acetic-formic anhydride was prepared as previously published.[10] (*p*S)-1-Phthalimido-2-methylferrocene was synthesized by Dr. Stephan Deplazes.[11] All other reagents were obtained from commercial sources and used as received.

IV.3.2 Synthesis of ($_p$S)-1-amino-2-methylferrocene (4.1)

Hydrazine monohydrate (3.8 mL, 77.5 mmol) was added via syringe to a stirring solution of (*p*S)-1-phthalimido-2-methylferrocene (0.705 g, 2.04 mmol) in 30 mL of deoxygenated absolute ethanol. The resulting mixture was refluxed for 2 hr. Then, 20 mL of H_2O was added to cause precipitation of a light orange solid. This mixture was transferred into a separatory funnel containing 50 mL of H_2O and 30 mL of Et_2O to dissolve all of the solid. The organic layer was separated and the aqueous layer was extracted with additional Et_2O (4 × 20 mL). The combined organic fractions were dried over anhydrous Na_2SO_4 for 2 hr and filtered. All solvent was removed from the filtrate *in vacuo* to afford a 92% yield of **4.1** (0.404 g, 1.88 mmol) as a yellow powder. Mp: 101-103 °C (dec). $[\alpha]_D^{22}$ = -48 (*c* 0.2, CH_2Cl_2). ^{1}H NMR (400 MHz, $CDCl_3$, 25 °C): δ 1.91 (s, 3H, C*H*$_3$), 2.41 (s, 2H, N*H*$_2$), 3.77 (s br, 1H, C_5H_3), 3.90 (s, br, 1H, C_5H_3), 4.00 (s, 1H, C_5H_3), 4.03 (s, 5H, C_5H_5) ppm. ^{13}C{^{1}H} NMR (100.6 MHz, $CDCl_3$, 25 °C): δ 12.6 (*C*H$_3$), 58.3, 61.0, 65.7, 69.4, 72.48 (*cyclopentadienyl C atoms*) ppm.

IV.3.3 Synthesis of ($_p$S)-1-formamido-2-methylferrocene (4.2)

Acetic-formic anhydride (0.503 g, 5.71 mmol) dissolved in 10 mL of CH_2Cl_2 was added dropwise to an orange solution of **4.1** (0.350 g, 1.63 mmol) at room temperature. After stirring for 1 hr, all solvent was removed from the reaction mixture under vacuum to give an orange-brown oil. This oil was then subject to flash column chromatography on silica gel using neat Et_2O as eluent to collect a yellow-orange band. Removal of all solvent under vacuum provided an orange oil that solidified upon cooling to -15 °C for several hours to afford yellow-orange **4.2** (0.286 g, 1.18 mmol) in a 72% yield. Mp: 118 °C (dec). $[\alpha]_D^{23}$ = -479 (*c* 0.2, CH_2Cl_2). HRMS (*m/z*, ES+): found for $[M]^+$ 243.0340; calcd for $C_{12}H_{13}FeNO$ 243.0347. FTIR (CH_2Cl_2): ν_{CO}

1693 cm^{-1}. In dichloromethane solutions (c ≈ 0.015 g/mL) at 25 °C, **4.2** exists as a 1.7:1 mixture of two conformational isomers due to hindered rotation about the formamide N-C bond. ^{1}H NMR (400 MHz, CD_2Cl_2, 25 °C): δ 2.01 (s, 3H, C*H*$_3$), 2.02 (s, 3H, C*H*$_3$), 3.93 (dd, $^{3}J_{HH(1)}$ = $^{3}J_{HH(2)}$ ≈ 2.5 Hz, 1H, C_5H_3), 3.96 (dd, $^{3}J_{HH(1)}$ = $^{3}J_{HH(2)}$ ≈ 2.5 Hz, 1H, C_5H_3), 4.00 (s br, 1H, C_5H_3), 4.07 (s br, 1H, C_5H_3), 4.08 (s, 5H, C_5H_5), 4.14 (s, 5H, C_5H_5), 4.26 (s br, 1H, C_5H_3), 4.69 (s br, 1H, C_5H_3), 6.88 (s br, 1H, N*H*), 7.74 (dd br, $^{3}J_{HH}$ ≈ 12 Hz, 1H, N*H*), 8.25 (s br, 1H, *formyl H*), 8.35 (d, $^{3}J_{HH}$ ≈ 12 Hz, 1H, *formyl H*) ppm. $^{13}C\{^{1}H\}$ NMR (100.6 MHz, CD_2Cl_2, 25 °C): δ 12.56, 12.81 (C*H*$_3$), 63.20, 63.80, 63.92, 64.02, 66.93, 67.92, 70.32, 70.46, 77.34, 78.35, 91.80, 92.74 (*cyclopentadienyl C atoms*), 160.15, 165.24 (*formyl C*) ppm.

IV.3.4 Synthesis of ($_p$S)-1-isocyano-2-methylferrocene (4.3)

Phosphorus oxychloride (0.100 mL, 0.997 mmol) was added dropwise to a stirring solution of **4.2** (0.240 g, 0.987 mmol) and diisopropyl amine (0.420 mL, 2.96 mmol) in 25 mL of CH_2Cl_2 over a 5 minute period. The reaction mixture was stirred for 4 hr at room temperature while changing from orange to orange-brown in color. Then, the mixture was quenched with 100 mL of aqueous K_2CO_3 (10 % by weight). The organic layer was separated, washed with water (2 × 50 mL), and dried over anhydrous $MgSO_4$ for 2 hr. The drying agent was removed by filtration and the filtrate was concentrated under vacuum. The resulting residue was subject to flash column chromatography on silica gel using a 1:1 Et_2O/hexanes mixture as eluent. The first eluted band provided a yellow-orange solution, from which all solvent was removed under reduced pressure. The product was dried at 10^{-2} Torr to give yellow-orange **4.3** (0.188 g, 0.835 mmol) in an 85% yield. Mp: = 44 – 46 °C. $[\alpha]_D^{23}$ = +21.5 (*c* 0.2, CH_2Cl_2). HRMS (*m/z*, ES+): found for $[M]^+$ 225.0237; calcd for $C_{12}H_{11}FeN$ 225.0241. FTIR (CH_2Cl_2): ν_{CN} 2127 cm^{-1}. ^{1}H

NMR (400 MHz, $CDCl_3$, 25 °C): δ 2.14 (s, 3H), 3.99 (s br, 1H, C_5H_3), 4.10 (s br, 1H, C_5H_3), 4.21 (s, 5H, C_5H_5), 4.48 (s br, 1H, C_5H_3) ppm. $^{13}C\{^1H\}$ NMR (100.6 MHz, $CDCl_3$, 25 °C): δ 12.44 (CH_3), 64.93, 65.65, 67.83, 71.27, 81.81 (*cyclopentadienyl C atoms*), 164.3 (-N*C*) ppm.

IV.3.5 Synthesis of trans-[PdI_2{($_p$S)-1-isocyano-2-methylferrocene}$_2$] (4.4)

A solution of **4.3** (0.110 g, 0.489 mmol) in 10 mL of CH_2Cl_2 was added to a stirring grey slurry of PdI_2 (0.088 g, 0.244 mmol) in 10 mL CH_2Cl_2 via cannula. The resulting mixture was stirred at room temperature for 2 hr, while changing from orange to red-orange in color. The mixture was then filtered through a plug of Celite to give a red-orange filtrate. All solvent was removed *in vacuo* from the filtrate and the product was dried at 10^{-2} Torr to afford red microcrystalline **4.4** (0.160 g, 0.197 mmol) in an 81% yield. Mp: 180 °C (dec). $[\alpha]_D^{22}$ = +136 (*c* 0.2, CH_2Cl_2). Anal. Calcd. for $C_{24}H_{22}Fe_2I_2N_2Pd$: C, 35.57; H, 2.74; N 3.46. Found: C, 35.61; H, 2.51; N, 3.51. FTIR (CH_2Cl_2): ν_{CN} 2204 cm^{-1}. ^1H NMR (400 MHz, $CDCl_3$, 25 °C): δ 2.27 (s, 3H), 4.13 (dd, 1H, $^3J_{HH(1)} = {}^3J_{HH(2)} \approx 2.5$ Hz, 1H, C_5H_3), 4.22 (dd br, 1H, $^3J_{HH}$ =2.6 Hz, $^4J_{HH}$ =1.5 Hz), 4.35 (s, 5H), 4.65 (dd, 1H, $^3J_{HH}$ =2.5 Hz, $^4J_{HH}$ =1.5 Hz) ppm. $^{13}C\{^1H\}$ NMR(100.6 MHz, $CDCl_3$, 25 °C): δ 12.73 (CH_3), 65.97, 66.19, 68.91, 71.79, 83.49 (*cyclopentadienyl C atoms*) ppm.

IV.4. Results and Discussion

Aminoferrocene, $FcNH_2$, has been known for more than fifty years.[12] However, the tedious multi-step procedures and very low overall yields associated with its preparation had prevented further development of aminoferrocene's chemistry until the turn of the century when several improved syntheses of this compound emerged.[13-15] A particularly facile route to $FcNH_2$, published by Bildstein and coworkers in 1999,[13] involves a high yielding sequence ferrocene → lithioferrocene → iodoferrocene → *N*-ferrocenyl phthalimide and constitutes a greatly improved modification of Nesmeyanov's original procedure.[16] Dr. Deplazes of the Barybin group applied the above method to the preparation of optically pure planar-chiral *($_p$S)*-1-amino-2-methylferrocene and its *($_p$R)*-congener (Scheme IV.1). Accordingly, refluxing enantiopure *($_p$S)*-1-bromo-2-methylferrocene, the synthesis of which has been developed by Richards *et al*.,[17] with phthalimide in the presence of Cu_2O afforded golden crystalline *($_p$S)*-1-phthalimido-2-methylferrocene in a 55% yield. Reductive cleavage of *($_p$S)*-1-phthalimido-2-methylferrocene with hydrazine monohydrate in EtOH quantitatively provided yellow *($_p$S)*-1-amino-2-methylferrocene (**4.1**). Interestingly, compound **4.1** exhibits somewhat better air- and thermal stability compared to $FcNH_2$. The *($_p$R)* congener of **4.1** can be prepared from *($_p$R)*-1-bromo-2-methylferrocene following the procedure identical to that described in Scheme IV.1.

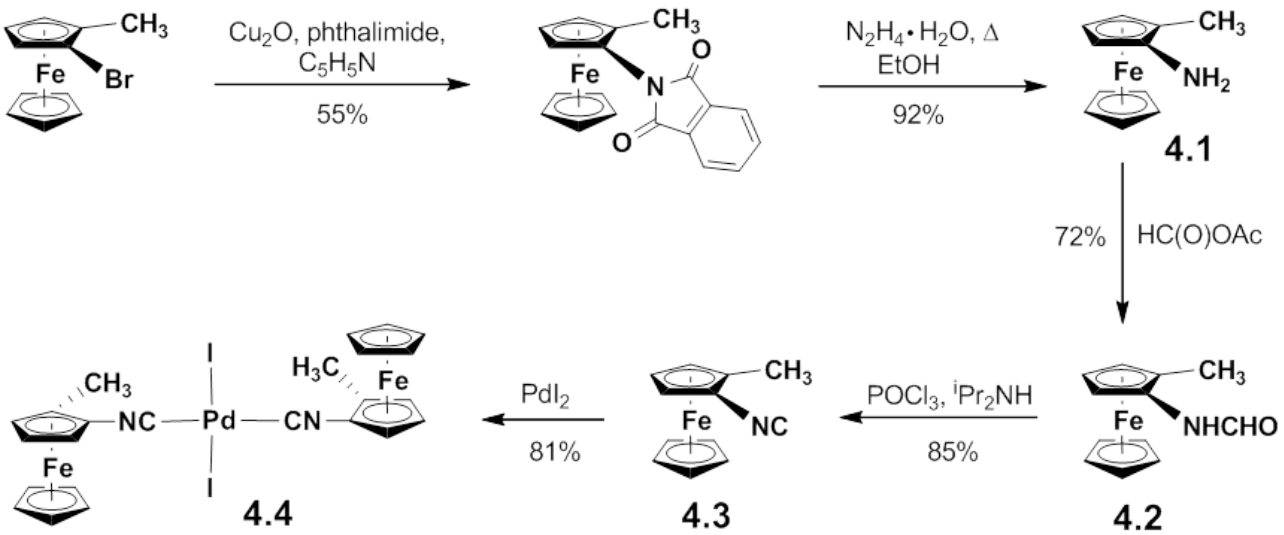

Scheme IV.1. Synthesis of compounds **4.1** – **4.4** from *(pS)*-1-bromo-2-methylferrocene.

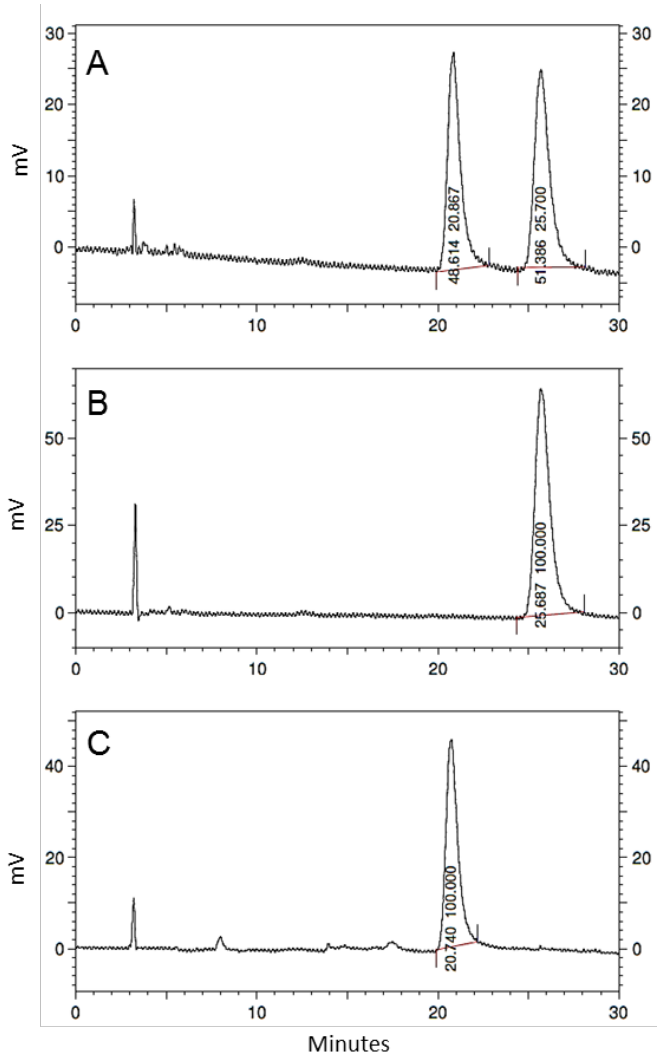

Figure IV.1. Chiral HPLC traces (identical conditions) for *rac*-1-amino-2-methylferrocene (A), *($_p$S)*- 1-amino-2-methylferrocene (B), and *($_p$R)*- 1-amino-2-methylferrocene (C). Adapted from S. F. Deplazes, Ph.D. Thesis, The University of Kansas, 2007.

Figure IV.1 compares chiral HPLC traces of *($_p$S)*-1-amino-2-methylferrocene and *($_p$R)*-1-amino-2-methylferrocene with that of a nearly racemic mixture thereof. The excellent enantiomeric purities (> 99% ee) of our samples of **4.1** and its *($_p$R)*-analogue stem from the retention of *($_p$S)* or *($_p$R)* planar chiralities of their 1-bromo-2-methylferrocene precursors,[17a] which in turn originate from the highly diastereoselective (100:1) ortholithiation of the corresponding *central*-chiral isopropyl-substituted ferrocenyloxazolines.[18] Notably, a non-

racemic mixture of *($_p$R)*- and *($_p$S)*-1-amino-2-methylferrocene with presumed 56% ee, prepared from the corresponding partially resolved *($_p$R)*-methylferrocene-α-carboxylic acid in four steps in an overall 26% yield, has been previously described.[19] This procedure involved alkaline hydrolysis of the *N*-ferrocenylbenzylurethan intermediate product obtained via a Curtius rearrangement of ferrocenylcarbonyl azide in benzyl alcohol.[19a]

Formylation of **4.1** with excess acetic-formic anhydride under mild conditions gave yellow-orange *($_p$S)*-1-formamido-2-methylferrocene (**4.2**) (Scheme IV.1). Formamide **4.2** exists as a mixture of two conformational isomers in dichloromethane solutions because of restricted rotation about the amide C-N bond.[20] The more abundant rotamer of **4.2** in solution features *trans* relationship of the hydrogen atoms within the H-N-C-H unit (or mutually *cis* orientation of the N-H and C=O bonds) as judged by the relatively large value of $^3J_{HH}$ = 12 Hz associated with its formamido moiety. While, generally speaking, this is *not* the thermodynamically preferred orientation of the formamido group,[21] such geometry is, in principle, well-suited for supporting intermolecular interactions between the molecules of **4** in solution through hydrogen bonding akin to the dimer formation postulated for solutions of FcNHCHO by Knox *et al.*[22] Dehydration of **4.2** with 1.0 equiv of $POCl_3$ provided yellow-orange *($_p$S)*-1-isocyano-2-methylferrocene (**4.3**) (Scheme IV.1). As in the case of the synthesis of FcNC,[23] it is important to avoid using excess dehydrating agent to achieve a high yield of the isocyanide. The spectroscopic signatures of the isocyano group in **5** (ν_{CN} = 2127 cm^{-1} in CH_2Cl_2 and $\delta(^{13}C)$ = 164.3 ppm in $CDCl_3$) are very similar to those documented for FcNC (ν_{CN} = 2122 cm^{-1} and $\delta(^{13}C)$ = 163.9 ppm) under the same conditions.[22,23]

Treatment of PdI_2 with 2 equiv of **4.3** affords air- and thermally stable, red crystalline *trans*-[PdI_2{*(pS)*-1-isocyano-2-methylferrocene}$_2$] (**4.4**) in a high yield (Scheme IV.1). The frequency of the ν_{CN} band documented for **4.4** is 77 cm^{-1} higher compared to that observed for uncoordinated **4.3** which indicates that the isocyanide ligands in **4.4** function essentially as σ-donors. Similar changes in the energy of ν_{CN} occur upon coordination of a number of other aryl isocyanides to PdI_2[24] and are caused by the fact that the lone pair of the terminal isocyanide carbon atom in R-N≡C is antibonding with respect to the N≡C bond.[4]

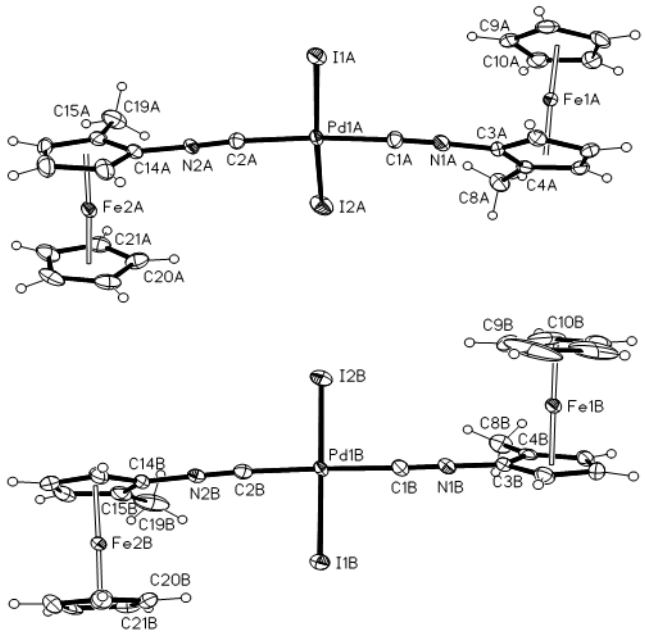

Figure IV.2. ORTEP diagrams of two independent molecules A (top) and B (bottom) in the asymmetric unit of **4.4**. Thermal ellipsoids are drawn at the 50% probability level.

Compound **4.4** crystallizes in the chiral space group $P2_1$. The asymmetric unit contains two crystallographically independent chiral molecules of **4.4** (A and B) that feature *trans* attachment of the *(pS)*-1-isocyano-2-methylferrocene ligands to the Pd(II) center (Figure IV.2). Selected bond distances and angles for both molecules are provided in Table IV.1. The metric parameters

of their square planar "$PdI_2(CN)_2$" cores are quite similar to those documented for a number of other crystallographically characterized *trans*-$PdI_2(CNAryl)_2$ complexes.[24] All C-N-C angles are essentially linear (175-178°). For **4.4**, the isocyanide N-C bond lengths vary from 1.144(5) to 1.164(6) Å and are comparable to the corresponding value of 1.157(3) Å found for "free" isocyanoferrocene.[25] The mutual orientation of the two ferrocenyl groups with respect to the C-N-C-Pd-C-N-C axis is best described as *anticlinal* for molecule A and *antiperiplanar* for molecule B because the dihedral angles defined by the centroids of the four cyclopentadienyl rings are 139° and 154° for molecules A and B, respectively. The cyclopentadienyl ring pairs sandwiching the iron atoms Fe(1A), Fe(2A), Fe(1B), and Fe(2B) deviate from the perfectly eclipsed conformation by 2°, 2°, 16°, and 4°, respectively.

Table IV.1. Selected bond distances (Å) and angles (°) for **4.4**.

	Molecule A	**Molecule B**
Pd-I(1)	2.5975(8)	2.5939(7)
Pd-I(2)	2.5981(8)	2.6000(7)
Pd-C(1)	1.953(4)	1.961(4)
Pd-C(2)	1.977(4)	1.946(4)
C(1)-N(1)	1.156(6)	1.144(6)
C(2)-N(2)	1.144(5)	1.164(6)
N(1)-C(3)	1.389(5)	1.400(6)
N(2)-C(14)	1.394(5)	1.378(6)
C(4)-C(8)	1.491(6)	1.482(6)
C(15)-C(19)	1.497(7)	1.486(8)
I(1)-Pd-I(2)	172.54(2)	179.48(2)
C(1)-Pd-C(2)	173.1(2)	178.1(2)
Pd-C(1)-N(1)	176.5(4)	177.6(4)
Pd-C(2)-N(2)	172.4(4)	176.1(4)
C(1)-N(1)-C(3)	177.2(4)	174.5(4)
C(2)-N(2)-C(14)	176.4(4)	178.2(4)

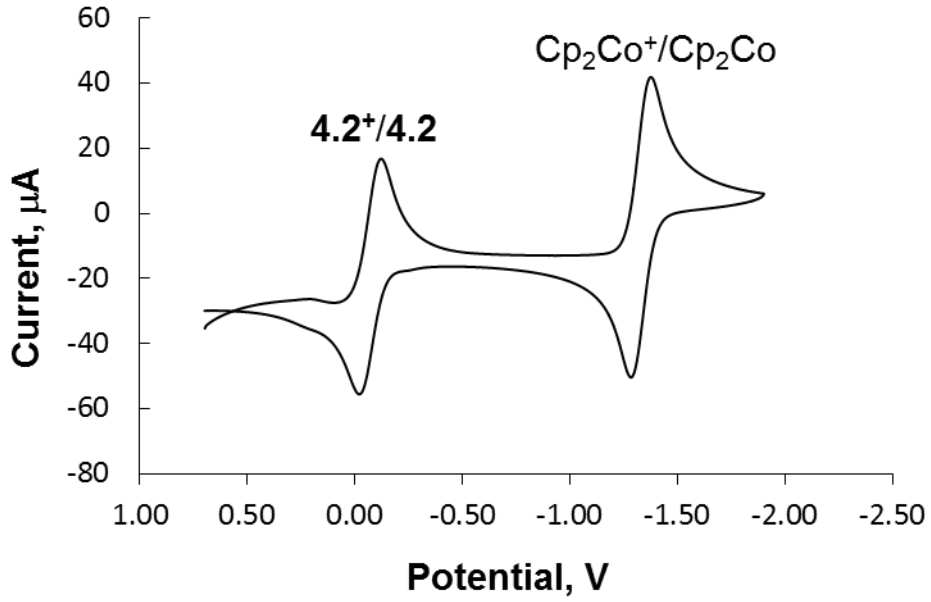

Figure IV.3. Cyclic voltammogram of **4.2** in 0.1 M [^{n}Bu$_4$N][PF$_6$]/CH$_2$Cl$_2$ vs. Cp$_2$Fe$^+$/Cp$_2$Fe. Scan rate = 100 mV/s. Internal Cp$_2$Co$^+$/Cp$_2$Co reference.

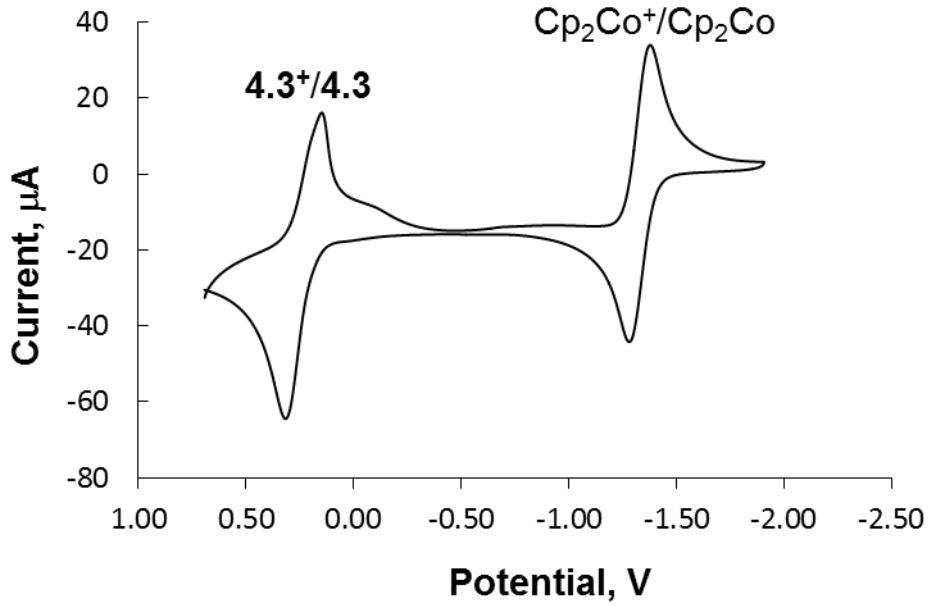

Figure IV.4. Cyclic voltammogram of **4.3** in 0.1 M [^{n}Bu$_4$N][PF$_6$]/CH$_2$Cl$_2$ vs. Cp$_2$Fe$^+$/Cp$_2$Fe. Scan rate = 100 mV/s. Internal Cp$_2$Co$^+$/Cp$_2$Co reference.

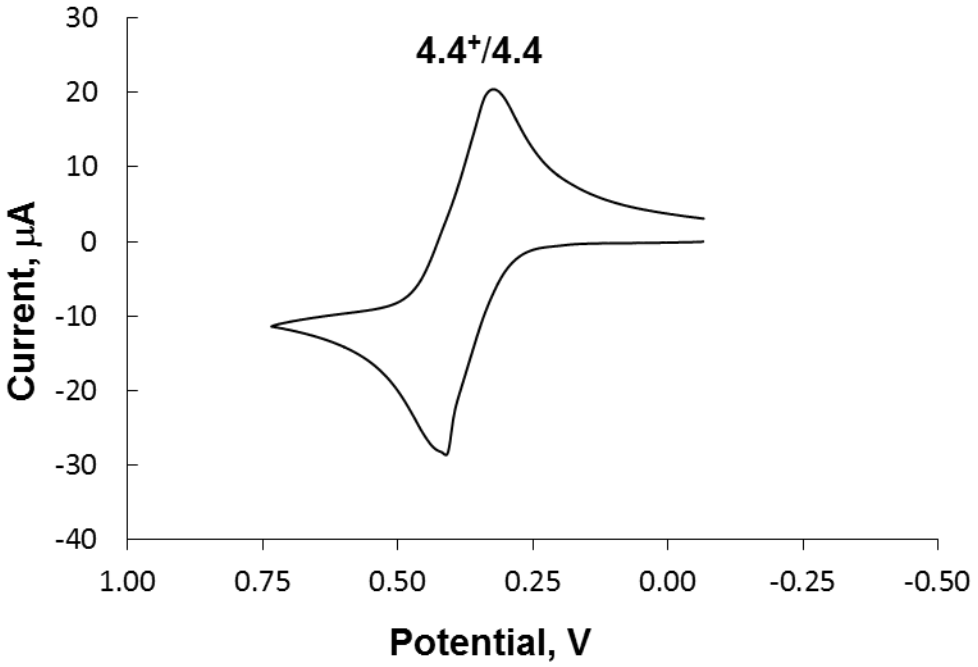

Figure IV.5. Cyclic voltammogram of **4.4** in 0.1 M [^{n}Bu$_4$N][PF$_6$]/CH$_2$Cl$_2$ at positive potentials vs. Cp$_2$Fe$^+$/Cp$_2$Fe. Scan rate = 100 mV/s. External Cp$_2$Fe$^+$/Cp$_2$Fe reference. Adapted from S. F. Deplazes, Ph.D. Thesis, The University of Kansas, 2007.

Figures IV.3, IV.4, and IV.5 show the cyclic voltammograms of solutions of **4.2**, **4.3**, and **4.4** in CH_2Cl_2. The half-wave potential ($E_{1/2}$) corresponding to the Fe^{2+}/Fe^{3+} couple increases in the order **4.2** < **4.3** < **4.4** (Table IV.2). This trend is a consequence of (a) the isocyano substituent being more electron-withdrawing / less electron-donating compared to the formamido substituent and (b) the 1-isocyano-2-methylferrocene ligands functioning primarily as σ-donors upon coordination to the Pd(II) center to form **4.4**. Indeed, engaging the lone pair of the terminal isocyanide carbon atom of **4.3** in bonding with the Pd(II) ion enhances the electron-withdrawing nature of the isocyanide junction with respect to the ferrocenyl moiety and, hence, makes the latter more difficult to oxidize. While the Fe^{2+}/Fe^{3+} couples for **4.2** and **4.4** are fully reversible ($i_{p,c}/i_{p,a} = 1.0$), this process for **4.3** is only partially reversible ($i_{p,c}/i_{p,a} \approx 0.6$) under the same conditions. Such electrochemical behavior of **4.3** appears to parallel the incomplete reversibility

of the Fe^{2+}/Fe^{3+} couple documented for its "parent" analogue, FcNC[7,23a] (Table IV.2). Notably, the $E_{1/2}$ value corresponding to the Fe^{2+}/Fe^{3+} couple for **4.3** is 33 mV less positive compared to that observed for FcNC due to the electron-donating influence of the methyl substituent in the former.

Table IV.2. Cyclic voltammetry data for FcNC, **4.2**, **4.3**, and **4.4**.[a]

Compound	$E_{1/2}(Fe^{2+}/Fe^{3+})$, V	$\Delta E_{p,c-p,a}$, mV	$i_{p,c}/i_{p,a}$
FcNC[b]	0.265	190	0.88
4.2	-0.071	168	1.0
4.3	0.232	103	0.62
4.4	0.368	89	1.0

[a] All measurements were performed in $CH_2Cl_2/[^nBu_4N][PF_6]$ at 22±2 °C to ensure quantitative comparison, scan rate = 100 mV/s. [b] Ref. 23a.

IV.5 Conclusions and Outlook

The work described herein has capitalized on the recent advancements in the syntheses of planar-chiral ferrocenyl halides, aminoferrocene, and isocyanoferrocene to access the first example of a planar-chiral isocyanide, **4.3**, in high enantiomeric purity. Upon complexation, this non-benzenoid aromatic isocyanide ligand exhibits robust redox activity, at least on the electrochemical time scale. Future efforts will include expanding the hitherto unavailable class of planar-chiral isocyanide ligands to include RNC species featuring "piano-stool" substituents R (e.g., see T. C. Holovics, Ph.D. Thesis, The University of Kansas, 2006) and applications of complexes of **4.3** and its derivatives in enantioselective catalysis.

IV.6 References

1) (a) Carson, M. J.; Simpson, J. S. *Natural Product Reports*. **2004**, *21*, 164.

   (b) Chang, C. W. J. *Progress in the Chemistry of Organic Natural Products*. **2000**, *80*, 1.

   (c) Chang, C. W. J.; Scheuer, P. J. *Topics in Current Chemistry*. **1993**, *167*, 33.

2) Nakano, T.; Okamoto, Y. *Chemical Reviews*. **2001**, *101*, 4013 and references therein.

3) Omenat, A.; Serrano, J.-L.; Sierra, T.; Amabilino, D. B.; Minguet, M.; Ramos, E.; Veciana, J. *Journal of Materials Chemistry*. **1999**, *9*, 2301.

4) Barybin, M. V. *Coordination Chemistry Reviews*. **2010**, *254*, 1240 and references therein.

5) (a) Deng, W.-P.; Snieckus, V.; Metallinos, C. *Stereoselective synthesis of planar chiral ferrocenes,* in: Dai, L.-X.; Hou, X.-L. (Eds.), *Chiral Ferrocenes in Asymmetric Catalysis,* Wiley-VCH, Weinheim, **2010**, pp. 15-54.

   (b) Blaser, H.-U.; Chen, W.; Camponovo, F.; Togni, A. *Chiral 1,2-disubstituted ferrocene diphosphines for asymmetric catalysis*, in: Štěpnička, P. (Ed.), *Ferrocenes: Ligands, Materials and Biomolecules*, John Wiley & Sons Ltd, West Sussex, England, **2008**, pp. 205-235.

   (c) Štěpnička, P.; Lamač, M. *Synthesis and catalytic use of planar chiral and polydentate ferrocene donors*, in: Štěpnička, P. (Ed.), *Ferrocenes: Ligands, Materials and Biomolecules*, John Wiley & Sons Ltd, West Sussex, England, **2008**, pp. 237-277.

   (d) Wagner, G.; Herrmann, R. *Chiral ferrocene derivatives. An introduction*, in: Togni, A.; Hayashi, T. (Eds.), *Ferrocenes*, VCH, Weinheim, **1995**, pp. 173-218.

6) Hida, N.; Takei, F.; Onitsuka, K.; Shiga, K.; Asaoka, S.; Iyoda, T.; Takahashi, S. *Angewandte Chemie*. **2003**, *115*, 4485.

7) El-Shihi, T.; Siglmüller, F.; Herrmann, R.; Carvalho, M. F. N. N., Pombeiro. *Journal of Organometallic Chemistry*. ***1987****, 335, 239.*

8) Gordon, A. J.; Ford, R. A. *The Chemist's Companion: A Handbook of Practical Data, Techinques, and References*, 1st ed., Wiley & Sons, New York, **1973**.

9) Connelly, N. G.; Geiger, W. E. *Chemical Reviews*. **1996**, *96*, 877.

10) Krimen, L. I. *Organic Synthesis*. **1970**, *50*, 1.

11) Deplazes, S. F. *Ligand Design, Coordination, and Electrochemistry of Nonbenzenoid Aryl Isocyanides*. **2007**, *Ph. D. Thesis*, The University of Kansas.

12) Plesske, K. *Angewandte Chemie International Edition*. **1962**, *1*, 394 and references therein.

13) Bildstein, B.; Malaun, M.; Kopacka, H.; Wurst, K.; Mitterböck, M.; Ongania, K.-H.; Opromolla, G.; Zanello, P. *Organometallics*. **1999**, *18*, 4325.

14) van Leusen, D.; Hessen, B. *Organometallics*. **2001**, *20*, 224.

15) Kavallieratos, K.; Hwang, S.; Crabtree, R. H. *Inorganic Chemistry*. **1999**, *38*, 5184.

16) (a) Nesmeyanov, A. N.; Sazonova, V. A.; Drozd, V. N. *Doklady Akademii Nauk S. S. S. R.* **1959**, *126*, 1004.

(b) Nesmeyanov, A. N.; Sazonova, V. A.; Drozd, V. N. *Chemische Berichte*. **1960**, *93*, 2717.

17) (a) Pickett, T. E.; Roca, F. X.; Richards, C. J. *Journal of Organic Chemistry*. **2003**, *68*, 2592.

(b) Pickett, T. E.; Richards, C. J. *Tetrahedron Letters*. **2001**, *42*, 3767.

18) Sammakia, T.; Latham, H. A. *Journal of Organic Chemistry*. **1995**, *60*, 6002.

19) (a) Lehner, H.; Schlögl, K.; *Monatshefte fur Chemie*. **1970**, *101*, 895.

(b) Rapić, V.; Schlögl, K., Steinitz, B. *Monatshefte fur Chemie*. **1977**, *108*, 767.

20) Kessler, H. *Angewandte Chemie International Edition*. **1970**, *9*, 219.

21) Schulz, G. E. Schirman, R. H. *Principles of Protein Structure*, Springer, New York, **1979**.

22) Knox, G. R.; Pauson, P. L.; Willison, D. *Organometallics*. **1990**, *9*, 301.

23) (a) Holovics, T. C.; Deplazes, S. F.; Toriyama, M.; Powell, D. R.; Lushington, G. H.; Barybin, M. V. *Organometallics*. **2004**, *23*, 2927.

(b) Barybin, M. V., Holovics, T. C.; Deplazes, S. F.; Lushington, G. H.; Powell, D. R., Toriyama, M. *Journal of the American Chemical Society*. **2002**, *124*, 13668.

24) (a) Lau, K. Y.; Mayr, A.; Cheung, K.-K. *Inorganica Chimica Acta*. **1999**, *285*, 223.

(b) Mayr, A.; Guo, J. *Inorganic Chemistry*. **1999**, *38*, 921.

(c) Mayr, A.; Mao, L.-F. *Inorganic Chemistry*. **1998**, *37*, 5776 and references therein.

25) Wrackmeyer, B.; Maisel, H. E.; Tok, O. L.; Milius, W.; Herberhold, M. *Zeitschrift fur Anorganische und Allgemeine Chemie*. **2004**, *630*, 2106.

Appendix 1

Crystallographic Data for compound 2.8

Table 1. Crystal data and structure refinement for Compound 2.8

Identification code	k34f	
Empirical formula	C61.50 H77 Au2 Cl F6 N2 O14 P2 S2	
Formula weight	1737.69	
Temperature	100(2) K	
Wavelength	0.71073 Å	
Crystal system	Triclinic	
Space group	P-1	
Unit cell dimensions	a = 12.7241(10) Å	α= 94.3280(10)°.
	b = 14.4095(11) Å	β= 97.6300(10)°.
	c = 19.5432(15) Å	γ = 113.3680(10)°.
Volume	3227.7(4) $Å^3$	
Z	2	
Density (calculated)	1.788 Mg/m^3	
Absorption coefficient	4.779 mm^{-1}	
F(000)	1726	
Crystal size	0.35 x 0.32 x 0.16 mm^3	
Theta range for data collection	2.45 to 30.53°.	
Index ranges	-18<=h<=18, -20<=k<=20, -27<=l<=27	
Reflections collected	37150	
Independent reflections	18761 [R(int) = 0.0296]	
Completeness to theta = 30.53°	95.0 %	
Absorption correction	Multi-scan	
Max. and min. transmission	1.000 and 0.582	
Refinement method	Full-matrix least-squares on F^2	
Data / restraints / parameters	18761 / 3 / 821	
Goodness-of-fit on F^2	1.006	
Final R indices [I>2sigma(I)]	R1 = 0.0380, wR2 = 0.0903	
R indices (all data)	R1 = 0.0553, wR2 = 0.0948	
Largest diff. peak and hole	2.663 and -2.280 e.$Å^{-3}$	

Table 2. Atomic coordinates (x 10^4) and equivalent isotropic displacement parameters ($Å^2$x 10^3) for Compound 2.8 U(eq) is defined as one third of the trace of the orthogonalized U_{ij} tensor.

	x	y	z	U(eq)
Au(1)	986(1)	2490(1)	2326(1)	16(1)
Au(2)	3621(1)	3532(1)	2390(1)	16(1)
P(1)	1278(1)	3088(1)	3486(1)	15(1)
P(2)	3522(1)	2769(1)	3386(1)	15(1)
O(11)	462(3)	3453(2)	455(1)	20(1)
O(12)	67(3)	3699(2)	-646(2)	29(1)
O(13)	1743(3)	-363(2)	-401(2)	23(1)
O(14)	1703(3)	323(2)	662(2)	26(1)
O(31)	3078(3)	5944(2)	1134(1)	22(1)
O(32)	2647(3)	6677(2)	226(2)	24(1)
O(33)	4175(3)	2866(2)	350(2)	23(1)
O(34)	4264(3)	2715(3)	-786(2)	30(1)
N(1)	967(3)	1874(3)	748(2)	19(1)
N(2)	3586(3)	4307(2)	930(2)	17(1)
C(1)	911(3)	2028(3)	1317(2)	19(1)
C(2)	3667(3)	4102(3)	1485(2)	19(1)
C(3)	2660(3)	3128(3)	3946(2)	17(1)
C(11)	704(3)	2395(3)	-415(2)	19(1)
C(12)	989(3)	1786(3)	40(2)	17(1)
C(13)	1280(3)	1058(3)	-318(2)	18(1)
C(14)	1428(4)	683(3)	-1572(2)	22(1)
C(15)	1389(4)	826(3)	-2269(2)	24(1)
C(16)	1083(4)	1500(3)	-2619(2)	24(1)
C(17)	720(4)	2229(3)	-2367(2)	24(1)
C(18)	603(4)	2475(3)	-1684(2)	23(1)
C(19)	808(3)	2053(3)	-1088(2)	18(1)
C(20)	1172(3)	1218(3)	-1032(2)	18(1)
C(21)	373(4)	3240(3)	-234(2)	20(1)
C(22)	114(4)	4256(3)	676(2)	22(1)
C(23)	176(4)	4314(3)	1453(2)	26(1)

C(24)	1599(3)	319(3)	38(2)	20(1)
C(25)	2066(4)	-1132(3)	-103(2)	22(1)
C(26)	3363(4)	-752(3)	90(2)	26(1)
C(31)	3157(3)	5276(3)	25(2)	18(1)
C(32)	3471(3)	4504(3)	244(2)	17(1)
C(33)	3664(3)	3951(3)	-316(2)	18(1)
C(34)	3513(4)	4014(3)	-1592(2)	23(1)
C(35)	3280(4)	4343(3)	-2212(2)	26(1)
C(36)	2929(4)	5124(4)	-2329(2)	28(1)
C(37)	2705(4)	5756(3)	-1865(2)	24(1)
C(38)	2785(4)	5804(3)	-1149(2)	22(1)
C(39)	3103(3)	5194(3)	-715(2)	18(1)
C(40)	3431(3)	4364(3)	-924(2)	17(1)
C(41)	2933(3)	6037(3)	452(2)	18(1)
C(42)	2890(4)	6685(3)	1597(2)	27(1)
C(43)	3914(4)	7704(3)	1730(2)	31(1)
C(44)	4055(4)	3114(3)	-291(2)	20(1)
C(45)	4640(4)	2095(3)	415(2)	25(1)
C(46)	4605(4)	1855(3)	1147(2)	26(1)
C(51)	133(3)	2273(3)	3925(2)	17(1)
C(52)	38(4)	1179(3)	3840(2)	20(1)
C(53)	-992(4)	488(3)	4144(2)	22(1)
C(54)	-861(4)	872(3)	4911(2)	28(1)
C(55)	-735(4)	1974(3)	5019(2)	24(1)
C(56)	271(4)	2680(3)	4696(2)	21(1)
C(61)	1386(3)	4393(3)	3668(2)	16(1)
C(62)	2358(4)	5171(3)	3362(2)	20(1)
C(63)	2422(4)	6244(3)	3530(2)	22(1)
C(64)	1266(4)	6303(3)	3290(2)	24(1)
C(65)	284(4)	5520(3)	3592(2)	26(1)
C(66)	212(4)	4440(3)	3424(2)	19(1)
C(71)	2752(3)	1373(3)	3171(2)	16(1)
C(72)	3004(4)	976(3)	2482(2)	20(1)
C(73)	2325(4)	-171(3)	2294(2)	25(1)
C(74)	2548(4)	-734(3)	2880(2)	27(1)
C(75)	2251(4)	-365(3)	3553(2)	25(1)

C(76)	2949(4)	791(3)	3763(2)	20(1)
C(81)	4915(3)	3111(3)	3951(2)	16(1)
C(82)	5715(4)	2704(3)	3643(2)	20(1)
C(83)	6850(4)	2997(3)	4157(2)	25(1)
C(84)	7474(4)	4150(3)	4360(2)	24(1)
C(85)	6690(3)	4595(3)	4643(2)	21(1)
C(86)	5534(3)	4279(3)	4136(2)	19(1)
S(1A)	3427(1)	2781(1)	5831(1)	32(1)
F(1A)	4786(3)	1942(3)	6362(3)	71(1)
F(2A)	4907(3)	3278(3)	6998(2)	45(1)
F(3A)	3423(3)	1842(3)	6923(2)	59(1)
O(1A)	2782(3)	3245(3)	6161(2)	37(1)
O(2A)	2715(4)	1817(3)	5394(2)	62(1)
O(3A)	4372(4)	3460(3)	5539(2)	52(1)
C(1A)	4171(4)	2444(4)	6569(3)	36(1)
S(2A)	7657(1)	1711(1)	2186(1)	22(1)
F(4A)	5463(2)	686(2)	2277(2)	40(1)
F(5A)	6192(3)	-167(2)	1711(2)	54(1)
F(6A)	6634(3)	159(3)	2828(2)	54(1)
O(4A)	8583(3)	1377(2)	2212(2)	33(1)
O(5A)	7749(3)	2408(3)	2780(2)	35(1)
O(6A)	7319(3)	1983(2)	1526(2)	30(1)
C(2A)	6429(4)	552(4)	2264(3)	31(1)
Cl(1S)	4240(2)	-353(2)	5501(1)	87(1)
C(1S)	5213(9)	740(2)	5204(4)	71(5)

Table 3. Bond lengths [Å] and angles [°] for Compound 2.8.

Au(1)-C(1)	2.010(4)
Au(1)-P(1)	2.2910(10)
Au(1)-Au(2)	3.0621(3)
Au(2)-C(2)	2.002(4)
Au(2)-P(2)	2.3007(10)
P(1)-C(61)	1.833(4)
P(1)-C(51)	1.833(4)
P(1)-C(3)	1.841(4)
P(2)-C(81)	1.819(4)
P(2)-C(3)	1.832(4)
P(2)-C(71)	1.839(4)
O(11)-C(21)	1.339(5)
O(11)-C(22)	1.450(5)
O(12)-C(21)	1.199(5)
O(13)-C(24)	1.340(5)
O(13)-C(25)	1.459(5)
O(14)-C(24)	1.208(5)
O(31)-C(41)	1.345(4)
O(31)-C(42)	1.459(5)
O(32)-C(41)	1.210(5)
O(33)-C(44)	1.335(5)
O(33)-C(45)	1.457(5)
O(34)-C(44)	1.202(5)
N(1)-C(1)	1.135(5)
N(1)-C(12)	1.386(5)
N(2)-C(2)	1.148(5)
N(2)-C(32)	1.392(5)
C(3)-H(3A)	0.9900
C(3)-H(3B)	0.9900
C(11)-C(12)	1.406(6)
C(11)-C(19)	1.410(5)
C(11)-C(21)	1.471(6)
C(12)-C(13)	1.411(5)
C(13)-C(20)	1.428(5)

C(13)-C(24)	1.472(6)
C(14)-C(15)	1.390(6)
C(14)-C(20)	1.408(5)
C(14)-H(14A)	0.9500
C(15)-C(16)	1.375(6)
C(15)-H(15A)	0.9500
C(16)-C(17)	1.389(6)
C(16)-H(16A)	0.9500
C(17)-C(18)	1.397(6)
C(17)-H(17A)	0.9500
C(18)-C(19)	1.396(6)
C(18)-H(18A)	0.9500
C(19)-C(20)	1.457(6)
C(22)-C(23)	1.505(6)
C(22)-H(22A)	0.9900
C(22)-H(22B)	0.9900
C(23)-H(23A)	0.9800
C(23)-H(23B)	0.9800
C(23)-H(23C)	0.9800
C(25)-C(26)	1.501(6)
C(25)-H(25A)	0.9900
C(25)-H(25B)	0.9900
C(26)-H(26A)	0.9800
C(26)-H(26B)	0.9800
C(26)-H(26C)	0.9800
C(31)-C(32)	1.400(5)
C(31)-C(39)	1.431(5)
C(31)-C(41)	1.468(5)
C(32)-C(33)	1.411(5)
C(33)-C(40)	1.417(5)
C(33)-C(44)	1.477(6)
C(34)-C(35)	1.372(6)
C(34)-C(40)	1.396(5)
C(34)-H(34A)	0.9500
C(35)-C(36)	1.389(6)
C(35)-H(35A)	0.9500

C(36)-C(37)	1.374(6)
C(36)-H(36A)	0.9500
C(37)-C(38)	1.384(6)
C(37)-H(37A)	0.9500
C(38)-C(39)	1.401(6)
C(38)-H(38A)	0.9500
C(39)-C(40)	1.462(6)
C(42)-C(43)	1.502(6)
C(42)-H(42A)	0.9900
C(42)-H(42B)	0.9900
C(43)-H(43A)	0.9800
C(43)-H(43B)	0.9800
C(43)-H(43C)	0.9800
C(45)-C(46)	1.499(6)
C(45)-H(45A)	0.9900
C(45)-H(45B)	0.9900
C(46)-H(46A)	0.9800
C(46)-H(46B)	0.9800
C(46)-H(46C)	0.9800
C(51)-C(52)	1.527(5)
C(51)-C(56)	1.536(5)
C(51)-H(51A)	1.0000
C(52)-C(53)	1.525(5)
C(52)-H(52A)	0.9900
C(52)-H(52B)	0.9900
C(53)-C(54)	1.521(6)
C(53)-H(53A)	0.9900
C(53)-H(53B)	0.9900
C(54)-C(55)	1.526(6)
C(54)-H(54A)	0.9900
C(54)-H(54B)	0.9900
C(55)-C(56)	1.534(6)
C(55)-H(55A)	0.9900
C(55)-H(55B)	0.9900
C(56)-H(56A)	0.9900
C(56)-H(56B)	0.9900

C(61)-C(62)	1.530(5)
C(61)-C(66)	1.536(5)
C(61)-H(61A)	1.0000
C(62)-C(63)	1.524(6)
C(62)-H(62A)	0.9900
C(62)-H(62B)	0.9900
C(63)-C(64)	1.520(6)
C(63)-H(63A)	0.9900
C(63)-H(63B)	0.9900
C(64)-C(65)	1.537(6)
C(64)-H(64A)	0.9900
C(64)-H(64B)	0.9900
C(65)-C(66)	1.530(6)
C(65)-H(65A)	0.9900
C(65)-H(65B)	0.9900
C(66)-H(66A)	0.9900
C(66)-H(66B)	0.9900
C(71)-C(76)	1.530(5)
C(71)-C(72)	1.545(5)
C(71)-H(71A)	1.0000
C(72)-C(73)	1.517(6)
C(72)-H(72A)	0.9900
C(72)-H(72B)	0.9900
C(73)-C(74)	1.512(6)
C(73)-H(73A)	0.9900
C(73)-H(73B)	0.9900
C(74)-C(75)	1.530(6)
C(74)-H(74A)	0.9900
C(74)-H(74B)	0.9900
C(75)-C(76)	1.535(6)
C(75)-H(75A)	0.9900
C(75)-H(75B)	0.9900
C(76)-H(76A)	0.9900
C(76)-H(76B)	0.9900
C(81)-C(82)	1.524(5)
C(81)-C(86)	1.537(5)

C(81)-H(81A)	1.0000
C(82)-C(83)	1.531(6)
C(82)-H(82A)	0.9900
C(82)-H(82B)	0.9900
C(83)-C(84)	1.523(6)
C(83)-H(83A)	0.9900
C(83)-H(83B)	0.9900
C(84)-C(85)	1.521(6)
C(84)-H(84A)	0.9900
C(84)-H(84B)	0.9900
C(85)-C(86)	1.539(5)
C(85)-H(85A)	0.9900
C(85)-H(85B)	0.9900
C(86)-H(86A)	0.9900
C(86)-H(86B)	0.9900
S(1A)-O(1A)	1.429(4)
S(1A)-O(3A)	1.435(4)
S(1A)-O(2A)	1.449(4)
S(1A)-C(1A)	1.822(6)
F(1A)-C(1A)	1.336(6)
F(2A)-C(1A)	1.330(6)
F(3A)-C(1A)	1.322(5)
S(2A)-O(4A)	1.436(3)
S(2A)-O(6A)	1.436(3)
S(2A)-O(5A)	1.437(3)
S(2A)-C(2A)	1.813(5)
F(4A)-C(2A)	1.321(5)
F(5A)-C(2A)	1.351(6)
F(6A)-C(2A)	1.319(5)
Cl(1S)-C(1S)	1.770(3)
Cl(1S)-C(1S)#1	1.771(3)
C(1S)-Cl(1S)#1	1.771(3)
C(1S)-H(1SA)	0.9900
C(1S)-H(1SB)	0.9900

C(1)-Au(1)-P(1)	174.04(12)

C(1)-Au(1)-Au(2)	85.46(11)
P(1)-Au(1)-Au(2)	88.59(3)
C(2)-Au(2)-P(2)	176.12(11)
C(2)-Au(2)-Au(1)	99.98(11)
P(2)-Au(2)-Au(1)	78.81(3)
C(61)-P(1)-C(51)	107.14(17)
C(61)-P(1)-C(3)	104.97(18)
C(51)-P(1)-C(3)	106.51(18)
C(61)-P(1)-Au(1)	114.57(13)
C(51)-P(1)-Au(1)	112.44(13)
C(3)-P(1)-Au(1)	110.64(12)
C(81)-P(2)-C(3)	104.09(17)
C(81)-P(2)-C(71)	110.33(18)
C(3)-P(2)-C(71)	104.38(18)
C(81)-P(2)-Au(2)	114.91(12)
C(3)-P(2)-Au(2)	111.72(13)
C(71)-P(2)-Au(2)	110.73(12)
C(21)-O(11)-C(22)	115.4(3)
C(24)-O(13)-C(25)	117.7(3)
C(41)-O(31)-C(42)	115.7(3)
C(44)-O(33)-C(45)	114.4(3)
C(1)-N(1)-C(12)	172.6(4)
C(2)-N(2)-C(32)	177.1(4)
N(1)-C(1)-Au(1)	172.2(4)
N(2)-C(2)-Au(2)	171.2(4)
P(2)-C(3)-P(1)	114.9(2)
P(2)-C(3)-H(3A)	108.5
P(1)-C(3)-H(3A)	108.5
P(2)-C(3)-H(3B)	108.5
P(1)-C(3)-H(3B)	108.5
H(3A)-C(3)-H(3B)	107.5
C(12)-C(11)-C(19)	106.9(4)
C(12)-C(11)-C(21)	127.3(3)
C(19)-C(11)-C(21)	125.8(4)
N(1)-C(12)-C(11)	124.4(3)
N(1)-C(12)-C(13)	124.1(4)

C(11)-C(12)-C(13)	111.5(3)
C(12)-C(13)-C(20)	105.8(3)
C(12)-C(13)-C(24)	122.2(3)
C(20)-C(13)-C(24)	131.9(4)
C(15)-C(14)-C(20)	128.2(4)
C(15)-C(14)-H(14A)	115.9
C(20)-C(14)-H(14A)	115.9
C(16)-C(15)-C(14)	130.4(4)
C(16)-C(15)-H(15A)	114.8
C(14)-C(15)-H(15A)	114.8
C(15)-C(16)-C(17)	129.1(4)
C(15)-C(16)-H(16A)	115.5
C(17)-C(16)-H(16A)	115.5
C(16)-C(17)-C(18)	128.1(4)
C(16)-C(17)-H(17A)	115.9
C(18)-C(17)-H(17A)	115.9
C(19)-C(18)-C(17)	129.3(4)
C(19)-C(18)-H(18A)	115.3
C(17)-C(18)-H(18A)	115.3
C(18)-C(19)-C(11)	124.2(4)
C(18)-C(19)-C(20)	128.0(4)
C(11)-C(19)-C(20)	107.8(4)
C(14)-C(20)-C(13)	125.1(4)
C(14)-C(20)-C(19)	126.9(4)
C(13)-C(20)-C(19)	108.0(3)
O(12)-C(21)-O(11)	123.0(4)
O(12)-C(21)-C(11)	125.1(4)
O(11)-C(21)-C(11)	112.0(3)
O(11)-C(22)-C(23)	107.2(3)
O(11)-C(22)-H(22A)	110.3
C(23)-C(22)-H(22A)	110.3
O(11)-C(22)-H(22B)	110.3
C(23)-C(22)-H(22B)	110.3
H(22A)-C(22)-H(22B)	108.5
C(22)-C(23)-H(23A)	109.5
C(22)-C(23)-H(23B)	109.5

H(23A)-C(23)-H(23B)	109.5
C(22)-C(23)-H(23C)	109.5
H(23A)-C(23)-H(23C)	109.5
H(23B)-C(23)-H(23C)	109.5
O(14)-C(24)-O(13)	123.8(4)
O(14)-C(24)-C(13)	123.1(4)
O(13)-C(24)-C(13)	113.0(3)
O(13)-C(25)-C(26)	111.1(3)
O(13)-C(25)-H(25A)	109.4
C(26)-C(25)-H(25A)	109.4
O(13)-C(25)-H(25B)	109.4
C(26)-C(25)-H(25B)	109.4
H(25A)-C(25)-H(25B)	108.0
C(25)-C(26)-H(26A)	109.5
C(25)-C(26)-H(26B)	109.5
H(26A)-C(26)-H(26B)	109.5
C(25)-C(26)-H(26C)	109.5
H(26A)-C(26)-H(26C)	109.5
H(26B)-C(26)-H(26C)	109.5
C(32)-C(31)-C(39)	106.3(3)
C(32)-C(31)-C(41)	128.1(4)
C(39)-C(31)-C(41)	125.6(4)
N(2)-C(32)-C(31)	124.4(3)
N(2)-C(32)-C(33)	123.9(4)
C(31)-C(32)-C(33)	111.6(4)
C(32)-C(33)-C(40)	106.7(4)
C(32)-C(33)-C(44)	127.8(4)
C(40)-C(33)-C(44)	125.4(3)
C(35)-C(34)-C(40)	128.8(4)
C(35)-C(34)-H(34A)	115.6
C(40)-C(34)-H(34A)	115.6
C(34)-C(35)-C(36)	128.6(4)
C(34)-C(35)-H(35A)	115.7
C(36)-C(35)-H(35A)	115.7
C(37)-C(36)-C(35)	129.7(4)
C(37)-C(36)-H(36A)	115.2

C(35)-C(36)-H(36A)	115.2
C(36)-C(37)-C(38)	129.7(4)
C(36)-C(37)-H(37A)	115.1
C(38)-C(37)-H(37A)	115.1
C(37)-C(38)-C(39)	128.0(4)
C(37)-C(38)-H(38A)	116.0
C(39)-C(38)-H(38A)	116.0
C(38)-C(39)-C(31)	125.2(4)
C(38)-C(39)-C(40)	127.1(4)
C(31)-C(39)-C(40)	107.7(3)
C(34)-C(40)-C(33)	124.3(4)
C(34)-C(40)-C(39)	128.1(4)
C(33)-C(40)-C(39)	107.6(3)
O(32)-C(41)-O(31)	123.1(4)
O(32)-C(41)-C(31)	124.7(4)
O(31)-C(41)-C(31)	112.3(3)
O(31)-C(42)-C(43)	111.7(4)
O(31)-C(42)-H(42A)	109.3
C(43)-C(42)-H(42A)	109.3
O(31)-C(42)-H(42B)	109.3
C(43)-C(42)-H(42B)	109.3
H(42A)-C(42)-H(42B)	107.9
C(42)-C(43)-H(43A)	109.5
C(42)-C(43)-H(43B)	109.5
H(43A)-C(43)-H(43B)	109.5
C(42)-C(43)-H(43C)	109.5
H(43A)-C(43)-H(43C)	109.5
H(43B)-C(43)-H(43C)	109.5
O(34)-C(44)-O(33)	123.7(4)
O(34)-C(44)-C(33)	124.1(4)
O(33)-C(44)-C(33)	112.2(3)
O(33)-C(45)-C(46)	106.2(3)
O(33)-C(45)-H(45A)	110.5
C(46)-C(45)-H(45A)	110.5
O(33)-C(45)-H(45B)	110.5
C(46)-C(45)-H(45B)	110.5

H(45A)-C(45)-H(45B)	108.7
C(45)-C(46)-H(46A)	109.5
C(45)-C(46)-H(46B)	109.5
H(46A)-C(46)-H(46B)	109.5
C(45)-C(46)-H(46C)	109.5
H(46A)-C(46)-H(46C)	109.5
H(46B)-C(46)-H(46C)	109.5
C(52)-C(51)-C(56)	111.1(3)
C(52)-C(51)-P(1)	110.6(3)
C(56)-C(51)-P(1)	113.8(3)
C(52)-C(51)-H(51A)	107.0
C(56)-C(51)-H(51A)	107.0
P(1)-C(51)-H(51A)	107.0
C(53)-C(52)-C(51)	110.1(3)
C(53)-C(52)-H(52A)	109.6
C(51)-C(52)-H(52A)	109.6
C(53)-C(52)-H(52B)	109.6
C(51)-C(52)-H(52B)	109.6
H(52A)-C(52)-H(52B)	108.2
C(54)-C(53)-C(52)	110.5(4)
C(54)-C(53)-H(53A)	109.6
C(52)-C(53)-H(53A)	109.6
C(54)-C(53)-H(53B)	109.6
C(52)-C(53)-H(53B)	109.6
H(53A)-C(53)-H(53B)	108.1
C(53)-C(54)-C(55)	111.7(4)
C(53)-C(54)-H(54A)	109.3
C(55)-C(54)-H(54A)	109.3
C(53)-C(54)-H(54B)	109.3
C(55)-C(54)-H(54B)	109.3
H(54A)-C(54)-H(54B)	107.9
C(54)-C(55)-C(56)	111.3(3)
C(54)-C(55)-H(55A)	109.4
C(56)-C(55)-H(55A)	109.4
C(54)-C(55)-H(55B)	109.4
C(56)-C(55)-H(55B)	109.4

H(55A)-C(55)-H(55B)	108.0
C(55)-C(56)-C(51)	110.6(3)
C(55)-C(56)-H(56A)	109.5
C(51)-C(56)-H(56A)	109.5
C(55)-C(56)-H(56B)	109.5
C(51)-C(56)-H(56B)	109.5
H(56A)-C(56)-H(56B)	108.1
C(62)-C(61)-C(66)	111.2(3)
C(62)-C(61)-P(1)	112.9(3)
C(66)-C(61)-P(1)	111.0(3)
C(62)-C(61)-H(61A)	107.1
C(66)-C(61)-H(61A)	107.1
P(1)-C(61)-H(61A)	107.1
C(63)-C(62)-C(61)	111.1(3)
C(63)-C(62)-H(62A)	109.4
C(61)-C(62)-H(62A)	109.4
C(63)-C(62)-H(62B)	109.4
C(61)-C(62)-H(62B)	109.4
H(62A)-C(62)-H(62B)	108.0
C(64)-C(63)-C(62)	112.3(4)
C(64)-C(63)-H(63A)	109.1
C(62)-C(63)-H(63A)	109.1
C(64)-C(63)-H(63B)	109.1
C(62)-C(63)-H(63B)	109.1
H(63A)-C(63)-H(63B)	107.9
C(63)-C(64)-C(65)	111.1(4)
C(63)-C(64)-H(64A)	109.4
C(65)-C(64)-H(64A)	109.4
C(63)-C(64)-H(64B)	109.4
C(65)-C(64)-H(64B)	109.4
H(64A)-C(64)-H(64B)	108.0
C(66)-C(65)-C(64)	111.4(3)
C(66)-C(65)-H(65A)	109.3
C(64)-C(65)-H(65A)	109.3
C(66)-C(65)-H(65B)	109.3
C(64)-C(65)-H(65B)	109.3

H(65A)-C(65)-H(65B)	108.0
C(65)-C(66)-C(61)	111.4(3)
C(65)-C(66)-H(66A)	109.4
C(61)-C(66)-H(66A)	109.4
C(65)-C(66)-H(66B)	109.4
C(61)-C(66)-H(66B)	109.4
H(66A)-C(66)-H(66B)	108.0
C(76)-C(71)-C(72)	111.7(3)
C(76)-C(71)-P(2)	114.0(3)
C(72)-C(71)-P(2)	111.8(3)
C(76)-C(71)-H(71A)	106.2
C(72)-C(71)-H(71A)	106.2
P(2)-C(71)-H(71A)	106.2
C(73)-C(72)-C(71)	111.3(3)
C(73)-C(72)-H(72A)	109.4
C(71)-C(72)-H(72A)	109.4
C(73)-C(72)-H(72B)	109.4
C(71)-C(72)-H(72B)	109.4
H(72A)-C(72)-H(72B)	108.0
C(74)-C(73)-C(72)	111.7(4)
C(74)-C(73)-H(73A)	109.3
C(72)-C(73)-H(73A)	109.3
C(74)-C(73)-H(73B)	109.3
C(72)-C(73)-H(73B)	109.3
H(73A)-C(73)-H(73B)	107.9
C(73)-C(74)-C(75)	111.0(4)
C(73)-C(74)-H(74A)	109.4
C(75)-C(74)-H(74A)	109.4
C(73)-C(74)-H(74B)	109.4
C(75)-C(74)-H(74B)	109.4
H(74A)-C(74)-H(74B)	108.0
C(74)-C(75)-C(76)	110.8(3)
C(74)-C(75)-H(75A)	109.5
C(76)-C(75)-H(75A)	109.5
C(74)-C(75)-H(75B)	109.5
C(76)-C(75)-H(75B)	109.5

H(75A)-C(75)-H(75B)	108.1
C(71)-C(76)-C(75)	110.9(3)
C(71)-C(76)-H(76A)	109.4
C(75)-C(76)-H(76A)	109.4
C(71)-C(76)-H(76B)	109.4
C(75)-C(76)-H(76B)	109.4
H(76A)-C(76)-H(76B)	108.0
C(82)-C(81)-C(86)	109.8(3)
C(82)-C(81)-P(2)	113.9(3)
C(86)-C(81)-P(2)	109.5(3)
C(82)-C(81)-H(81A)	107.8
C(86)-C(81)-H(81A)	107.8
P(2)-C(81)-H(81A)	107.8
C(81)-C(82)-C(83)	110.8(3)
C(81)-C(82)-H(82A)	109.5
C(83)-C(82)-H(82A)	109.5
C(81)-C(82)-H(82B)	109.5
C(83)-C(82)-H(82B)	109.5
H(82A)-C(82)-H(82B)	108.1
C(84)-C(83)-C(82)	111.1(4)
C(84)-C(83)-H(83A)	109.4
C(82)-C(83)-H(83A)	109.4
C(84)-C(83)-H(83B)	109.4
C(82)-C(83)-H(83B)	109.4
H(83A)-C(83)-H(83B)	108.0
C(85)-C(84)-C(83)	111.6(3)
C(85)-C(84)-H(84A)	109.3
C(83)-C(84)-H(84A)	109.3
C(85)-C(84)-H(84B)	109.3
C(83)-C(84)-H(84B)	109.3
H(84A)-C(84)-H(84B)	108.0
C(84)-C(85)-C(86)	111.7(3)
C(84)-C(85)-H(85A)	109.3
C(86)-C(85)-H(85A)	109.3
C(84)-C(85)-H(85B)	109.3
C(86)-C(85)-H(85B)	109.3

H(85A)-C(85)-H(85B)	107.9
C(81)-C(86)-C(85)	111.0(3)
C(81)-C(86)-H(86A)	109.4
C(85)-C(86)-H(86A)	109.4
C(81)-C(86)-H(86B)	109.4
C(85)-C(86)-H(86B)	109.4
H(86A)-C(86)-H(86B)	108.0
O(1A)-S(1A)-O(3A)	115.6(2)
O(1A)-S(1A)-O(2A)	114.3(3)
O(3A)-S(1A)-O(2A)	114.9(2)
O(1A)-S(1A)-C(1A)	102.3(2)
O(3A)-S(1A)-C(1A)	102.8(3)
O(2A)-S(1A)-C(1A)	104.6(3)
F(3A)-C(1A)-F(2A)	108.7(5)
F(3A)-C(1A)-F(1A)	106.9(4)
F(2A)-C(1A)-F(1A)	107.5(4)
F(3A)-C(1A)-S(1A)	111.3(3)
F(2A)-C(1A)-S(1A)	110.7(3)
F(1A)-C(1A)-S(1A)	111.7(4)
O(4A)-S(2A)-O(6A)	115.0(2)
O(4A)-S(2A)-O(5A)	115.2(2)
O(6A)-S(2A)-O(5A)	114.3(2)
O(4A)-S(2A)-C(2A)	102.1(2)
O(6A)-S(2A)-C(2A)	104.4(2)
O(5A)-S(2A)-C(2A)	103.5(2)
F(6A)-C(2A)-F(4A)	107.8(4)
F(6A)-C(2A)-F(5A)	107.1(4)
F(4A)-C(2A)-F(5A)	106.1(4)
F(6A)-C(2A)-S(2A)	112.0(3)
F(4A)-C(2A)-S(2A)	113.1(3)
F(5A)-C(2A)-S(2A)	110.4(3)
C(1S)-Cl(1S)-C(1S)#1	70.57(13)
Cl(1S)-C(1S)-Cl(1S)#1	109.43(13)
Cl(1S)-C(1S)-H(1SA)	109.8
Cl(1S)#1-C(1S)-H(1SA)	109.8
Cl(1S)-C(1S)-H(1SB)	109.8

Cl(1S)#1-C(1S)-H(1SB) 109.8
H(1SA)-C(1S)-H(1SB) 108.2

Symmetry transformations used to generate equivalent atoms:
#1 -x+1,-y,-z+1

Table 4. Anisotropic displacement parameters ($Å^2 x\ 10^3$) for Compound 2.8. The anisotropic displacement factor exponent takes the form: $-2\pi^2[\ h^2\ a^{*2}U^{11} + ... + 2\ h\ k\ a^*\ b^*\ U^{12}\ ]$

	U^{11}	U^{22}	U^{33}	U^{23}	U^{13}	U^{12}
Au(1)	19(1)	22(1)	9(1)	1(1)	5(1)	10(1)
Au(2)	20(1)	21(1)	9(1)	3(1)	6(1)	10(1)
P(1)	18(1)	21(1)	9(1)	1(1)	5(1)	10(1)
P(2)	17(1)	20(1)	9(1)	1(1)	5(1)	10(1)
O(11)	31(2)	26(2)	11(1)	1(1)	8(1)	17(1)
O(12)	47(2)	37(2)	15(2)	2(1)	8(1)	29(2)
O(13)	27(2)	30(2)	16(1)	-1(1)	5(1)	17(1)
O(14)	36(2)	36(2)	13(1)	4(1)	7(1)	20(2)
O(31)	34(2)	25(2)	11(1)	3(1)	10(1)	16(1)
O(32)	31(2)	28(2)	18(2)	2(1)	4(1)	16(1)
O(33)	32(2)	29(2)	15(1)	6(1)	9(1)	19(1)
O(34)	46(2)	40(2)	19(2)	4(1)	12(1)	29(2)
N(1)	21(2)	24(2)	13(2)	0(1)	3(1)	11(1)
N(2)	19(2)	22(2)	13(2)	2(1)	8(1)	10(1)
C(1)	21(2)	24(2)	14(2)	2(2)	7(2)	11(2)
C(2)	19(2)	20(2)	17(2)	0(2)	4(2)	9(2)
C(3)	19(2)	27(2)	8(2)	1(1)	5(1)	12(2)
C(11)	22(2)	29(2)	8(2)	-1(2)	5(1)	11(2)
C(12)	17(2)	22(2)	12(2)	-1(1)	5(1)	9(2)
C(13)	18(2)	26(2)	11(2)	-1(2)	3(1)	11(2)
C(14)	24(2)	27(2)	16(2)	-1(2)	5(2)	11(2)
C(15)	28(2)	31(2)	16(2)	-3(2)	7(2)	13(2)
C(16)	30(2)	30(2)	12(2)	-1(2)	8(2)	13(2)
C(17)	29(2)	31(2)	14(2)	4(2)	5(2)	13(2)
C(18)	28(2)	26(2)	16(2)	1(2)	8(2)	13(2)
C(19)	21(2)	23(2)	13(2)	-3(1)	5(2)	9(2)
C(20)	17(2)	23(2)	14(2)	2(2)	4(1)	8(2)
C(21)	20(2)	23(2)	18(2)	-1(2)	6(2)	7(2)
C(22)	29(2)	23(2)	16(2)	-1(2)	6(2)	14(2)
C(23)	35(2)	30(2)	20(2)	3(2)	10(2)	18(2)
C(24)	18(2)	25(2)	16(2)	-1(2)	5(2)	9(2)

C(25)	29(2)	22(2)	21(2)	4(2)	9(2)	13(2)
C(26)	27(2)	27(2)	28(2)	5(2)	5(2)	14(2)
C(31)	20(2)	20(2)	17(2)	4(2)	6(2)	10(2)
C(32)	19(2)	22(2)	10(2)	1(1)	4(1)	8(2)
C(33)	21(2)	22(2)	11(2)	1(1)	6(2)	7(2)
C(34)	27(2)	25(2)	17(2)	3(2)	6(2)	11(2)
C(35)	32(2)	31(2)	13(2)	0(2)	9(2)	10(2)
C(36)	32(2)	38(3)	13(2)	6(2)	6(2)	12(2)
C(37)	28(2)	27(2)	19(2)	8(2)	5(2)	12(2)
C(38)	27(2)	22(2)	18(2)	4(2)	6(2)	10(2)
C(39)	18(2)	21(2)	14(2)	1(1)	6(2)	6(2)
C(40)	18(2)	19(2)	14(2)	2(1)	5(1)	5(2)
C(41)	19(2)	23(2)	11(2)	4(1)	6(1)	8(2)
C(42)	42(3)	31(2)	14(2)	0(2)	12(2)	20(2)
C(43)	41(3)	31(2)	23(2)	0(2)	10(2)	16(2)
C(44)	21(2)	24(2)	14(2)	2(2)	6(2)	9(2)
C(45)	30(2)	25(2)	26(2)	4(2)	14(2)	15(2)
C(46)	30(2)	31(2)	21(2)	8(2)	3(2)	17(2)
C(51)	18(2)	22(2)	14(2)	0(1)	8(1)	9(2)
C(52)	25(2)	24(2)	16(2)	2(2)	8(2)	13(2)
C(53)	27(2)	20(2)	20(2)	6(2)	11(2)	8(2)
C(54)	35(3)	32(2)	23(2)	9(2)	15(2)	17(2)
C(55)	30(2)	26(2)	21(2)	6(2)	14(2)	14(2)
C(56)	27(2)	25(2)	14(2)	2(2)	9(2)	13(2)
C(61)	19(2)	20(2)	11(2)	-2(1)	2(1)	11(2)
C(62)	19(2)	25(2)	16(2)	2(2)	7(2)	8(2)
C(63)	28(2)	22(2)	17(2)	1(2)	7(2)	10(2)
C(64)	31(2)	21(2)	22(2)	4(2)	8(2)	10(2)
C(65)	29(2)	27(2)	26(2)	5(2)	9(2)	15(2)
C(66)	23(2)	23(2)	15(2)	4(2)	7(2)	12(2)
C(71)	20(2)	20(2)	11(2)	1(1)	6(1)	10(2)
C(72)	26(2)	25(2)	10(2)	-1(1)	3(2)	13(2)
C(73)	35(2)	25(2)	15(2)	2(2)	6(2)	12(2)
C(74)	43(3)	20(2)	21(2)	1(2)	15(2)	14(2)
C(75)	31(2)	25(2)	22(2)	7(2)	14(2)	12(2)
C(76)	27(2)	21(2)	14(2)	3(2)	8(2)	11(2)

C(81)	18(2)	22(2)	12(2)	4(1)	8(1)	10(2)
C(82)	25(2)	28(2)	13(2)	3(2)	7(2)	15(2)
C(83)	25(2)	38(2)	17(2)	4(2)	6(2)	18(2)
C(84)	16(2)	38(2)	15(2)	4(2)	4(2)	8(2)
C(85)	22(2)	26(2)	12(2)	1(2)	1(2)	8(2)
C(86)	21(2)	21(2)	15(2)	2(2)	3(2)	9(2)
S(1A)	56(1)	28(1)	15(1)	4(1)	13(1)	16(1)
F(1A)	43(2)	41(2)	144(4)	14(2)	36(2)	27(2)
F(2A)	36(2)	59(2)	43(2)	8(2)	3(1)	23(2)
F(3A)	39(2)	83(3)	65(2)	58(2)	20(2)	24(2)
O(1A)	46(2)	46(2)	27(2)	5(2)	2(2)	29(2)
O(2A)	100(4)	37(2)	28(2)	-8(2)	14(2)	6(2)
O(3A)	88(3)	34(2)	32(2)	9(2)	40(2)	15(2)
C(1A)	27(2)	40(3)	50(3)	17(2)	18(2)	18(2)
S(2A)	22(1)	24(1)	20(1)	-1(1)	6(1)	11(1)
F(4A)	27(2)	59(2)	49(2)	30(2)	18(1)	25(1)
F(5A)	42(2)	33(2)	71(2)	-12(2)	18(2)	1(1)
F(6A)	40(2)	67(2)	64(2)	46(2)	11(2)	24(2)
O(4A)	20(2)	25(2)	52(2)	0(2)	7(2)	7(1)
O(5A)	45(2)	41(2)	22(2)	-6(1)	3(2)	23(2)
O(6A)	35(2)	38(2)	19(2)	4(1)	11(1)	15(2)
C(2A)	25(2)	43(3)	32(3)	10(2)	5(2)	22(2)
Cl(1S)	85(1)	59(1)	121(2)	8(1)	-9(1)	41(1)
C(1S)	102(12)	43(7)	70(9)	-17(6)	-36(8)	51(8)

Table 5. Hydrogen coordinates (x 10^4) and isotropic displacement parameters (Å^{2}x 10^3) for Compound 2.8.

	x	y	z	U(eq)
H(3A)	3135	3829	4190	20
H(3B)	2488	2665	4304	20
H(14A)	1655	158	-1444	26
H(15A)	1609	389	-2548	29
H(16A)	1127	1460	-3102	29
H(17A)	526	2609	-2701	29
H(18A)	347	3006	-1616	27
H(22A)	-688	4097	441	26
H(22B)	642	4916	556	26
H(23A)	-55	4850	1622	40
H(23B)	975	4472	1679	40
H(23C)	-350	3656	1565	40
H(25A)	1760	-1760	-446	27
H(25B)	1711	-1305	317	27
H(26A)	3557	-1284	285	40
H(26B)	3664	-140	439	40
H(26C)	3715	-586	-326	40
H(34A)	3765	3476	-1622	27
H(35A)	3372	3989	-2615	31
H(36A)	2829	5237	-2801	34
H(37A)	2457	6232	-2065	29
H(38A)	2602	6314	-924	26
H(42A)	2753	6424	2046	32
H(42B)	2187	6768	1386	32
H(43A)	3756	8182	2041	46
H(43B)	4045	7968	1287	46
H(43C)	4607	7626	1950	46
H(45A)	5449	2361	327	30
H(45B)	4161	1475	76	30
H(46A)	4911	1337	1218	39

H(46B)	3800	1596	1226	39
H(46C)	5081	2477	1476	39
H(51A)	-620	2253	3682	21
H(52A)	-65	929	3339	24
H(52B)	764	1162	4081	24
H(53A)	-1722	474	3884	26
H(53B)	-1039	-217	4094	26
H(54A)	-168	828	5176	33
H(54B)	-1551	430	5094	33
H(55A)	-594	2213	5525	28
H(55B)	-1468	2005	4805	28
H(56A)	1019	2727	4954	25
H(56B)	286	3374	4735	25
H(61A)	1581	4587	4186	19
H(62A)	3112	5159	3556	24
H(62B)	2215	4982	2850	24
H(63A)	2659	6463	4040	27
H(63B)	3023	6722	3301	27
H(64A)	1075	6171	2774	29
H(64B)	1333	6998	3441	29
H(65A)	423	5706	4104	31
H(65B)	-466	5535	3397	31
H(66A)	-26	4219	2914	23
H(66B)	-387	3963	3655	23
H(71A)	1903	1218	3088	20
H(72A)	2792	1320	2102	23
H(72B)	3847	1145	2530	23
H(73A)	1483	-332	2188	30
H(73B)	2549	-407	1871	30
H(74A)	3376	-623	2960	32
H(74B)	2069	-1476	2746	32
H(75A)	2429	-727	3932	30
H(75B)	1408	-527	3485	30
H(76A)	2708	1019	4183	24
H(76B)	3787	944	3881	24
H(81A)	4758	2818	4393	19

H(82A)	5890	2988	3205	25
H(82B)	5316	1951	3530	25
H(83A)	6678	2671	4581	30
H(83B)	7364	2741	3943	30
H(84A)	8173	4313	4718	29
H(84B)	7734	4468	3946	29
H(85A)	7097	5349	4726	25
H(85B)	6528	4357	5096	25
H(86A)	5023	4536	4352	23
H(86B)	5687	4590	3705	23
H(1SA)	5864	1152	5588	86
H(1SB)	4804	1167	5050	86

Table 6. Torsion angles [°] for Compound 2.8.

C(1)-Au(1)-Au(2)-C(2)	41.71(16)
P(1)-Au(1)-Au(2)-C(2)	-138.72(12)
C(1)-Au(1)-Au(2)-P(2)	-134.54(12)
P(1)-Au(1)-Au(2)-P(2)	45.03(4)
C(1)-Au(1)-P(1)-C(61)	88.8(11)
Au(2)-Au(1)-P(1)-C(61)	84.71(14)
C(1)-Au(1)-P(1)-C(51)	-148.5(11)
Au(2)-Au(1)-P(1)-C(51)	-152.65(14)
C(1)-Au(1)-P(1)-C(3)	-29.6(11)
Au(2)-Au(1)-P(1)-C(3)	-33.70(14)
C(2)-Au(2)-P(2)-C(81)	115.5(17)
Au(1)-Au(2)-P(2)-C(81)	-172.40(14)
C(2)-Au(2)-P(2)-C(3)	-126.2(17)
Au(1)-Au(2)-P(2)-C(3)	-54.11(14)
C(2)-Au(2)-P(2)-C(71)	-10.4(17)
Au(1)-Au(2)-P(2)-C(71)	61.78(13)
C(12)-N(1)-C(1)-Au(1)	-64(5)
P(1)-Au(1)-C(1)-N(1)	-42(4)
Au(2)-Au(1)-C(1)-N(1)	-38(3)
C(32)-N(2)-C(2)-Au(2)	-27(10)
P(2)-Au(2)-C(2)-N(2)	25(4)
Au(1)-Au(2)-C(2)-N(2)	-47(2)
C(81)-P(2)-C(3)-P(1)	169.7(2)
C(71)-P(2)-C(3)-P(1)	-74.5(2)
Au(2)-P(2)-C(3)-P(1)	45.2(2)
C(61)-P(1)-C(3)-P(2)	-120.6(2)
C(51)-P(1)-C(3)-P(2)	125.9(2)
Au(1)-P(1)-C(3)-P(2)	3.5(3)
C(1)-N(1)-C(12)-C(11)	0(3)
C(1)-N(1)-C(12)-C(13)	-179(100)
C(19)-C(11)-C(12)-N(1)	-178.6(4)
C(21)-C(11)-C(12)-N(1)	2.0(7)
C(19)-C(11)-C(12)-C(13)	0.2(5)
C(21)-C(11)-C(12)-C(13)	-179.1(4)

N(1)-C(12)-C(13)-C(20)	178.8(4)
C(11)-C(12)-C(13)-C(20)	0.0(5)
N(1)-C(12)-C(13)-C(24)	-0.5(6)
C(11)-C(12)-C(13)-C(24)	-179.3(4)
C(20)-C(14)-C(15)-C(16)	-1.0(8)
C(14)-C(15)-C(16)-C(17)	-0.3(8)
C(15)-C(16)-C(17)-C(18)	1.7(8)
C(16)-C(17)-C(18)-C(19)	-0.6(8)
C(17)-C(18)-C(19)-C(11)	177.3(4)
C(17)-C(18)-C(19)-C(20)	-1.8(8)
C(12)-C(11)-C(19)-C(18)	-179.6(4)
C(21)-C(11)-C(19)-C(18)	-0.2(7)
C(12)-C(11)-C(19)-C(20)	-0.3(4)
C(21)-C(11)-C(19)-C(20)	179.0(4)
C(15)-C(14)-C(20)-C(13)	-177.1(4)
C(15)-C(14)-C(20)-C(19)	-0.2(7)
C(12)-C(13)-C(20)-C(14)	177.3(4)
C(24)-C(13)-C(20)-C(14)	-3.5(7)
C(12)-C(13)-C(20)-C(19)	-0.2(4)
C(24)-C(13)-C(20)-C(19)	179.0(4)
C(18)-C(19)-C(20)-C(14)	2.1(7)
C(11)-C(19)-C(20)-C(14)	-177.1(4)
C(18)-C(19)-C(20)-C(13)	179.5(4)
C(11)-C(19)-C(20)-C(13)	0.3(4)
C(22)-O(11)-C(21)-O(12)	2.5(6)
C(22)-O(11)-C(21)-C(11)	-178.0(3)
C(12)-C(11)-C(21)-O(12)	-175.1(4)
C(19)-C(11)-C(21)-O(12)	5.7(7)
C(12)-C(11)-C(21)-O(11)	5.5(6)
C(19)-C(11)-C(21)-O(11)	-173.7(4)
C(21)-O(11)-C(22)-C(23)	175.1(3)
C(25)-O(13)-C(24)-O(14)	-1.3(6)
C(25)-O(13)-C(24)-C(13)	179.8(3)
C(12)-C(13)-C(24)-O(14)	-4.6(6)
C(20)-C(13)-C(24)-O(14)	176.3(4)
C(12)-C(13)-C(24)-O(13)	174.4(4)

C(20)-C(13)-C(24)-O(13)	-4.8(6)
C(24)-O(13)-C(25)-C(26)	-88.2(4)
C(2)-N(2)-C(32)-C(31)	149(8)
C(2)-N(2)-C(32)-C(33)	-32(8)
C(39)-C(31)-C(32)-N(2)	-178.2(4)
C(41)-C(31)-C(32)-N(2)	2.5(7)
C(39)-C(31)-C(32)-C(33)	2.1(5)
C(41)-C(31)-C(32)-C(33)	-177.2(4)
N(2)-C(32)-C(33)-C(40)	178.5(3)
C(31)-C(32)-C(33)-C(40)	-1.7(5)
N(2)-C(32)-C(33)-C(44)	-2.6(7)
C(31)-C(32)-C(33)-C(44)	177.2(4)
C(40)-C(34)-C(35)-C(36)	1.7(8)
C(34)-C(35)-C(36)-C(37)	-1.2(8)
C(35)-C(36)-C(37)-C(38)	1.2(8)
C(36)-C(37)-C(38)-C(39)	-1.2(8)
C(37)-C(38)-C(39)-C(31)	-179.2(4)
C(37)-C(38)-C(39)-C(40)	0.3(7)
C(32)-C(31)-C(39)-C(38)	178.0(4)
C(41)-C(31)-C(39)-C(38)	-2.6(7)
C(32)-C(31)-C(39)-C(40)	-1.6(4)
C(41)-C(31)-C(39)-C(40)	177.8(4)
C(35)-C(34)-C(40)-C(33)	178.3(4)
C(35)-C(34)-C(40)-C(39)	-1.9(7)
C(32)-C(33)-C(40)-C(34)	-179.5(4)
C(44)-C(33)-C(40)-C(34)	1.6(7)
C(32)-C(33)-C(40)-C(39)	0.7(4)
C(44)-C(33)-C(40)-C(39)	-178.3(4)
C(38)-C(39)-C(40)-C(34)	1.1(7)
C(31)-C(39)-C(40)-C(34)	-179.3(4)
C(38)-C(39)-C(40)-C(33)	-179.0(4)
C(31)-C(39)-C(40)-C(33)	0.6(4)
C(42)-O(31)-C(41)-O(32)	-1.2(6)
C(42)-O(31)-C(41)-C(31)	179.0(3)
C(32)-C(31)-C(41)-O(32)	-178.9(4)
C(39)-C(31)-C(41)-O(32)	1.9(7)

C(32)-C(31)-C(41)-O(31)	0.8(6)
C(39)-C(31)-C(41)-O(31)	-178.4(4)
C(41)-O(31)-C(42)-C(43)	-77.9(5)
C(45)-O(33)-C(44)-O(34)	2.8(6)
C(45)-O(33)-C(44)-C(33)	-175.7(3)
C(32)-C(33)-C(44)-O(34)	-175.6(4)
C(40)-C(33)-C(44)-O(34)	3.1(7)
C(32)-C(33)-C(44)-O(33)	3.0(6)
C(40)-C(33)-C(44)-O(33)	-178.3(4)
C(44)-O(33)-C(45)-C(46)	-174.9(4)
C(61)-P(1)-C(51)-C(52)	-176.3(3)
C(3)-P(1)-C(51)-C(52)	-64.4(3)
Au(1)-P(1)-C(51)-C(52)	56.9(3)
C(61)-P(1)-C(51)-C(56)	-50.5(3)
C(3)-P(1)-C(51)-C(56)	61.4(3)
Au(1)-P(1)-C(51)-C(56)	-177.2(2)
C(56)-C(51)-C(52)-C(53)	58.2(4)
P(1)-C(51)-C(52)-C(53)	-174.5(3)
C(51)-C(52)-C(53)-C(54)	-58.2(5)
C(52)-C(53)-C(54)-C(55)	56.9(5)
C(53)-C(54)-C(55)-C(56)	-54.9(5)
C(54)-C(55)-C(56)-C(51)	53.9(5)
C(52)-C(51)-C(56)-C(55)	-56.0(4)
P(1)-C(51)-C(56)-C(55)	178.4(3)
C(51)-P(1)-C(61)-C(62)	177.1(3)
C(3)-P(1)-C(61)-C(62)	64.1(3)
Au(1)-P(1)-C(61)-C(62)	-57.5(3)
C(51)-P(1)-C(61)-C(66)	-57.3(3)
C(3)-P(1)-C(61)-C(66)	-170.2(3)
Au(1)-P(1)-C(61)-C(66)	68.2(3)
C(66)-C(61)-C(62)-C(63)	54.9(4)
P(1)-C(61)-C(62)-C(63)	-179.6(3)
C(61)-C(62)-C(63)-C(64)	-55.3(5)
C(62)-C(63)-C(64)-C(65)	54.9(5)
C(63)-C(64)-C(65)-C(66)	-54.4(5)
C(64)-C(65)-C(66)-C(61)	54.8(5)

C(62)-C(61)-C(66)-C(65)	-55.1(4)
P(1)-C(61)-C(66)-C(65)	178.3(3)
C(81)-P(2)-C(71)-C(76)	34.8(3)
C(3)-P(2)-C(71)-C(76)	-76.5(3)
Au(2)-P(2)-C(71)-C(76)	163.1(2)
C(81)-P(2)-C(71)-C(72)	-93.1(3)
C(3)-P(2)-C(71)-C(72)	155.6(3)
Au(2)-P(2)-C(71)-C(72)	35.3(3)
C(76)-C(71)-C(72)-C(73)	53.3(5)
P(2)-C(71)-C(72)-C(73)	-177.6(3)
C(71)-C(72)-C(73)-C(74)	-54.9(5)
C(72)-C(73)-C(74)-C(75)	57.1(5)
C(73)-C(74)-C(75)-C(76)	-57.2(5)
C(72)-C(71)-C(76)-C(75)	-53.8(4)
P(2)-C(71)-C(76)-C(75)	178.3(3)
C(74)-C(75)-C(76)-C(71)	55.7(5)
C(3)-P(2)-C(81)-C(82)	169.2(3)
C(71)-P(2)-C(81)-C(82)	57.7(3)
Au(2)-P(2)-C(81)-C(82)	-68.3(3)
C(3)-P(2)-C(81)-C(86)	-67.4(3)
C(71)-P(2)-C(81)-C(86)	-178.9(2)
Au(2)-P(2)-C(81)-C(86)	55.1(3)
C(86)-C(81)-C(82)-C(83)	58.5(4)
P(2)-C(81)-C(82)-C(83)	-178.3(3)
C(81)-C(82)-C(83)-C(84)	-57.6(4)
C(82)-C(83)-C(84)-C(85)	54.8(4)
C(83)-C(84)-C(85)-C(86)	-53.6(5)
C(82)-C(81)-C(86)-C(85)	-57.0(4)
P(2)-C(81)-C(86)-C(85)	177.2(3)
C(84)-C(85)-C(86)-C(81)	54.8(4)
O(1A)-S(1A)-C(1A)-F(3A)	57.3(4)
O(3A)-S(1A)-C(1A)-F(3A)	177.5(4)
O(2A)-S(1A)-C(1A)-F(3A)	-62.1(5)
O(1A)-S(1A)-C(1A)-F(2A)	-63.7(4)
O(3A)-S(1A)-C(1A)-F(2A)	56.5(4)
O(2A)-S(1A)-C(1A)-F(2A)	176.9(4)

O(1A)-S(1A)-C(1A)-F(1A)	176.6(4)
O(3A)-S(1A)-C(1A)-F(1A)	-63.2(4)
O(2A)-S(1A)-C(1A)-F(1A)	57.2(4)
O(4A)-S(2A)-C(2A)-F(6A)	55.7(4)
O(6A)-S(2A)-C(2A)-F(6A)	175.7(3)
O(5A)-S(2A)-C(2A)-F(6A)	-64.3(4)
O(4A)-S(2A)-C(2A)-F(4A)	177.7(3)
O(6A)-S(2A)-C(2A)-F(4A)	-62.2(4)
O(5A)-S(2A)-C(2A)-F(4A)	57.8(4)
O(4A)-S(2A)-C(2A)-F(5A)	-63.6(4)
O(6A)-S(2A)-C(2A)-F(5A)	56.5(4)
O(5A)-S(2A)-C(2A)-F(5A)	176.5(3)
C(1S)#1-Cl(1S)-C(1S)-Cl(1S)#1	0.0

Symmetry transformations used to generate equivalent atoms:
#1 -x+1,-y,-z+1

Appendix 2

Preliminary Crystallographic Data for compound 3.1

Table 1. Crystal data and structure refinement for **3.1**.

Identification code	q68a	
Empirical formula	C20 H15 N	
Formula weight	269.33	
Temperature	100(2) K	
Wavelength	1.54178 Å	
Crystal system	Orthorhombic	
Space group	Pna2(1)	
Unit cell dimensions	a = 12.7468(9) Å	α= 90°.
	b = 14.3461(11) Å	β= 90°.
	c = 7.4079(6) Å	γ = 90°.
Volume	1354.66(18) $Å^3$	
Z	4	
Density (calculated)	1.321 Mg/m^3	
Absorption coefficient	0.585 mm^{-1}	
F(000)	568	
Crystal size	0.24 x 0.05 x 0.04 mm^3	
Theta range for data collection	6.73 to 67.79°.	
Index ranges	0<=h<=14, 0<=k<=16, 0<=l<=8	
Reflections collected	1248	
Independent reflections	1248 [R(int) = 0.0000]	
Completeness to theta = 67.79°	93.8 %	
Absorption correction	Multi-scan	
Max. and min. transmission	1.000 and 0.836	
Refinement method	Full-matrix least-squares on F^2	
Data / restraints / parameters	1248 / 13 / 190	
Goodness-of-fit on F^2	1.090	
Final R indices [I>2sigma(I)]	R1 = 0.1289, wR2 = 0.2980	
R indices (all data)	R1 = 0.1407, wR2 = 0.3047	
Absolute structure parameter	1(5)	
Largest diff. peak and hole	1.004 and -0.553 $e.Å^{-3}$	

Table 2. Atomic coordinates (x 10^4) and equivalent isotropic displacement parameters ($Å^2$x 10^3) for **3.1**. U(eq) is defined as one third of the trace of the orthogonalized U^{ij} tensor.

	x	y	z	U(eq)
N(1)	2025(7)	515(7)	6301(14)	44(3)
C(1)	2763(8)	4512(7)	6714(14)	32(2)
C(2)	3740(6)	4850(7)	5953(13)	24(2)
C(3)	4250(7)	4049(7)	5200(14)	28(2)
C(4)	3880(8)	2337(8)	5056(14)	33(3)
C(5)	3381(8)	1529(8)	5341(15)	31(2)
C(6)	2392(7)	1378(8)	6210(15)	31(2)
C(7)	1710(7)	2098(8)	6932(12)	28(2)
C(8)	1820(7)	2996(8)	7053(13)	32(3)
C(9)	2686(7)	3593(7)	6496(12)	25(2)
C(10)	3655(6)	3253(6)	5484(13)	22(2)
C(11)	3536(7)	6554(7)	6722(13)	28(2)
C(12)	4092(7)	5804(7)	5985(14)	27(2)
C(13)	5008(6)	6178(7)	5293(14)	25(2)
C(14)	5822(6)	7746(6)	4998(12)	18(2)
C(15)	5905(8)	8696(8)	5168(16)	36(3)
C(16)	5190(7)	9304(7)	6017(16)	33(2)
C(17)	4232(8)	9095(8)	6852(16)	35(2)
C(18)	3738(7)	8242(7)	7014(15)	30(2)
C(19)	4033(7)	7363(7)	6515(13)	27(2)
C(20)	5051(7)	7124(7)	5526(13)	27(2)

Table 3. Bond lengths [Å] and angles [°] for **3.1**.

N(1)-C(6)	1.325(14)
N(1)-H(1N1)	0.8800
N(1)-H(1N2)	0.8800
C(1)-C(9)	1.333(15)
C(1)-C(2)	1.450(13)
C(1)-H(1)	0.9500
C(2)-C(3)	1.433(13)
C(2)-C(12)	1.440(13)
C(3)-C(10)	1.387(13)
C(3)-H(3)	0.9500
C(4)-C(5)	1.340(15)
C(4)-C(10)	1.381(14)
C(4)-H(4)	0.9500
C(5)-C(6)	1.431(13)
C(5)-H(5)	0.9500
C(6)-C(7)	1.452(14)
C(7)-C(8)	1.300(15)
C(7)-H(7)	0.9500
C(8)-C(9)	1.457(13)
C(8)-H(8)	0.9500
C(9)-C(10)	1.525(12)
C(11)-C(19)	1.331(14)
C(11)-C(12)	1.400(13)
C(11)-H(11)	0.9500
C(12)-C(13)	1.384(13)
C(13)-C(20)	1.369(14)
C(13)-H(13)	0.9500
C(14)-C(15)	1.373(14)
C(14)-C(20)	1.383(13)
C(14)-H(14)	0.9500
C(15)-C(16)	1.410(14)
C(15)-H(15)	0.9500
C(16)-C(17)	1.401(15)
C(16)-H(16)	0.9500

C(17)-C(18)	1.382(15)
C(17)-H(17)	0.9500
C(18)-C(19)	1.367(14)
C(18)-H(18)	0.9500
C(19)-C(20)	1.530(14)

C(6)-N(1)-H(1N1)	120.0
C(6)-N(1)-H(1N2)	120.0
H(1N1)-N(1)-H(1N2)	120.0
C(9)-C(1)-C(2)	110.3(9)
C(9)-C(1)-H(1)	124.9
C(2)-C(1)-H(1)	124.9
C(3)-C(2)-C(12)	128.8(8)
C(3)-C(2)-C(1)	105.8(8)
C(12)-C(2)-C(1)	125.3(8)
C(10)-C(3)-C(2)	110.7(8)
C(10)-C(3)-H(3)	124.6
C(2)-C(3)-H(3)	124.6
C(5)-C(4)-C(10)	133.5(10)
C(5)-C(4)-H(4)	113.3
C(10)-C(4)-H(4)	113.3
C(4)-C(5)-C(6)	128.4(10)
C(4)-C(5)-H(5)	115.8
C(6)-C(5)-H(5)	115.8
N(1)-C(6)-C(5)	118.4(10)
N(1)-C(6)-C(7)	115.7(9)
C(5)-C(6)-C(7)	125.8(9)
C(8)-C(7)-C(6)	131.8(9)
C(8)-C(7)-H(7)	114.1
C(6)-C(7)-H(7)	114.1
C(7)-C(8)-C(9)	130.1(9)
C(7)-C(8)-H(8)	114.9
C(9)-C(8)-H(8)	114.9
C(1)-C(9)-C(8)	127.1(9)
C(1)-C(9)-C(10)	108.4(8)
C(8)-C(9)-C(10)	124.5(9)

C(4)-C(10)-C(3)	129.4(9)
C(4)-C(10)-C(9)	125.8(9)
C(3)-C(10)-C(9)	104.7(8)
C(19)-C(11)-C(12)	112.6(9)
C(19)-C(11)-H(11)	123.7
C(12)-C(11)-H(11)	123.7
C(13)-C(12)-C(11)	105.9(9)
C(13)-C(12)-C(2)	128.7(9)
C(11)-C(12)-C(2)	125.4(8)
C(20)-C(13)-C(12)	111.8(9)
C(20)-C(13)-H(13)	124.1
C(12)-C(13)-H(13)	124.1
C(15)-C(14)-C(20)	132.0(9)
C(15)-C(14)-H(14)	114.0
C(20)-C(14)-H(14)	114.0
C(14)-C(15)-C(16)	127.3(10)
C(14)-C(15)-H(15)	116.4
C(16)-C(15)-H(15)	116.4
C(17)-C(16)-C(15)	128.9(10)
C(17)-C(16)-H(16)	115.5
C(15)-C(16)-H(16)	115.5
C(18)-C(17)-C(16)	128.7(10)
C(18)-C(17)-H(17)	115.7
C(16)-C(17)-H(17)	115.7
C(19)-C(18)-C(17)	132.0(10)
C(19)-C(18)-H(18)	114.0
C(17)-C(18)-H(18)	114.0
C(11)-C(19)-C(18)	130.0(10)
C(11)-C(19)-C(20)	105.3(9)
C(18)-C(19)-C(20)	124.7(9)
C(13)-C(20)-C(14)	129.2(9)
C(13)-C(20)-C(19)	104.4(8)
C(14)-C(20)-C(19)	126.4(9)

Symmetry transformations used to generate equivalent atoms:

Table 4. Anisotropic displacement parameters ($Å^2 x\ 10^3$) for **3.1**. The anisotropic displacement factor exponent takes the form: $-2\pi^2[\ h^2\ a^{*2}U^{11} + ...\ + 2\ h\ k\ a^*\ b^*\ U^{12}\ ]$

	U^{11}	U^{22}	U^{33}	U^{23}	U^{13}	U^{12}
N(1)	39(5)	52(6)	40(6)	1(5)	1(5)	6(4)
C(1)	34(5)	44(6)	18(5)	9(5)	10(4)	14(4)
C(2)	13(4)	47(6)	10(4)	7(4)	-3(3)	11(4)
C(3)	24(5)	45(6)	14(5)	2(4)	-1(4)	3(4)
C(4)	27(5)	55(7)	16(6)	4(5)	-8(5)	-1(4)
C(5)	30(5)	47(6)	17(5)	3(5)	0(5)	5(4)
C(6)	16(4)	52(6)	24(5)	-6(5)	4(4)	-12(4)
C(7)	12(4)	65(7)	5(5)	6(5)	2(4)	-4(4)
C(8)	16(4)	71(8)	8(5)	4(5)	5(4)	7(5)
C(9)	20(4)	46(6)	8(5)	5(4)	5(4)	-1(4)
C(10)	16(4)	36(5)	15(5)	1(4)	-7(4)	10(4)
C(11)	27(5)	49(6)	7(4)	4(4)	-2(4)	14(4)
C(12)	22(4)	45(6)	13(5)	2(4)	3(4)	7(4)
C(13)	13(4)	43(6)	18(5)	6(4)	0(4)	1(3)
C(14)	11(3)	31(4)	14(4)	1(3)	-7(3)	-2(3)
C(15)	28(5)	51(7)	29(6)	0(5)	-2(5)	10(5)
C(16)	29(5)	40(6)	30(6)	0(5)	0(5)	6(4)
C(17)	33(5)	44(6)	26(6)	-4(5)	-1(5)	9(4)
C(18)	21(4)	46(6)	23(5)	-3(5)	-7(4)	9(4)
C(19)	29(4)	33(4)	19(4)	-1(3)	-11(3)	3(3)
C(20)	26(4)	47(6)	7(5)	-1(4)	-8(4)	7(4)

Table 5. Hydrogen coordinates (x 10^4) and isotropic displacement parameters ($Å^2$x 10^3) for **3.1**.

	x	y	z	U(eq)
H(1N1)	2387	52	5834	52
H(1N2)	1419	406	6829	52
H(1)	2251	4892	7286	38
H(3)	4905	4062	4589	33
H(4)	4525	2266	4426	39
H(5)	3727	986	4911	38
H(7)	1066	1870	7402	33
H(8)	1244	3314	7589	38
H(11)	2876	6493	7306	33
H(13)	5542	5821	4725	30
H(14)	6402	7463	4407	22
H(15)	6513	8975	4658	43
H(16)	5384	9943	6023	40
H(17)	3875	9609	7377	41
H(18)	3070	8272	7578	36

Table 6. Torsion angles [°] for **3.1**.

C(9)-C(1)-C(2)-C(3)	1.4(12)
C(9)-C(1)-C(2)-C(12)	-178.5(9)
C(12)-C(2)-C(3)-C(10)	178.8(9)
C(1)-C(2)-C(3)-C(10)	-1.1(11)
C(10)-C(4)-C(5)-C(6)	1(2)
C(4)-C(5)-C(6)-N(1)	178.0(11)
C(4)-C(5)-C(6)-C(7)	1.6(19)
N(1)-C(6)-C(7)-C(8)	-179.8(11)
C(5)-C(6)-C(7)-C(8)	-3.4(19)
C(6)-C(7)-C(8)-C(9)	-0.2(19)
C(2)-C(1)-C(9)-C(8)	-179.2(9)
C(2)-C(1)-C(9)-C(10)	-1.2(11)
C(7)-C(8)-C(9)-C(1)	-177.6(11)
C(7)-C(8)-C(9)-C(10)	4.7(17)
C(5)-C(4)-C(10)-C(3)	176.8(11)
C(5)-C(4)-C(10)-C(9)	0.3(18)
C(2)-C(3)-C(10)-C(4)	-176.7(10)
C(2)-C(3)-C(10)-C(9)	0.4(11)
C(1)-C(9)-C(10)-C(4)	177.7(10)
C(8)-C(9)-C(10)-C(4)	-4.3(15)
C(1)-C(9)-C(10)-C(3)	0.5(11)
C(8)-C(9)-C(10)-C(3)	178.6(9)
C(19)-C(11)-C(12)-C(13)	0.8(12)
C(19)-C(11)-C(12)-C(2)	-178.0(9)
C(3)-C(2)-C(12)-C(13)	0.1(16)
C(1)-C(2)-C(12)-C(13)	180.0(11)
C(3)-C(2)-C(12)-C(11)	178.7(10)
C(1)-C(2)-C(12)-C(11)	-1.4(15)
C(11)-C(12)-C(13)-C(20)	-1.0(12)
C(2)-C(12)-C(13)-C(20)	177.8(9)
C(20)-C(14)-C(15)-C(16)	1.8(19)
C(14)-C(15)-C(16)-C(17)	-1(2)
C(15)-C(16)-C(17)-C(18)	-2(2)
C(16)-C(17)-C(18)-C(19)	3(2)

C(12)-C(11)-C(19)-C(18)	178.7(11)
C(12)-C(11)-C(19)-C(20)	-0.4(11)
C(17)-C(18)-C(19)-C(11)	178.9(11)
C(17)-C(18)-C(19)-C(20)	-2.2(18)
C(12)-C(13)-C(20)-C(14)	-178.8(10)
C(12)-C(13)-C(20)-C(19)	0.8(11)
C(15)-C(14)-C(20)-C(13)	179.0(11)
C(15)-C(14)-C(20)-C(19)	-0.5(17)
C(11)-C(19)-C(20)-C(13)	-0.3(11)
C(18)-C(19)-C(20)-C(13)	-179.4(9)
C(11)-C(19)-C(20)-C(14)	179.4(9)
C(18)-C(19)-C(20)-C(14)	0.3(16)

Symmetry transformations used to generate equivalent atoms:

Appendix 3

NMR Spectra of Selected Compounds from Chapter I

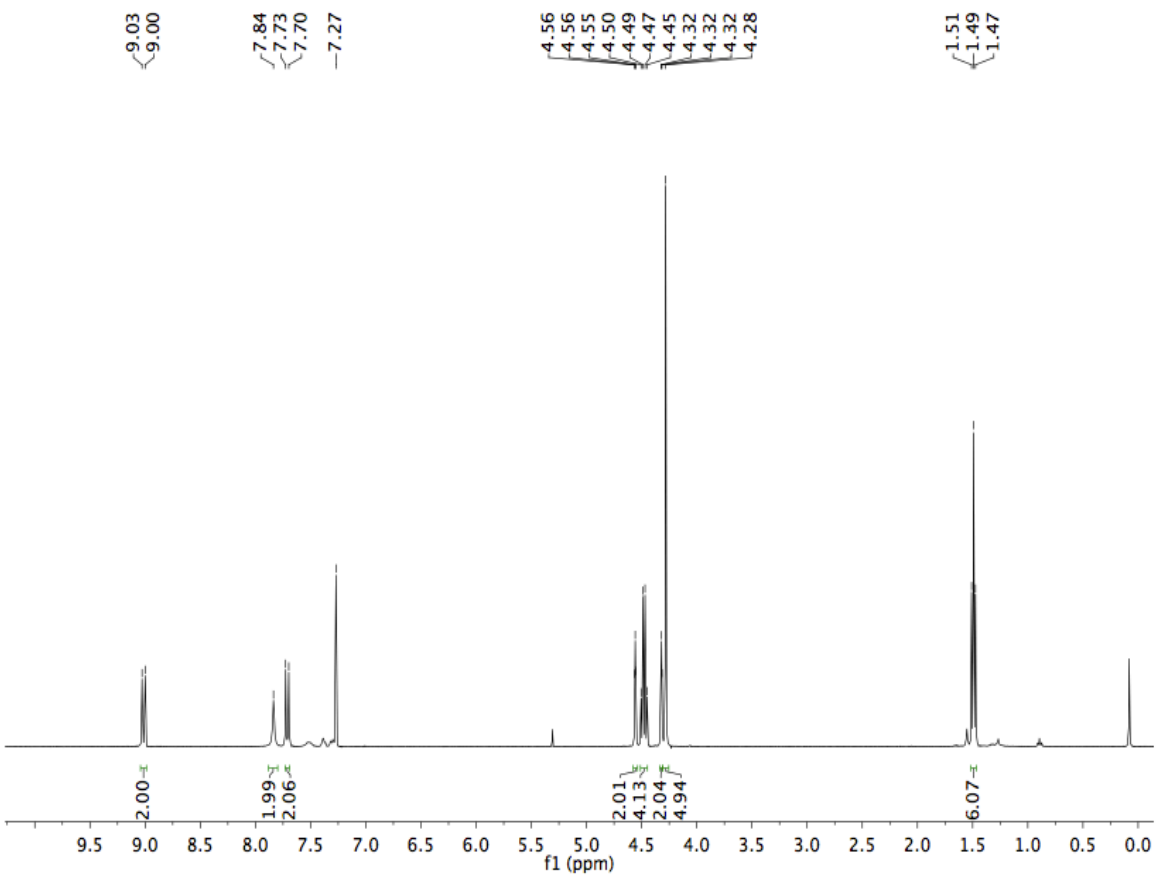

^{1}H NMR Spectrum of Compound 1.4 in $CDCl_3$

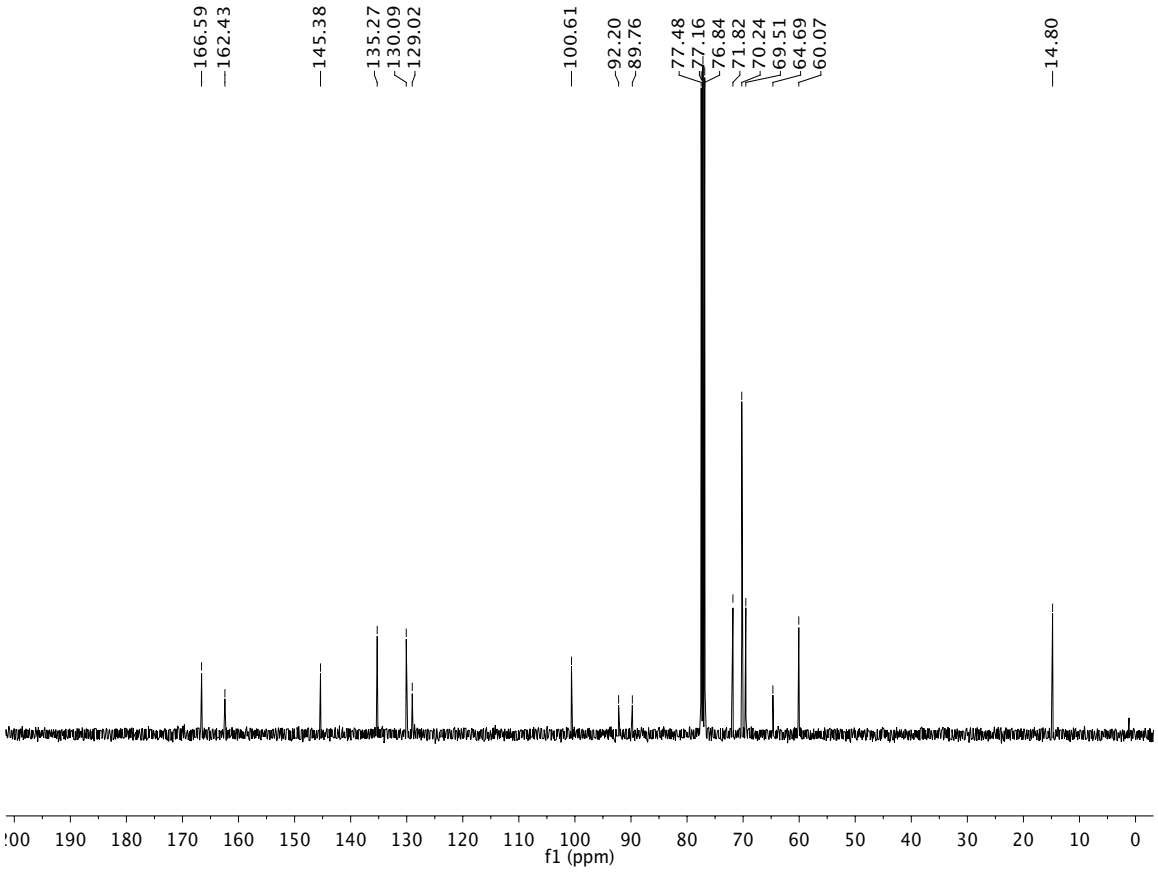

^{13}C NMR Spectrum of Compound 1.4 in $CDCl_3$

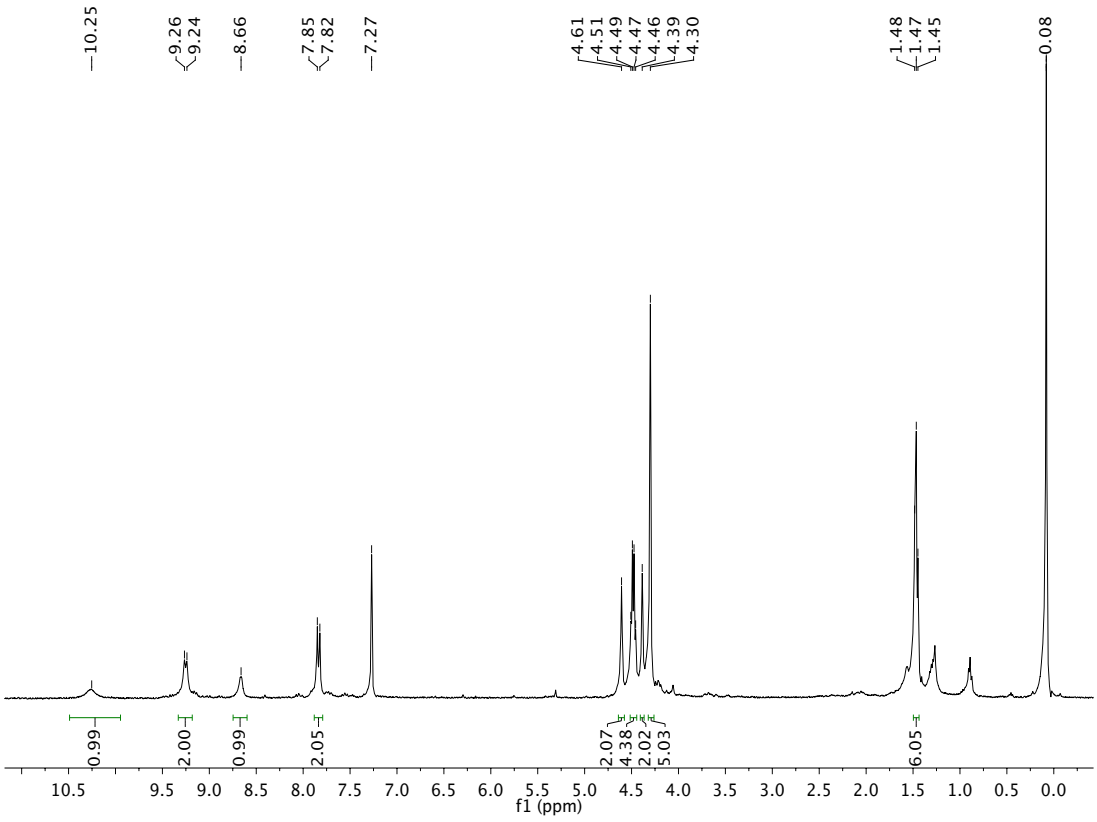

^{1}H NMR Spectrum of Compound 1.5 in $CDCl_3$

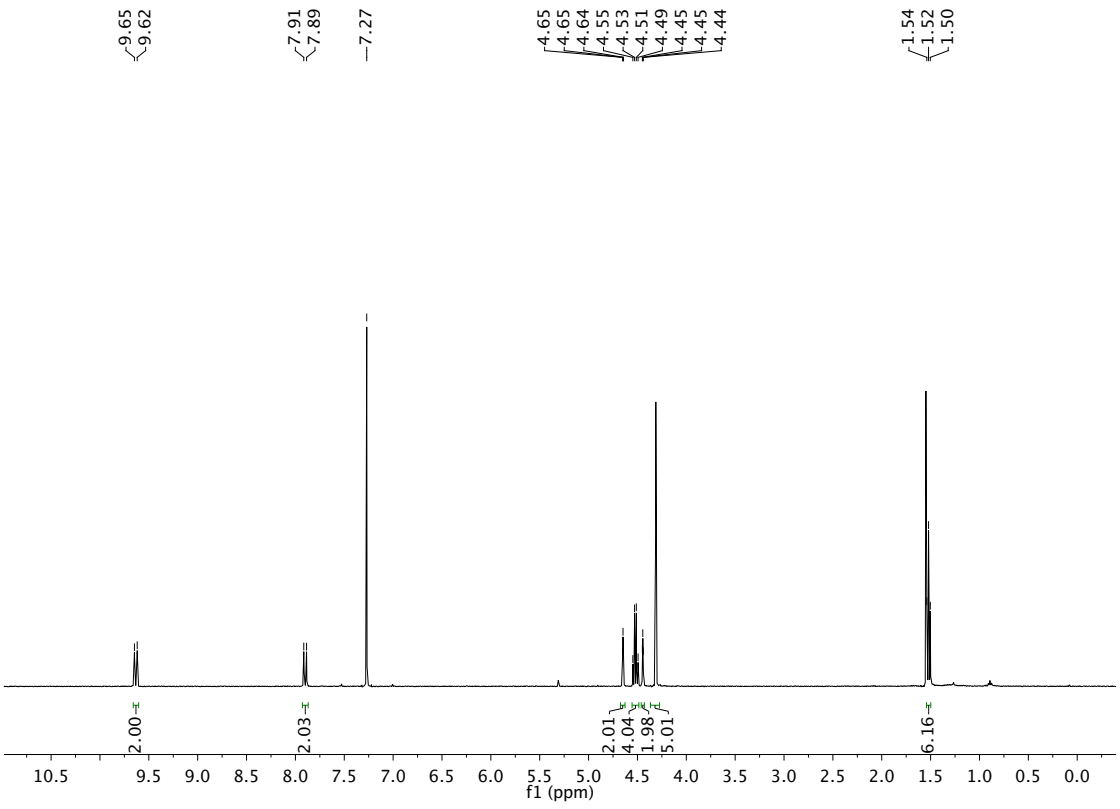

^{1}H NMR Spectrum of Compound 1.6 in $CDCl_3$

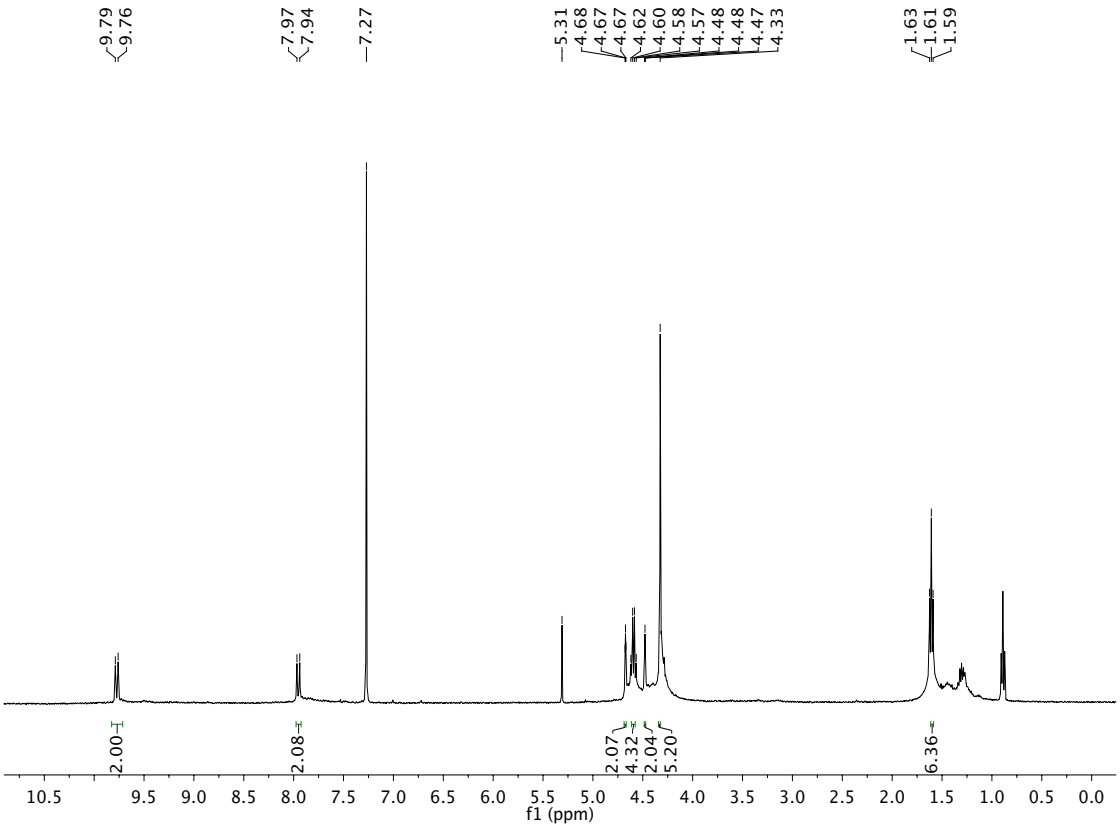

^{1}H NMR Spectrum of Compound 1.7 in $CDCl_3$

Appendix 4

NMR Spectra of Selected Compounds from Chapter II.

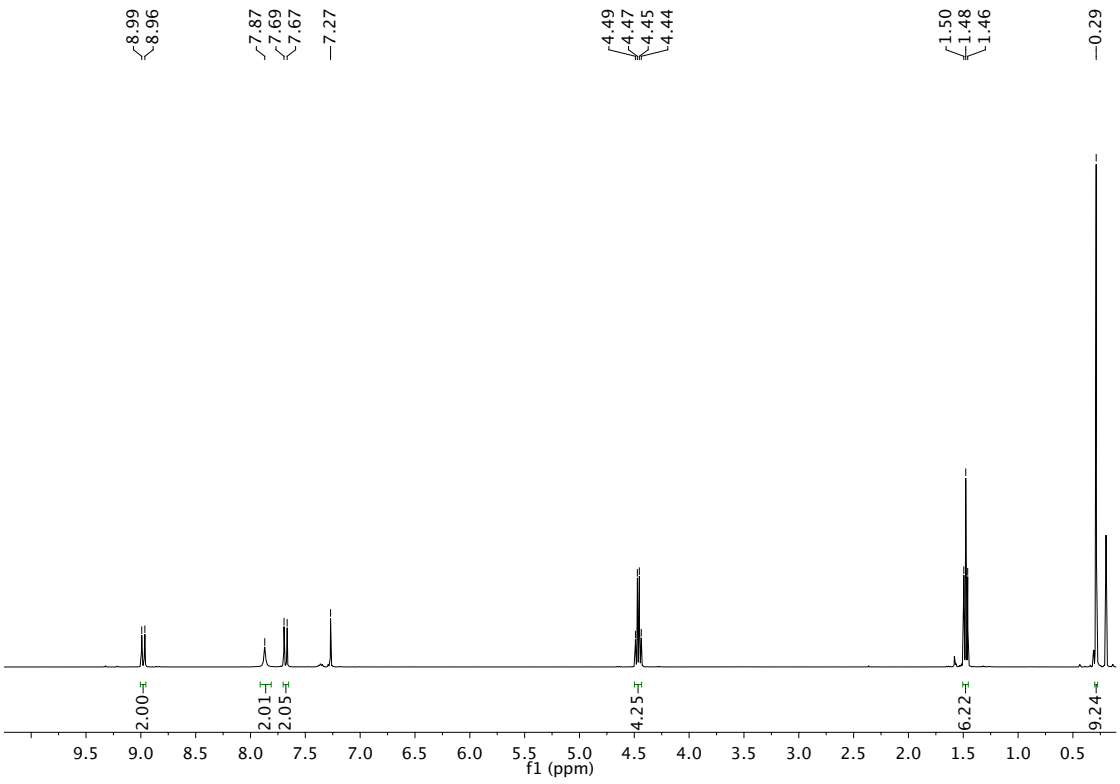

^{1}H NMR Spectrum of Compound 2.1 in $CDCl_3$

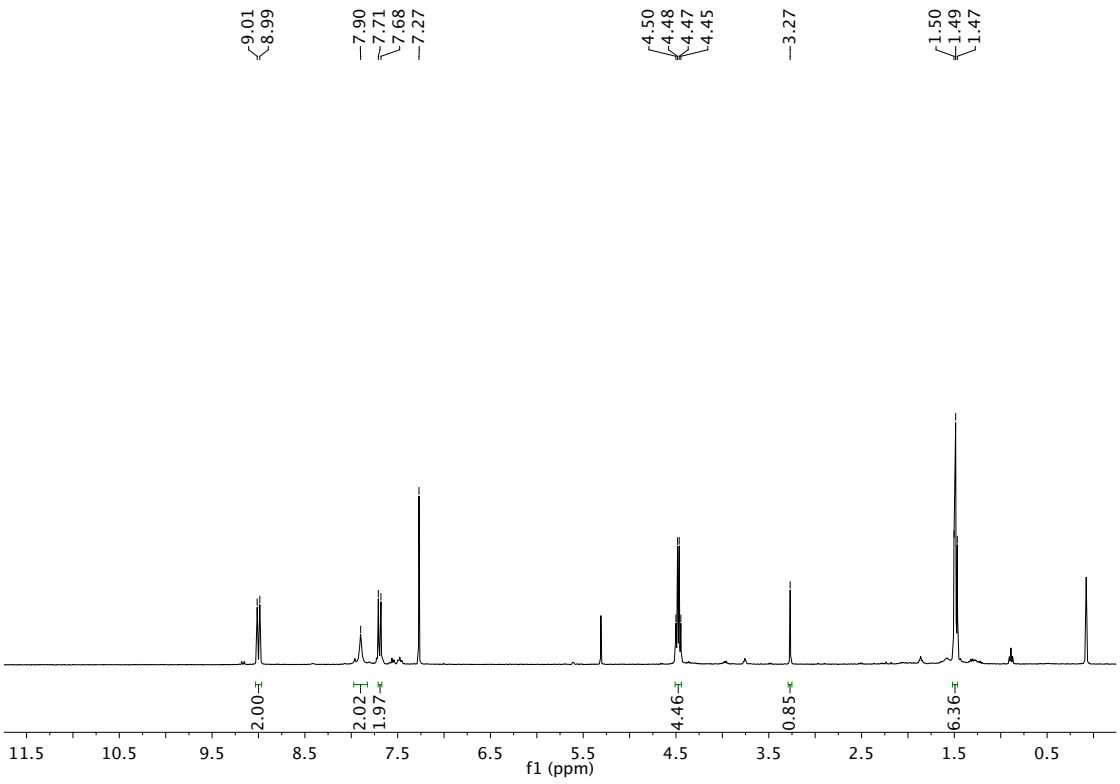

^{1}H NMR Spectrum of Compound 2.2 in $CDCl_3$

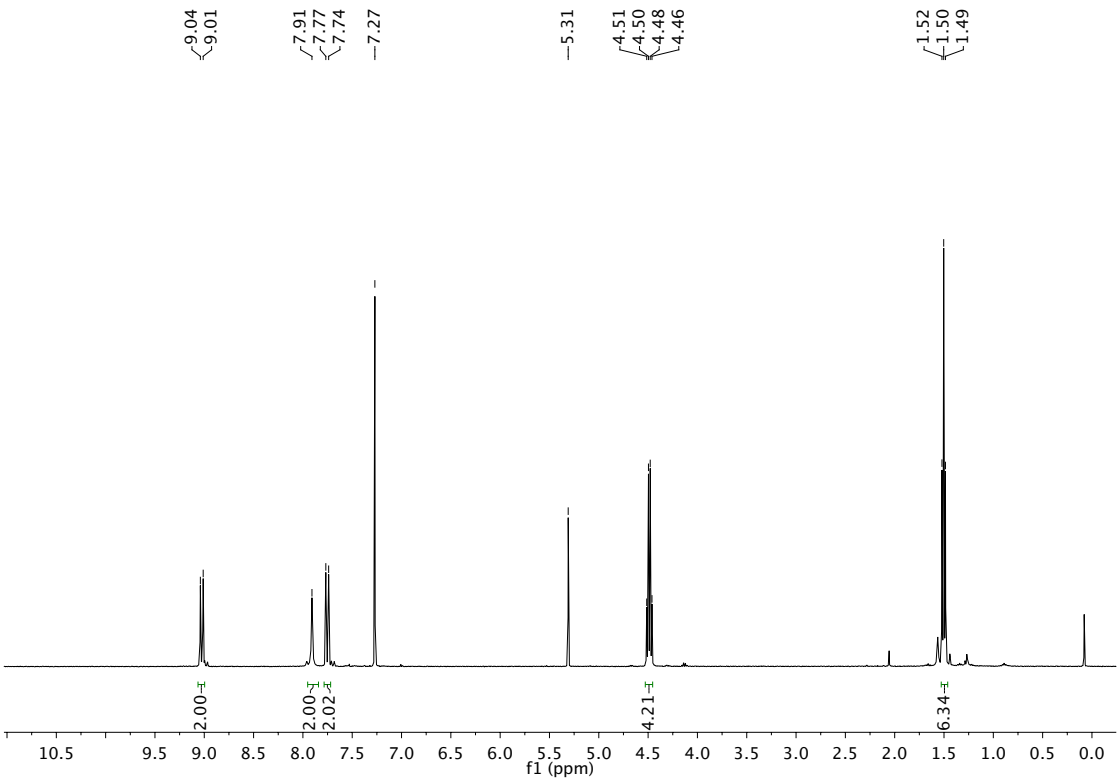

^{1}H NMR Spectrum of Compound 2.3 in $CDCl_3$

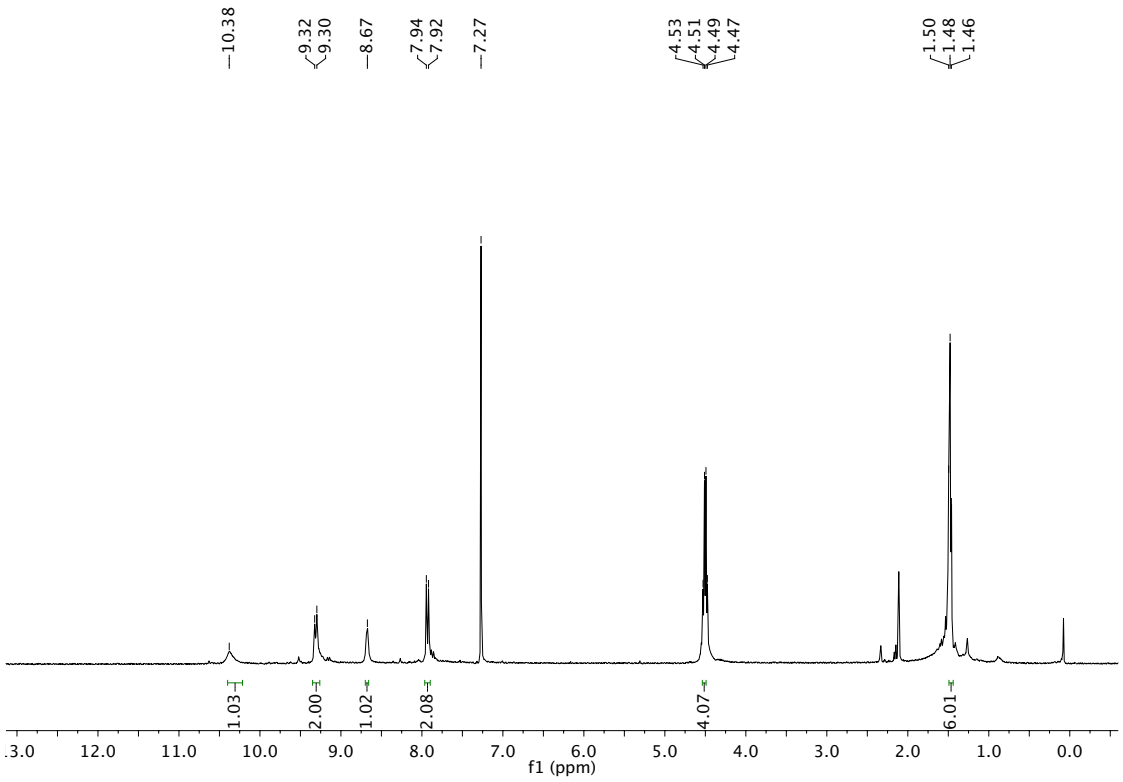

^{1}H NMR Spectrum of Compound 2.4 in $CDCl_3$

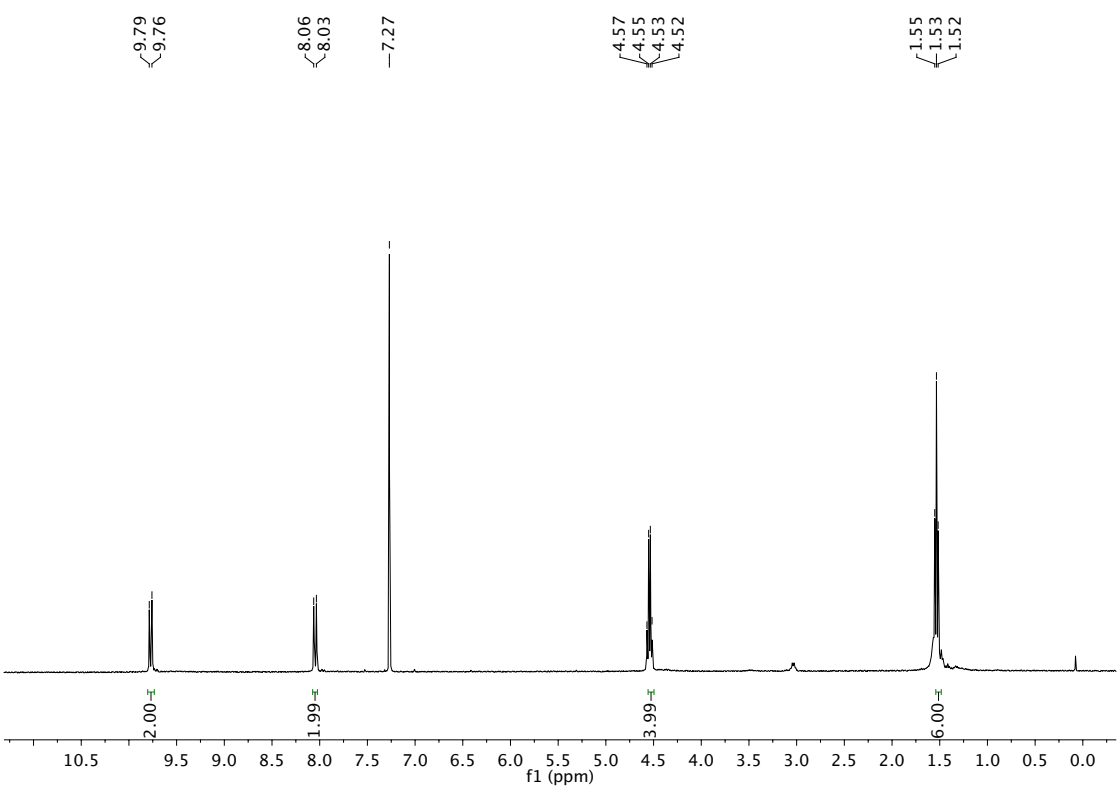

^{1}H NMR Spectrum of Compound 2.5 in $CDCl_3$

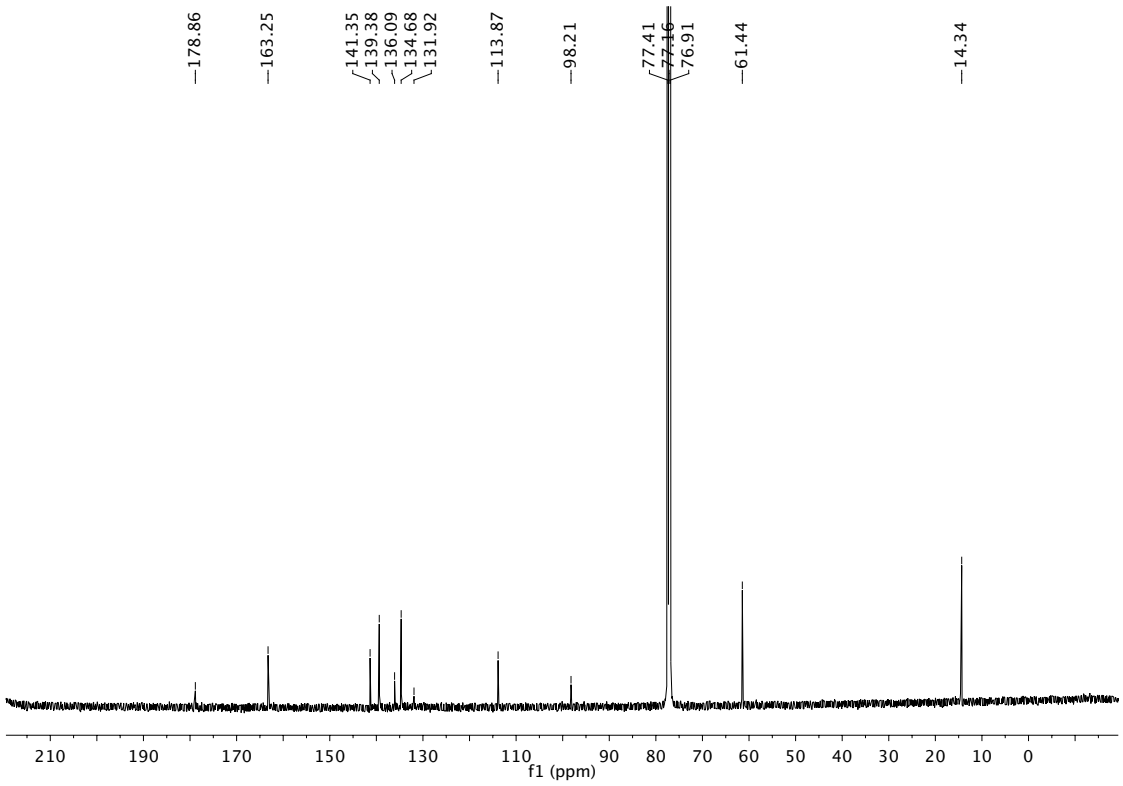

^{13}C NMR Spectra of Compound 2.5 in $CDCl_3$

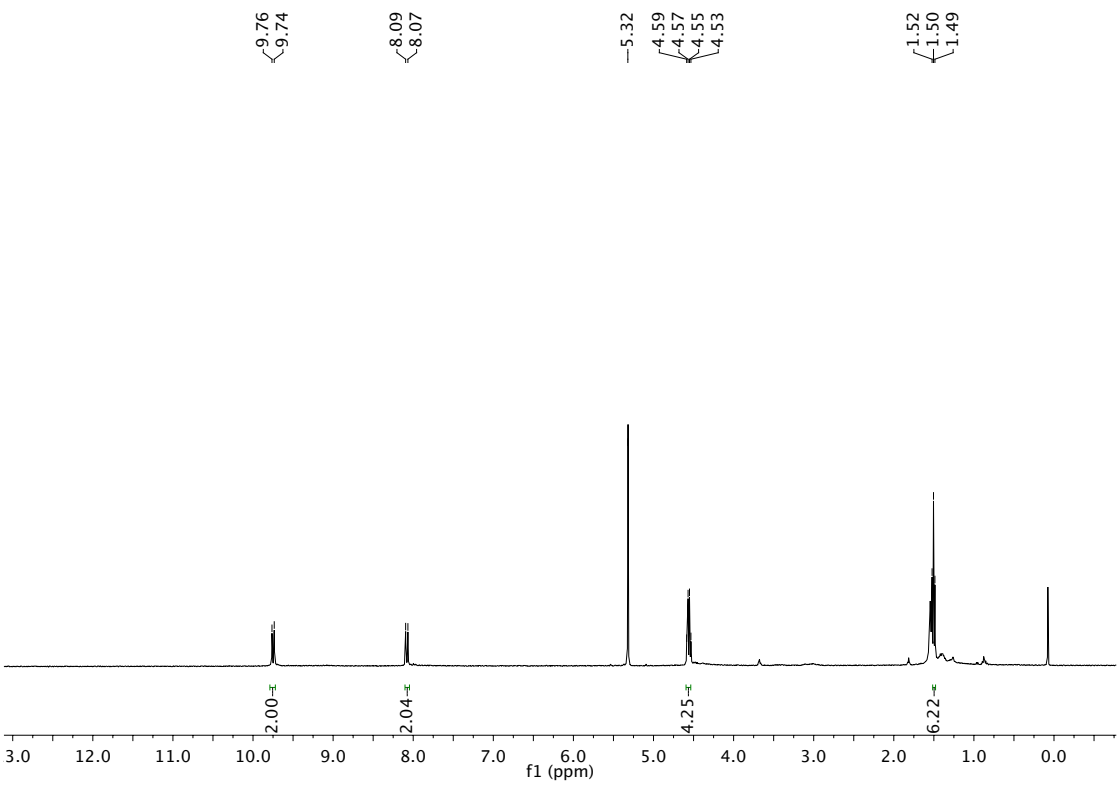

^{1}H NMR Spectra of Compound 2.6 in CD_2Cl_2

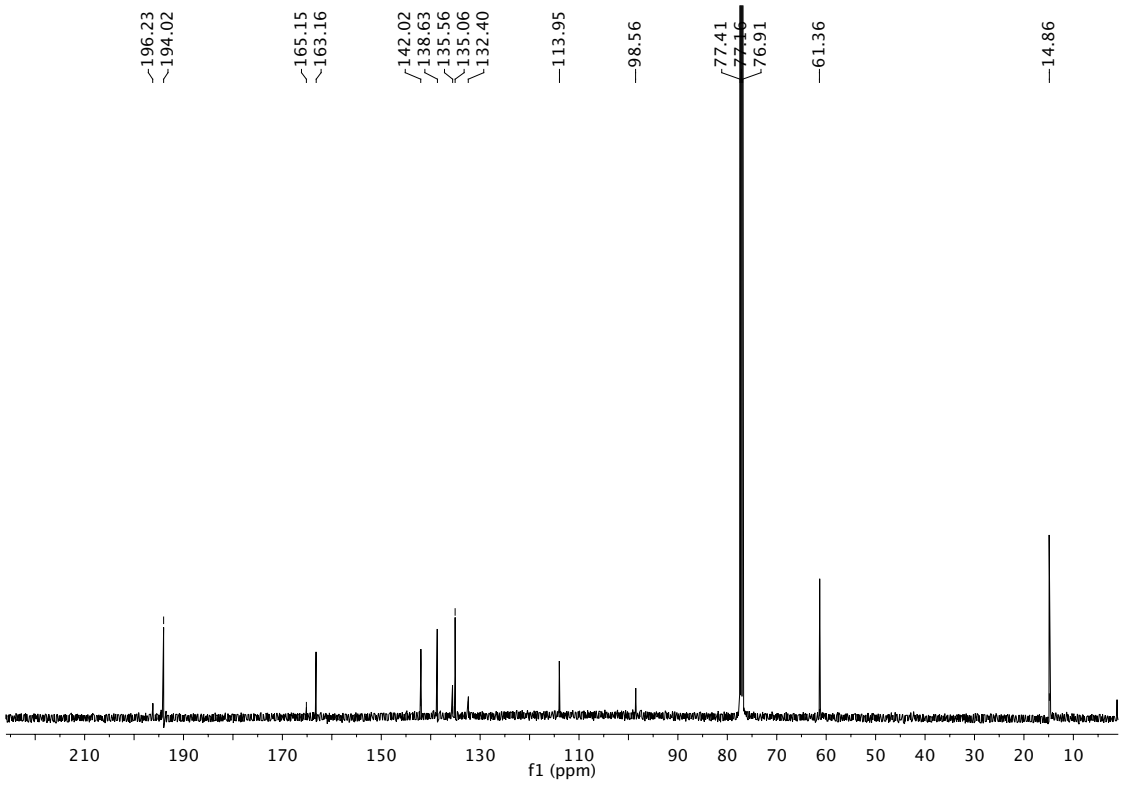

^{13}C NMR Spectra of Compound 2.6 in $CDCl_3$

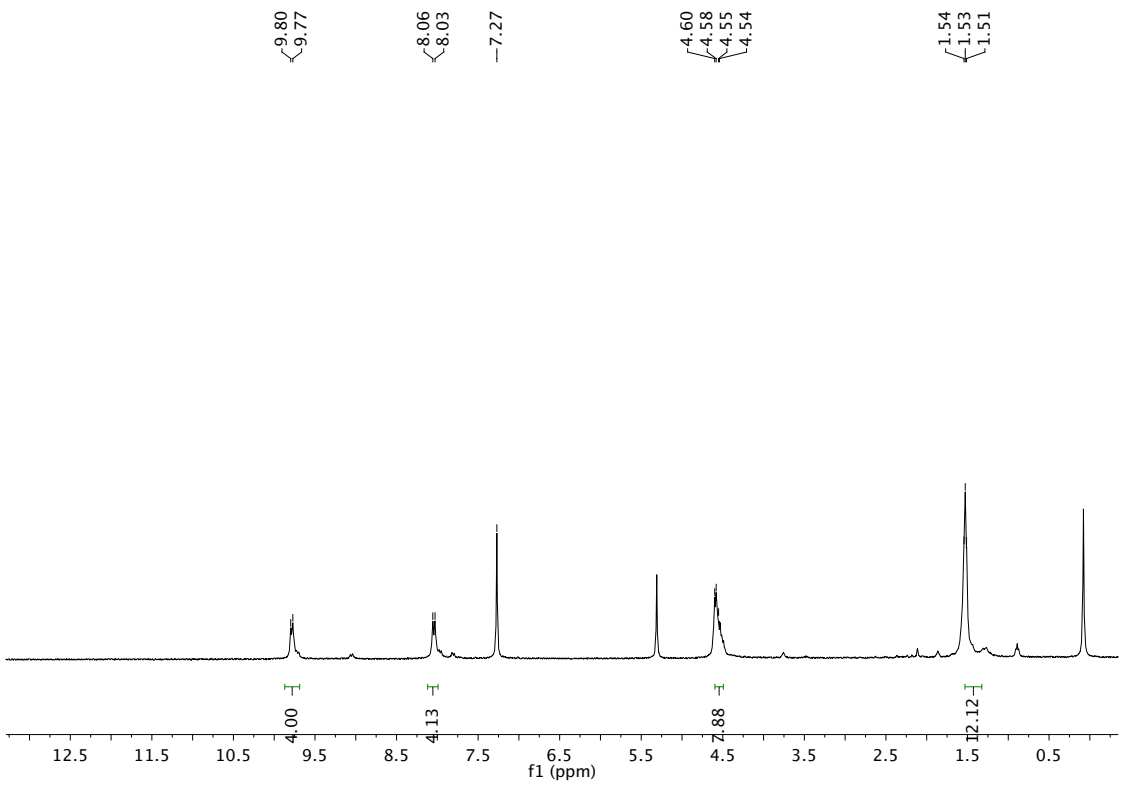

^{1}H NMR Spectra of Compound 2.7 in $CDCl_3$

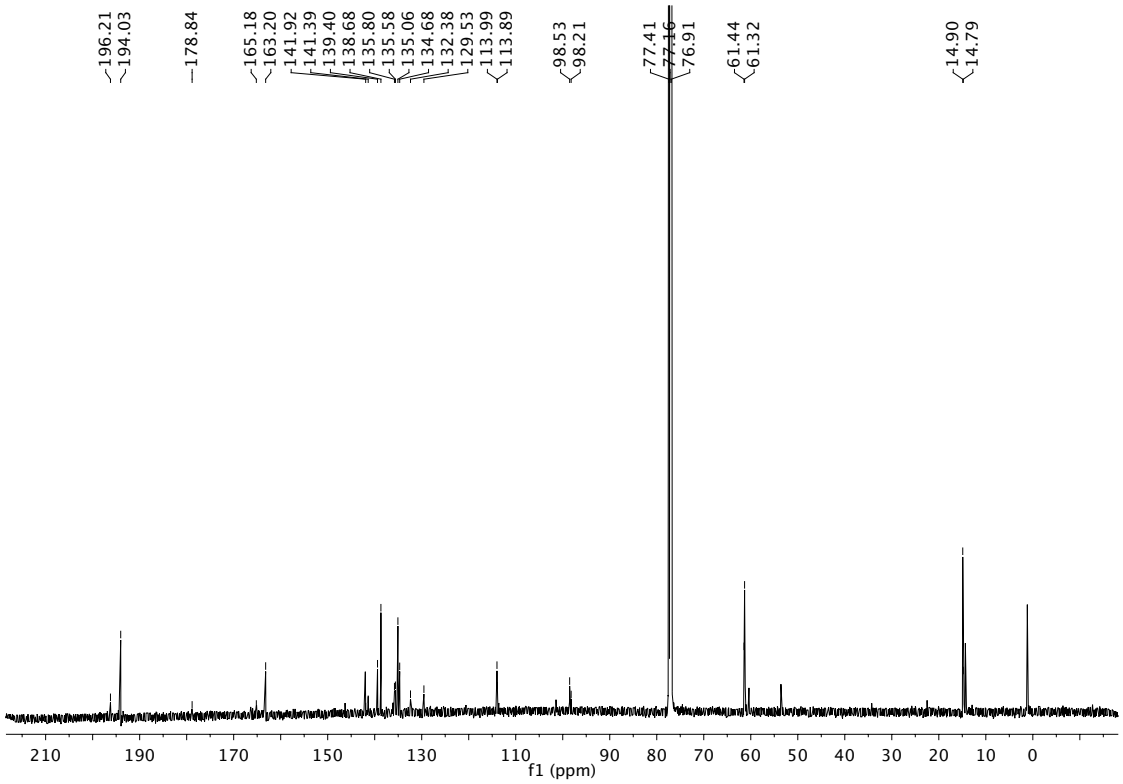

^{13}C NMR Spectra of Compound 2.7 in $CDCl_3$

Appendix 5

NMR Spectra of Selected Compounds from Chapter III

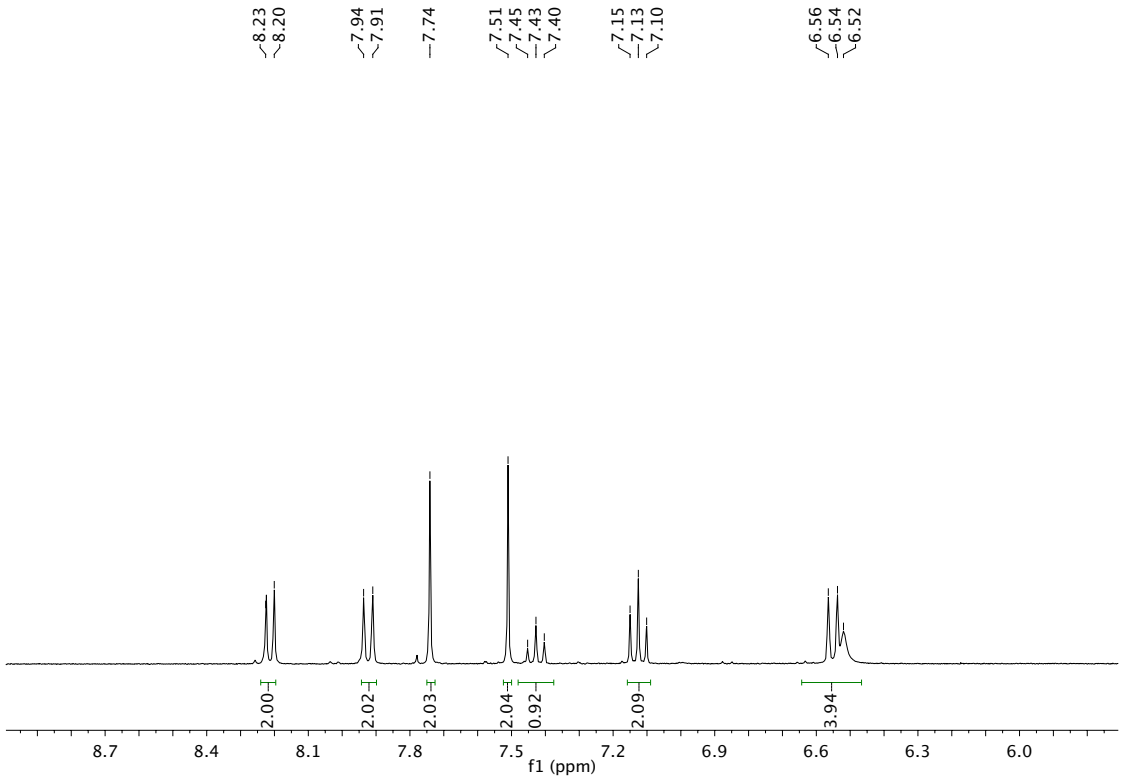

^{1}H NMR Spectra of Compound 3.1 in Acetone-d^{6}

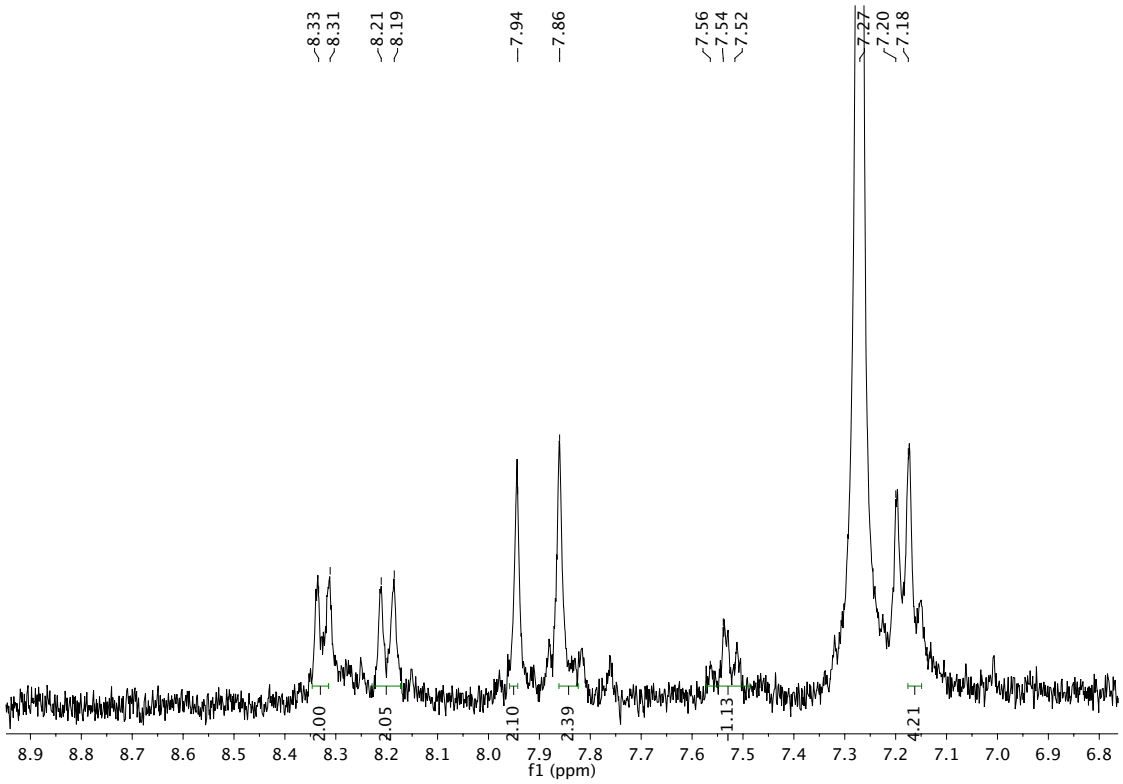

^{1}H NMR Spectra of Compound 3.3 in $CDCl_3$